CHANCE project

(Contract Number:755371)

R&D requests in the field of conditioned radioactive characterization

DELIVERABLE (D2.3)

Work Package 2

Authors: Bertrand Perot (CEA), Olivier Gueton (CEA), Denise Ricard (Andra), Barbara Ferrucci (ENEA), Grazyna Zakrzewska (INCT), Christophe Bruggeman (SCK CEN), Crina Bucur (RATEN), Christophe Mathonat (KEP), Guillaume Genoud (VTT), Jaap Velthuis (UoB), Eric Laloy (SCK CEN)

Reporting period 3: 01/06/2020 – 31/03/2022

Date of issue of this report: 31/03/2022

Start date of project: **01/06/2017** Duration: 58 Months

This project has received funding from the Euratom research and training programme 2014-2018 under grant agreement No 755371;

Dissemination Level		
PU	Public	X
CO	Confidential, only for partners of the CHANCE project and EC	

History chart			
Status	**Type of revision**	**Partner**	**Date**
Draft	Initial version	CEA	Nov 2019
Draft	Amended document	SCK CEN	May 2021
Draft	Amended document after internal review	ANDRA, CEA, SCK CEN	July 2021
Draft	Version for external review		November 2021
Final version			March 2022

Reviewed by

- WP2 contributors
- WP leader
- End-Users members: Amy Shelton (RWM), Jeroen Mertens (BelV) and Tomas Vandoorne (Ondraf/Niras)

Table of Contents

1. Introduction

The CHANCE project aims to address the specific issue of the characterization of conditioned radioactive waste. The characterization of fully or partly conditioned radioactive waste is a specific issue because unlike for raw waste, its characterization is more complex and therefore requires more advanced non-destructive techniques and methodologies.

The first objective of the CHANCE project is to establish at the European level a comprehensive understanding of current conditioned radioactive waste characterization and quality control schemes across the variety of different national radioactive waste management programmes, based on inputs from end-users members such as Waste Management Organizations and storage operators.

The second objective of CHANCE is to further develop, test and validate techniques already identified that will improve the characterization of conditioned radioactive waste, namely those that cannot easily be dealt with using conventional methods. Specifically, the work on conditioned radioactive waste characterization technology will focus on:

- Calorimetry as an innovative non-destructive technique to reduce uncertainties on the inventory of radionuclides;
- Muon Tomography to address the specific issue of non-destructive control of the content of large volume nuclear waste;
- Cavity Ring-Down Spectroscopy (CRDS) as an innovative technique to characterize outgassing of radioactive waste.

The present report focuses on activities from Work Package 2 related to the first objective of the CHANCE project, namely **the establishment of an overview of current conditioned radioactive waste characterization techniques employed over Europe**. In the framework of Task 2.1, information in terms of characterization requirements, particularly links and overlaps between these requirements and waste specifications from different national disposal programmes were collected from the CHANCE project End-User Group. A synthesis of the collected information was summarized in the CHANCE Deliverable 2.2.

The objective of Task 2.2 is **to identify the R&D needs on characterization of conditioned radioactive based on the outcomes of task 2.1**. To this end, the present report describes the state of the art regarding (RD&D on) waste characterization techniques and methodologies in view of the needs identified in the Task 2.1. It also highlights the techniques that can be improved/further developed in the future to improve characterization of conditioned radioactive wastes.

To recapitulate the main outcomes of task 2.1, CHANCE stakeholders and end-users highlighted following needs for radioactive waste characterization:

- Better quantification of the radiological inventory of specific wasteforms, including:
  - Quantification of difficult to measure (alpha and beta emitting) isotopes;
  - Fissile materials assessment in conditioned waste;
  - Quantification of the inventory of ^{3}H, ^{14}C and ^{36}Cl in irradiated graphite waste forms, and, if possible, the correlation of these isotopes with an easy to measure isotope as well as the ^{14}C speciation;
  - Quantification of ^{226}Ra activity levels in historical Ra-contaminated (NORM) waste;
- Quantification of chemical parameters considered in waste acceptance criteria ("WAC"), for example those related to:
  - Presence of complexing and chelating agents;
  - Presence of accelerators of leaching processes (e.g., chlorides, fluorides, nitrates, sulphates, carbonates)

    - Presence of toxic chemicals (referred to in the European regulation REACH);
    - Reactive phases (e.g., metals that react with water)
    - Presence of molecules which react with the matrix
    - Presence of forbidden compounds (e.g., those that present risk of explosion or ignition, unstable chemicals, strong reductants, etc.).
- Proper characterization of the conditioned legacy/ historical waste packages
- Visualization of waste forms to identify filling/void volumes;
- Development of transportable/in situ characterization devices;
- Monitoring waste drums during (extended) interim storage;
- Development of statistical approaches to demonstrate the representativeness of sampling for destructive measurements.

Within this report, we will describe the state-of-the-art of different methodologies used, or under development, in radioactive waste characterization. The emphasis of this report is on **non-destructive waste characterization methods**. After a general introduction to nuclear waste characterization (section 2), we will first discuss imaging methods (section 3) allowing to obtain a visual inspection of the inside and contents of a waste form. Hereafter, we will present passive measurement techniques, including gamma-based (section 4) and neutron-based methods (section 5). Both techniques are well-established and routinely used to obtain information on easy-to-measure isotopes present in the waste. From these sections onwards, we will detail how the complete radiological inventory of a waste form can be obtained, e.g., through scaling factors (section 6) or calorimetry (section 7). Then, we will discuss several technical more high-end techniques where developments are still very active in order to allow these techniques to tackle more challenging waste forms and/or isotope quantification. These include active interrogation techniques (section 8), cavity ring-down spectroscopy (section 9), coupling of different methods (section 10) and Bayesian approaches (section 11) that can greatly enhance insights and reduce uncertainties in waste form characterization. Then, we will discuss latest developments in mobile and transportable characterization techniques (section 12). The report ends with a concluding section (section 13) indicating needs for future RD&D.

2. Nuclear waste characterization

Radioactive waste can originate from different producers such as nuclear power plants, research facilities, nuclear medicine, etc. In the context of final radioactive waste disposal, the purpose of radioactive waste characterization is generally to verify that the waste (packages) complies with the acceptance criteria of the licensed disposal facility. These criteria differ depending on the form and type of radioactive waste and on the different (country-specific) regulations that apply for these facilities. Appropriate control procedures to ensure the compliance with these criteria are necessary for quality control. These procedures can take place at different stages of the waste management strategy, including during decommissioning of nuclear facilities (e.g., NEA, 2017). This report refers mostly to the characterization of waste before it enters a final disposal facility, in line with the scope of the CHANCE project.

Characterization of nuclear waste or nuclear waste packages is performed through both non-destructive and destructive measurement methods, allowing access to the physical (density, volume, shape, position of the waste and embedding matrices, mechanical toughness, cracking, diffusion coefficient, gas release, thermal power, etc.), chemical (elemental composition, content of toxic or reactive substances, etc.) and radiological characteristics (dose rate, α and β activity, isotopic composition and mass of nuclear materials, etc.) (Pérot *et al.*, 2018).

2.1. Destructive analysis

Destructive analysis (DA) provides the most accurate and unbiased activity determination, since pure alpha and beta emitting radionuclides or those emitting gamma or X-rays with a too small intensity or energy are extremely difficult to measure in already conditioned waste packages. Chemical and radiochemical treatment of the primary waste or waste form allows measurements to be performed that assure the traceability of the determined activity. This is not the case with NDA methods, which typically use standards calibration or modelling. As a consequence, there is greater uncertainty with NDA in terms of determining activity.

The DA process involves sampling, sample preparation and chemical separation methods. Sampling is a critical step in the characterization process. Designing the sampling procedures and checking the homogeneity and representation of the samples assures the reliability of the final results. Sample preparation by dissolution/mineralization has to be applied in accordance with the physicochemical characteristics of the matrix of waste forms or primary wastes and as a function of the behaviour of the specific element in the dissolution media (volatilization, precipitation). In some cases, it is possible to do a direct measurement of the radionuclide after dissolution/mineralization if the determination technique has the resolution required for it.

Chemical separation involves the chemical strategy to eliminate chemical interference (e.g., Ca in Sr determination) and radiological interference in the measurement through a chemical process such as precipitation, solvent extraction, or chromatography.

Radiometric determination is performed by instrumental analysis. Sophisticated methods are used such as liquid scintillation counters that allow beta spectrometry, alpha spectrometry with semiconductor detectors, high resolution gamma spectrometry for high and low energy gamma emitting nuclides, mass spectrometry that gives an accurate and efficient response for the analysis of the prepared and/or separated waste samples.

A review of methods on destructive analyses for the quality checking of radioactive waste packages is provided by Troiani *et al*. (2001).

2.2. Non-destructive analysis

Non-destructive testing methods are used in order to minimize the radiation dose to personnel, to avoid secondary radioactive waste production and to minimize costs. Furthermore, with destructive testing, there is always the essential question of taking a representative sample, especially for heterogeneous waste (Bücherl and Lierse von Gostomski, 2001).

Several non-destructive methods for quality checking of radioactive waste packages have been developed and tested. (Bücherl and Lierse von Gostomski, 2001) distinguish these by the measured quantity, and their operation mode (Table 1). Passive methods are based on the detection of neutrons and gamma-rays spontaneously emitted by the nuclides of interest. Such methods are easy to implement, but also impaired by the low intensity of radiations or self-attenuation inside the packages (e.g., in the case of low-energy gamma-rays emitted by actinides). To overcome these impairments, active methods may be employed. These methods are based on fission processes and on the detection of particles emitted after such processes (Carrel *et al*., 2010).

TABLE 1: MEASURING MODES CONVENTIONALLY USED IN QUALITY CONTROL OF RADIOACTIVE WASTE PACKAGES (BÜCHERL AND LIERSE VON GOSTOMSKI, 2001)

	gamma radiation	neutrons
passive	dose rate measurements gamma counting segmented gamma scanning	total neutron counting segmented neutron counting time correlation methods
active	radiography tomography interrogation techniques	interrogation techniques

According to the information collected in the Task 2.1 and described in CHANCE deliverable 2.2, one of the main needs in characterization of waste, is the development of new non-destructive methods especially for the characterization of conditioned wastes namely for legacy/historical waste packages. The most important parameters that need to be further characterized were identified to be radiologic parameters and composition of waste materials (chemical content).

Apart from non-destructive methods, also chemical, radiochemical and physical destructive analytical methods and techniques are used in the verification and characterization of waste forms and packages. A review of methods on destructive analyses for the quality checking of radioactive waste packages is provided by Troiani *et al*. (2001). These methods are only very briefly described in this report (section 3).

Thus, the objective of this deliverable is to describe latest developments in the area of (mainly non-) destructive (conditioned) waste characterization, referring also to adopted best practices in countries with operating disposal facilities.

3. Imaging

Imaging can be a powerful tool allowing the physical characterization of waste drums, including waste identification, density measurement, and integrity check of the package (Estre *et al*., 2015). Using X-rays, digital radiography (DR) and computed tomography (CT) can be performed on either small sub-samples (section 3.2) or on entire waste drums (section 3.3).

3.1 (Low-energy) X-ray tomography

In 1895, William Conrad Roentgen (1845-1923), accidentally discovered a new type of ionizing radiation, named X-rays. This discovery was soon followed by the invention of radiology, exposing films with various objects placed between a cathode ray tube (CRT) and the film. The radiographic technique consists of focusing a broad parallel beam of penetrating radiation upon a sample of interest and recording the effects of the unabsorbed portion of the beam upon the radiographic film (Hansen). The picture or image provided by the film represents the opacity of the sample, which varies dependent upon the density, thickness and atomic number (Z) of the sample.

Opacity differences as small as a few percent can be discerned under ideal conditions and high-quality images can be obtained which are nowadays an invaluable diagnostic for the medical and the industrial community. X-ray radiography works perfectly well to image materials that do not completely attenuate the beam, that have differences in attenuation (opacity) due to internal structure, and that can be oriented perpendicular to the X-ray beam.

Autoradiography is a technique for revealing fixed radioactivity that is difficult to measure in certain types of waste. Using sensitive screens, especially beta emitters such as tritium, and in some instances alpha emitters can be visualised (Pérot *et al*., 2018).

In recent years, new types of ionizing radiation, new detector types, and different configuration systems have been tested to provide better resolution, more penetrating depth, or even qualitative and quantitative information on the type of materials contained in a waste package.

These developments are in line with the evolving needs for chemical contents characterization. Indeed, the traceability of the chemical content is usually very low in the case of historical waste packages or when the packaging is done by the waste generator. Regarding the *chemical parameters* considered in waste acceptance criteria, in some situation attention is paid to the chemical reactivity to ensure the stability of the waste matrices and to avoid or limit perturbations of the engineered barriers and/or host rock: e.g., there may be limitations on amounts of complexing and chelating agents, accelerators of leaching processes (chlorides, fluorides, nitrates, sulphates, and carbonates), organic substances (frequently precursors of chelating agents), pyrophoric, flammable, explosive, corrosive or oxidizing materials. Biologically active wastes (infectious or putrescible) are generally forbidden.

Although most of these chemical characterizations are nowadays mostly performed by destructive measurements, replacement by new non-destructive controls is now being studied and the newest developments (such as those described in subsequent sections) already allow to assess some chemical elements or compounds.

Tomography was designed to solve the issue of rendering an object in three dimensions so that any arbitrary plane of interest can be displayed when the source and detector cannot be placed at right angles to the plane of interest (Hansen).

X-ray computed tomography (CT) scanning is a non-destructive technique that allows visualization of the internal structure of objects, determined mainly by variations in density and atomic composition (Mees *et al*., 2003). The most well-known application is a medical CT scanner for the visualization of the inside of patients, but also in the geosciences it has found widespread application for the petrography and characterization of drill cores (Mees *et al*., 2003; Engelberg *et al*., 2012). The result of a tomography is a virtual 3D presentation of the scanned object, both in- and outside. Three-dimensional microstructure representations are calculated numerically from the recorded projection images by a tomographic reconstruction algorithm "https://www.ugent.be/we/ugct/en/research/xrayct.htm".

During X-ray tomography, X-rays are directed onto the sample under investigation. As in any tomography experiment, 3D information is gathered by acquiring a series of 2D images while rotating either the source and detector, or the sample (typically between 0° and 180°). In transmission X-ray tomography, X-rays are attenuated through the object and detected by a dedicated system. Since interactions that are responsible for this attenuation are mainly Compton scattering (high energies) and photoelectric absorption (lower energies), the attenuation is material- and energy-dependent. Generally, the X-rays used are always polychromatic with a wide range in energy, which complicates quantitative analysis and creates artefacts in the CT images, due to the stronger attenuation of X-rays with lower energies. Monochromatisation by diffraction eliminates these problems, but results in a great decrease in beam intensity (Mees *et al*., 2003). The attenuation of X-rays decreases as a function of energy, for energies lower than 10 MeV. Therefore, the larger the object, the higher the required energy (Rizo *et al*., 2000).

From the set of all the attenuation measurements across a plane of the object, the attenuation coefficient of each point of the object in this plane can be reconstructed using a series of mathematical and image quality optimization algorithms. In order to provide reliable reconstructed values, the attenuation must be measured through the object and out of the object. With translation rotation scanners (Figure 1) such as those used for large objects, the detector must perform measurements in and out of the container. This therefore leads to a very high dynamic range for the detectors. Today the maximum dynamic range which can be reached is about 5 decades. Thanks to the rapid development of both the X-ray tubes as the detectors, objects can be imaged with continuously better resolution. The current state of the art tomography machines get resolutions of about 1 micrometre or better.

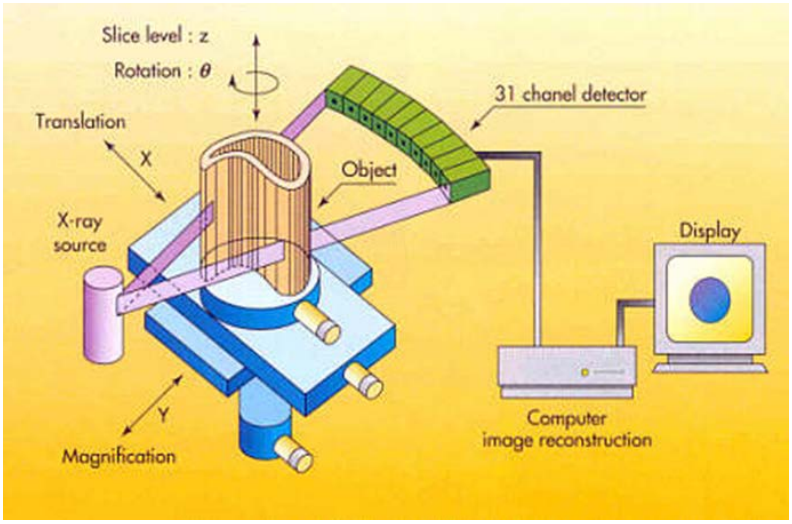

FIGURE 1: PRINCIPLE OF TRANSLATE ROTATE TOMOGRAPHIC SYSTEMS (RIZO ET AL., 2000)

Tomography allows to reconstruct the attenuation coefficient of each pixel in the object. Therefore, it can give access to the detection of voids, cracks and any structure leading to a sensible variation of the attenuation coefficient. The main limitation of this technique is the detection of liquids and the chemical characterisation of materials (Rizo *et al.*, 2000).

The geometric resolution of tomographic images is limited by the system geometry, the number of projections acquired and the resolution of these projections. The density resolution of the reconstruction is limited by the number of photons reaching the detectors. Considering the preceding constraints, it appears that the type of information that will be extracted from tomographic measurements will depend on the container size and density (Rizo *et al.*, 2000). For heavier objects, such as cemented (conditioned) waste drums, low energy X-rays are completely attenuated through the object, making the application domain restricted to small sub-samples of waste drums.

3.2 High-energy X-ray imaging

3.2.1 Current practice

Among radioactive objects, cemented waste drums and shielded containers are among the largest and heaviest. In broad outline they are made of a mix of materials, compacted or not, and surrounded by a hydraulic cement. Containers are typically composed of a 8 to 15-cm thick concrete shell or a 0.1 to 0.5-cm thick metallic shell. High energy X-ray applications for radiological testing and computerized tomography on such large or dense radioactive objects require X or γ rays of at least 1 MeV to reach sufficient S/N ratio in attenuation measurements. These high-energy photons are produced either by a ^{60}Co isotopic source (as monochromatic continuous beam) or by a Linear Accelerator of electrons (Linac) (Pettier *et al.*, 2004).

In a Linac, an electron canon produces electron packets which are accelerated in a network of cavities by a stationary HF wave, raising their energy up to a few MeV. The electrons are eventually projected onto a target made of heavy material (tungsten or tantalum). They then yield a fraction of their energy by emitting a braking radiation, or Bremsstrahlung (polychromated pulsed beam). The dose rates delivered by these machines are very high, ranging from 10 to 100 Gy.min^{-1} at a distance of 1 m from the target, in the axis of the beam (Pérot *et al.*, 2018).

The radiographic image provides a projection of the object of millimetre resolution, each pixel of the image being representative of the attenuation experienced by the beam along a linear path. The tomographic image is obtained by acquiring different angular projections (radiographies) of the package. The tomographic reconstruction is then carried out by dedicated algorithms allowing precise visualization of the interior of an object (values of the density) in planar sections. The principle of such a system is shown in Figure 2.

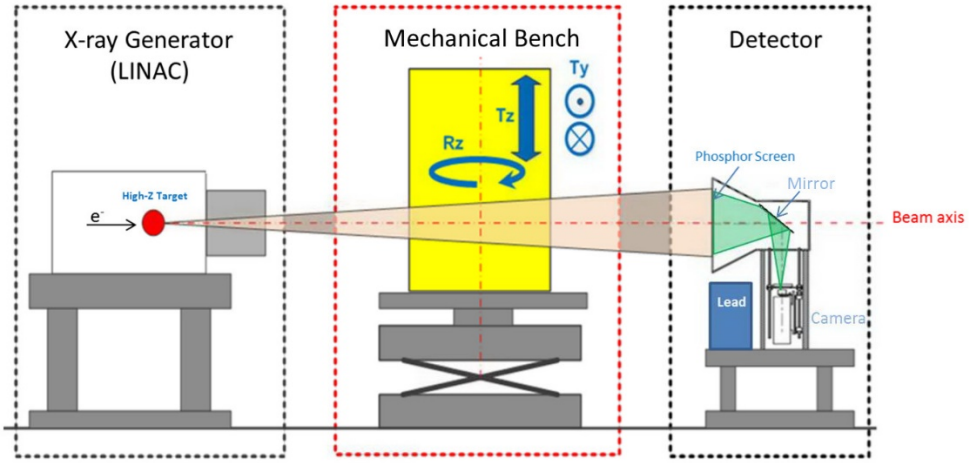

FIGURE 2: MAIN COMPONENTS OF THE HIGH-ENERGY IMAGING SYSTEM (PÉROT ET AL., 2018)

Bernardi and Martz (1995) describe the progress of a multi-modality system for a mobile semi-trailer mounted non-destructive examination (NDE) and assay (NDA) for nuclear waste drum characterization, developed for the USA's DOE. Among the characterization modalities, the system uses a 2 MeV high-energy accelerator as an externally transmitted radiation source. The high-energy source is needed to penetrate denser and thicker waste forms like glass, sludge and cemented drums, while allowing for an optimum inspection throughput. The use of energies higher than 2 MeV was not deemed practical because of the mobile requirements of the system, resulting in weight restrictions for radiation shielding limiting close operator interaction. The authors describe

the system as having better imaging capabilities for higher density materials and faster throughput for lighter waste forms, compared to more conventional (420 kV) radiography.

With higher levels of intensity and energy, it is possible to cross through more than a meter of concrete while keeping a detectable signal behind the object to be radiographed. In CEA Cadarache, such a system is implemented in the CINPHONIE buried casemate containing a 9 MeV LINAC (Pérot *et al.*, 2018). Because of these high energies, it is absolutely necessary to set up highly efficient biological protection in order to protect the personnel (Figure 3).

The high-energy photon imaging system allows the realization of X-ray radiography (2D imaging) or tomography (sectional reconstruction of the interior of the package, 3D imaging), see Figure 4. The imaging allows also the interfaces between waste, binder and container to be checked in order to make sure that there is no empty space as well as the absence of liquid. Using the 9 MeV imaging system of standards of known and calibrated materials, it has been established that spatial resolution of 1.5 mm and a precision on density lower than 10% can be achieved. Typical 1 m^3 packages can be inspected in less than 10 minutes for a complete radiography, and about 30 minutes for a tomographic cut.

FIGURE 3: THE CINPHONIE BURIED CASEMATE CELL AT CEA, CADARACHE, FRANCE, HOSTING A HIGH-ENERGY PHOTON IMAGING SYSTEM IN THE CHICADE BASIC NUCLEAR FACILITY, WITH A 9 MEV "MINI-LINATRON" LINAC (PÉROT ET AL., 2018)

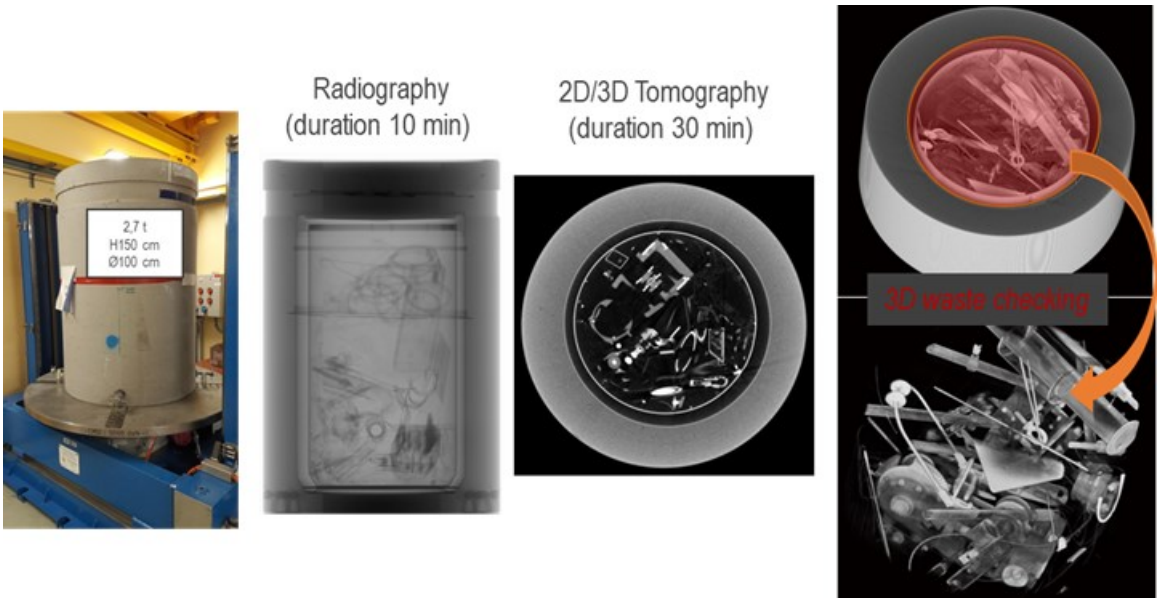

FIGURE 4: EXAMPLE OF X-RAY RADIOGRAPHY AND TOMOGRAPHY OF A CONCRETE PACKAGE (PICTURES FROM CEA, FRANCE)[1]

3.2.2 R&D on high-energy X-ray imaging

Recent RD&D include the development of newer detectors such as a large and continuous line of $CdWO_4$ scintillator needles (Kistler *et al.*, 2018) or CsI scintillators (Estre *et al.*, 2018) to avoid the horizontal sweeping scan of the package imposed by dead layers between the collimated CdTe, and thus to reduce acquisition time (Figure 5).

Also, higher energy (up to 15 MeV) and intensity Linacs are being tested (e.g., within CEA, France) with the goal to interrogate large and heavy waste packages up to 140 cm of concrete in diameter (vs. 100 cm for the current 9 MeV LINAC), with a sub-millimetre resolution thanks to a very small focal spot of the accelerated electron beam on the tungsten target (instead of about 2 mm with the current 9 MeV LINAC).

[1] Two acquisition systems are currently available at the CEA CINPHONIE facility: 1) a 2D wide-field screen of 80 × 60 cm² with a "Gadox" (Gd_2O_2S) phosphor coating for rapid imaging, with attenuation dynamics of about 3 decades, or in other words 1 m of concrete or 25 cm of steel, 2) a system of 25 CdTe semiconductor bar detectors, with collimators oriented towards the focal spot of the photon beam, for quantitative computed tomography with attenuation dynamics of approximately 5 decades, i.e. 1.5 m of concrete or 40 cm of steel.

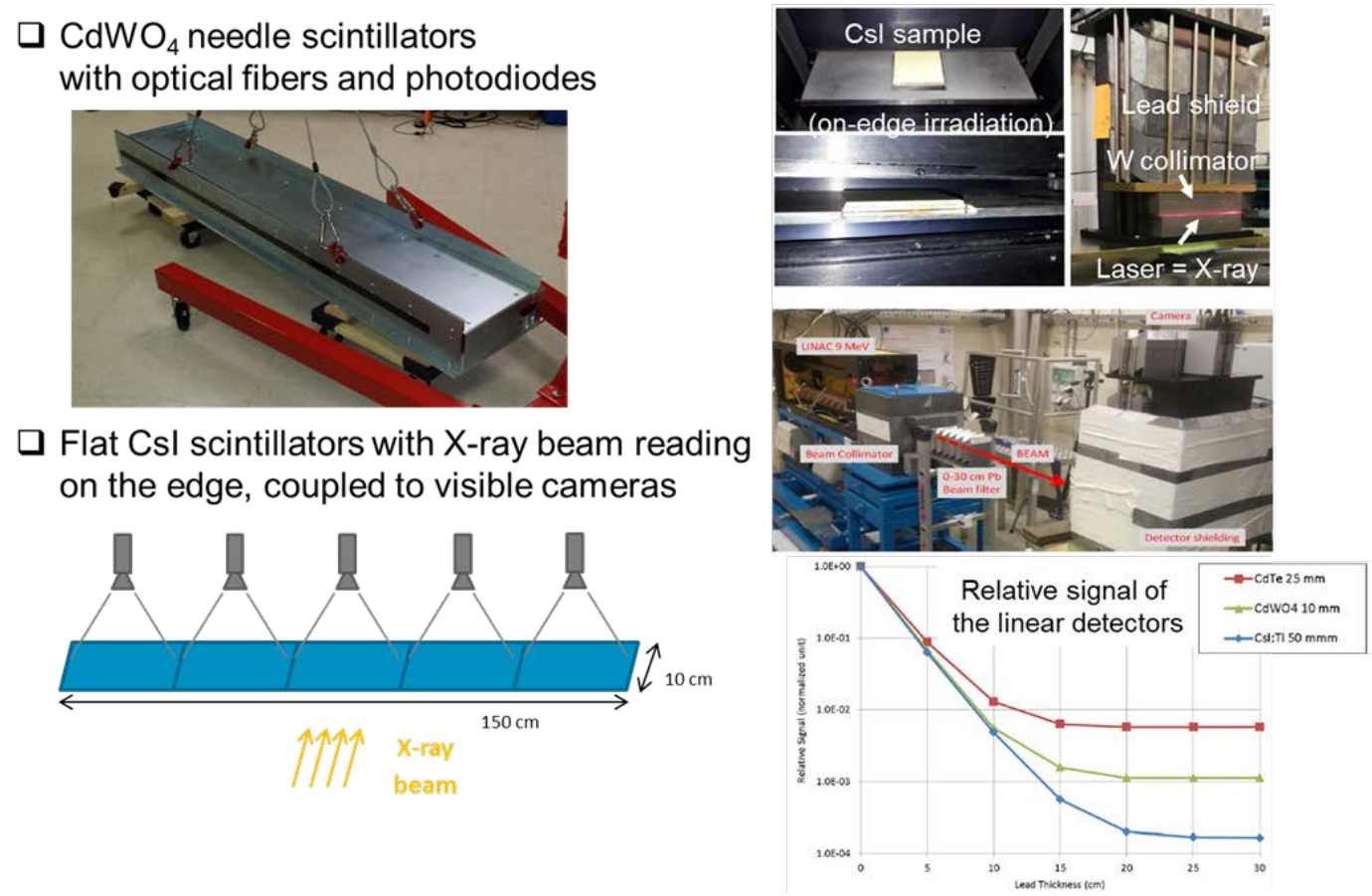

FIGURE 5: TESTS OF LINEAR DETECTORS BEHIND A TUNGSTEN ALLOY COLLIMATOR SURROUNDED BY A LEAD SHIELD (THE RED LASER BEAM REPRESENTS THE X-RAY BEAM). THE NORMALIZED ATTENUATION CURVES OBTAINED WITH AN INCREASING LEAD THICKNESS ALLOWS COMPARING THE DYNAMIC RANGE OF THE EXISTING CDTE DETECTION SYSTEM TO ALTERNATIVE LINEAR DETECTORS (ESTRE ET AL., 2018)

3.3 Dual energy X-ray imaging

Another information to be taken into account in tomography is that the attenuation coefficient depends on the density r and atomic effective number Z of the material at low energy up to 100 keV (photoelectric domain) and mainly on the density for energy from 200 keV up to 6 Mev (Compton domain). Therefore, using dual energy tomographic acquisition with objects of low attenuation, photoelectric and Compton information can be combined in order to obtain the effective atomic number and the density on each pixel of the slice. In that case it will be possible to distinguish organic materials, mineral and metals (Rizo *et al.*, 2000).

Dual energy imaging (e.g., 9 vs 6 MeV) is currently being tested within CEA, France, using Linac systems to determine an effective atomic number (Z_{eff}) of the imaged objects (Tamagno *et al.*, 2018). The principle illustrated in Figure 6 consists in taking advantage of the differences in attenuation according to X-ray energy spectrum and atomic number of the elements. In addition to the existing tomodensitometry measurement, this information will make it possible to refine the identification of materials thanks to a 2D analysis of Z_{eff} vs. density.

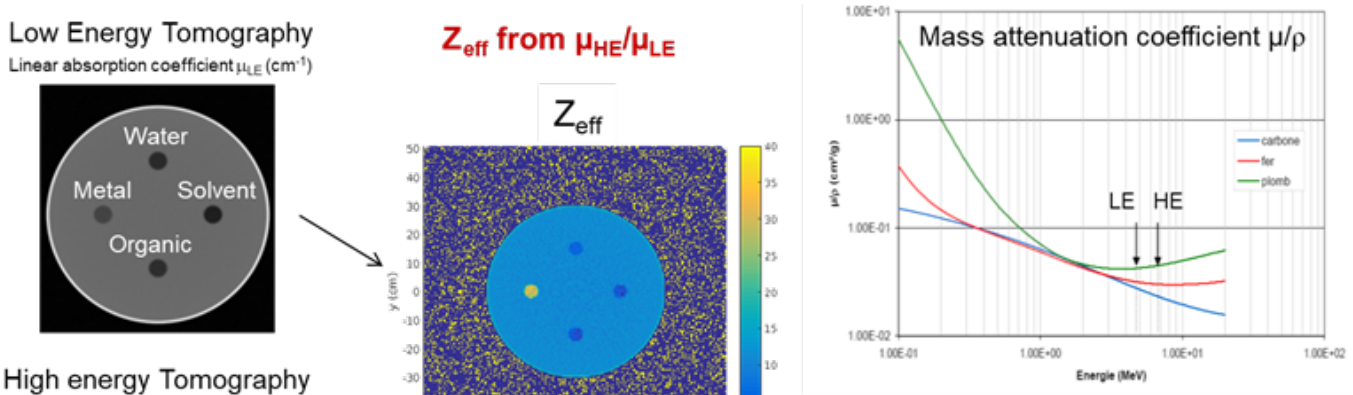

	Theoretical Z_{eff}	Extracted Z_{eff}	Reconstruction error
Water	6.60	5.72	-0.88
Solvent 1	4.60	3.61	-0.99
Solvent 2	5.37	4.68	-0.69
Solvent 3	6.06	5.36	-0.70
Graphite	6	5.39	-0.61
PVC	11.38	11.35	-0.03
Plaster	12.95	12.99	+0.04
ZrO_2 *	30.86	30.52	-0.34
PbO *	65.8	61.30	-4.50
Pb *	82	-	-

Table 1: Z_{eff} reconstruction of the 10 test materials inside a 200 L drum filled with concrete. (*) Density artificially reduced to 1.

FIGURE 6: PRINCIPLE OF DUAL-ENERGY IMAGING: TWO CROSS SECTIONS (IN GREY SCALE ON THE LEFT) OF THE SAME OBJECT ARE IMAGED USING DIFFERENT ENERGY SPECTRA FOR THE X-RAY SOURCE, HERE AT 9 AND 20 MEV, AND THE RATIO OF THE RECONSTRUCTED LINEAR ATTENUATION COEFFICIENT M (CM^{-1}) AT THE TWO ENERGIES (μHE/μLE) ALLOWS OBTAINING INFORMATION ON THE EFFECTIVE ATOMIC NUMBER ZEFF IN EACH PIXEL. THE TABLE REPORTS SIMULATION TESTS FOR 10 MATERIALS INSIDE A 200 L DRUM FILLED WITH CONCRETE, SEE DETAILS IN TAMAGNO ET AL. (2018)

3.4 Muon tomography

Because of their unique ability to penetrate matter, cosmic ray muons are used to image the interiors of structures. Since the early 2000's, several groups have extended the concept of muon radiography to the tracking of individual muons as they enter and exit a structure. Most current efforts have been geared toward demonstrating the potential for muon tomography to detect the smuggling of Special Nuclear Materials (SNMs) in cargo, the non-invasive characterization of legacy nuclear waste containers, and for nuclear material accountancy of spent fuel inside Dry Storage Containers used to store spent fuel (Jonkmans *et al.*, 2013).

Muons are charged particles created by the interaction of cosmic radiation with the upper layer of the atmosphere. Muons have the same electric charge as electrons, which make them easy to detect, but, in contrast, are much more massive ($m_\mu \approx 207 m_e$) and, on average, have a high momentum, which confers them with their strong penetrating ability. The vertical flux of energetic muons, above 1 GeV/c, at sea level is about 70 $m^{-2}s^{-1}sr^{-1}$ (or an integrated vertical flux ≈1 $cm^{-2}min^{-1}$). The mean muon energy is 3-4 GeV, which is sufficient to allow them to penetrate several meters of rock before being stopped. The first measurements with muons to image large structures date from the 1950s.

During the passage of the muon through matter, energy is transferred from the muon to the electrons and nuclei in the traversed material. In this process the muon loses energy and changes direction. The latter process is known as multiple scattering. As a result, the muon either gets absorbed in the traversed material or comes out under an angle. The spectrum of the angles depends on the muon momentum and the material traversed. The spectrum of scattering angles depends on the charge number *Z* of the target material. Thus, muon tomography allows discriminating between low, medium and high-*Z* materials. Image reconstruction techniques and/or statistical analysis of muon tracks are performed to image objects.

There are two ways to utilize muons: one is to record the number muons absorbed in the material, which is known as radiography, and the other is to measure the scattering, which is known as muon tomography. The radiography is particularly relevant for the scanning of large objects like waste silos, while tomography is utilized for objects like waste drums up to cargo containers.

Tomography provides high resolution information, but it requires to measure the incoming and outgoing directions are recorded for each muon. Hence, the entire scanned volume needs to be placed in between detectors. During the passage of the muon through the material, the muon undergoes a random walk as a result of the multiple scattering. Many algorithms have been developed to analyse the data. The simplest is the Point of Closest Approach (PoCA). In this algorithm the point of closest approach of the incoming and outgoing track is calculated. The volume is divided into voxels and for each voxel the number of scatterings is counted, thereby producing a 3D image of the interior of the inspected objects. The performance of the PoCA algorithm is in general poor. A much better performing algorithm is the Maximum Likelihood/Expectation Maximization algorithm (Schulz, *et al.*, 2007). This algorithm estimates the material density in each voxel and then iterates on the material content of each voxel until the measured spectrum of scattering is reproduced. It is a very powerful algorithm.

Other commonly used algorithms include the Angle Statistics Reconstruction algorithm (Stapleton *et al.*, 2014) and the Binned Cluster Algorithm (Thomay *et al.*, 2013). The ASR algorithm treats the projected deflection angles for each scattering location as independent measurements, assigns a score list for each voxel based on the muon momentum and scatter angle and based on the scores calculates a final reconstruction value for each voxel. This algorithm is much less computing intensive than the ML/EM algorithm. The BCA algorithm was initially developed for the detection of smuggled high Z objects hidden in cargo containers. It exploits the degree of spatial clustering of muon scattering vertices. A higher density of vertices corresponds to higher-*Z* materials as strong muon scatterings take place with greater frequency in such materials. This makes the algorithm very sensitive for the detection of high Z and low Z objects in a matrix. Figure 7 shows a ROC curve for the detection of a $10\times10\times10$ cm^3 uranium cube hidden in a 20ft cargo container filled to the weight limit of the container with scrap iron. The graphs show that within two minutes of data taking, the presence or absence of a uranium block can be determined or excluded with a very high degree of certainty.

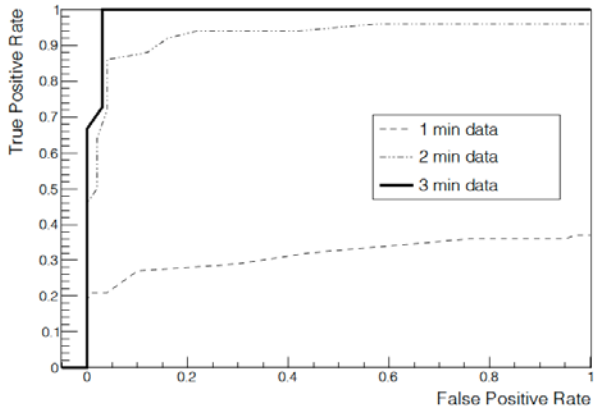

FIGURE 7 : ROC CURVE FOR THE DETECTION OF A 10×10×10 CM^3 CUBE OF A URANIUM CUBE HIDDEN INSIDE A 20 FOOT CARGO CONTAINER. TAKEN FROM THOMAY ET AL. (2013)

This technique can also be used to image nuclear waste drums. By using small voxels, the material content of each voxel and thus the entire waste drum can be determined. Figure 8 shows an image obtained using a muon flux equivalent to 2 weeks of data-taking, using bins of 1 cm side length. The cylindrical steel drum (diameter 26 cm, length 50 cm, with a steel flange at the top) is filled with concrete and contains dummy objects: a cylindrical U rod (1 cm radius, 10 cm height), a thin quadratic U sheet (0:5 10 10 cm3), three tungsten pennies of 1 cm thickness (1 cm, 2 cm, and 4 cm radius), and a cylindrical air enclosure with 5 cm thickness and 10 cm radius.

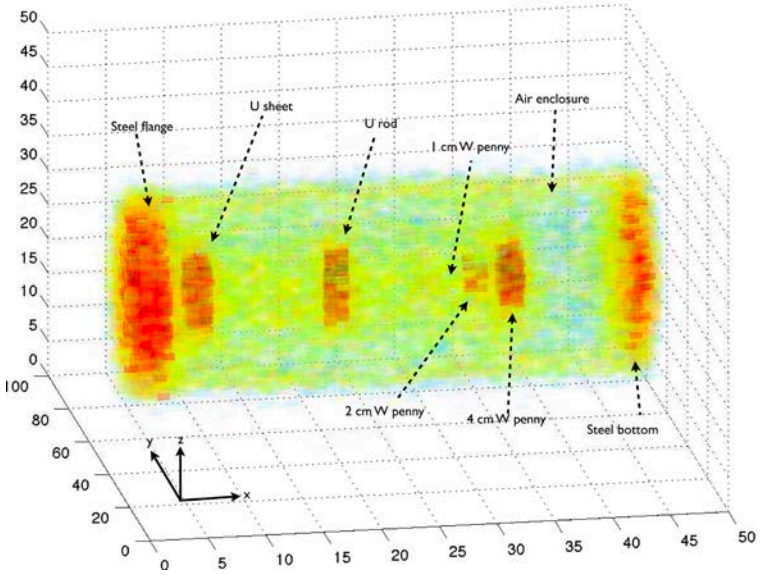

FIGURE 8 : WASTE DRUM 3D IMAGE PRODUCED WITH THE BCA. THE CONCRETE IS VISIBLE AS LIGHT YELLOW, AND DENSER OBJECTS ARE VISIBLE TOWARDS THE RED END OF THE SPECTRUM. AN AIR ENCLOSURE IS VISIBLE AS BLUE. ALL AXES ARE IN CM. TAKEN FROM THOMAY ET AL. (2016)

Since the scattering is dependent on Z, the technique can be used to identify materials as well. Using the same information, it is possible to distinguish between different materials. A study to distinguish between uranium and other heavy elements while inside concrete filled small nuclear waste containers was presented in (Frazão *et. al*, 2016). The waste drum was 40 cm long, with a 13 cm radius and is encased in steel with a thickness of 1.5 cm. Figure 9 shows the area under the curve for a ROC curve to distinguish between uranium and lead as function of time for different sizes of the objects. An AUC of 100% indicates perfect separation. Clearly, the objects can be distinguished after only a few hours of data taking.

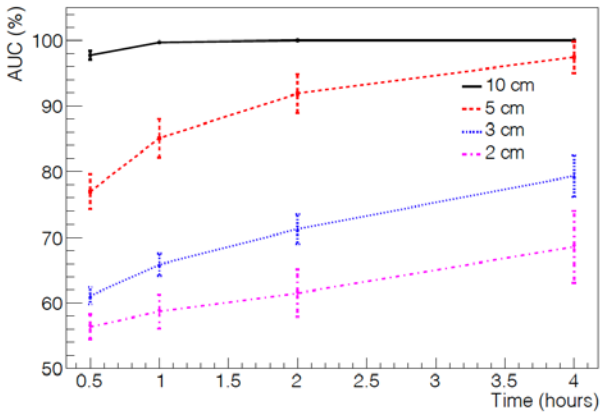

FIGURE 9 : AREA UNDER THE CURVE OF ROC CURVES DISTINGUISHING URANIUM FROM TUNGSTEN FOR DIFFERENT BLOCK SIZES. TAKEN FROM FRAZÃO ET AL. (2016)

A novel algorithm based on the BCA was used to improve the material identification using a multivariate analysis in the framework of Chance project. MVA classifiers trained on variables obtained from the distribution of the BCA metric values were shown to be effective at discriminating materials in waste drums. This was tested in a set of simulated drums containing 6 cm radius spheres of different materials (uranium, lead and iron) in randomly determined positions, the system performed with a true positive rate of $0.90^{+0.07}_{-0.12}$ and a false positive rate of $0.12^{+0.12}_{-0.07}$, in identifying uranium indicating this approach is effective at identifying uranium objects inside waste drums (Weekes, *et al.*, 2021).

The measurement resolution of the various algorithms is different and depends on the material inside the drum, their spacing, the exposure and object size. A comparison study performed in the framework of Chance project was published by (Stowell, *et al.*, 2019). An array of 8 cuboid uranium target objects was simulated, each with sides of 10 cm in the Y and Z dimension, see figure 7c. Starting at a X dimension of 3 cm, the thickness in the X dimension is then scaled by a factor of 75% for each successive target object, whilst the object spacing is kept fixed. Scanning from left to right, the number of observable features gives a metric for the smallest observable feature when objects are not in close proximity to one another. As shown in Figure 10, using 25 days of simulated muon exposure the PoCA algorithm is only capable of clearly resolving 5 objects, corresponding to a smallest observable object of 0.95cm, comparable to the voxel size. In contrast, the ASR and BCA both show much cleaner, rectangular features for all 8 objects, resolving the presence of a target object down to 4mm thickness.

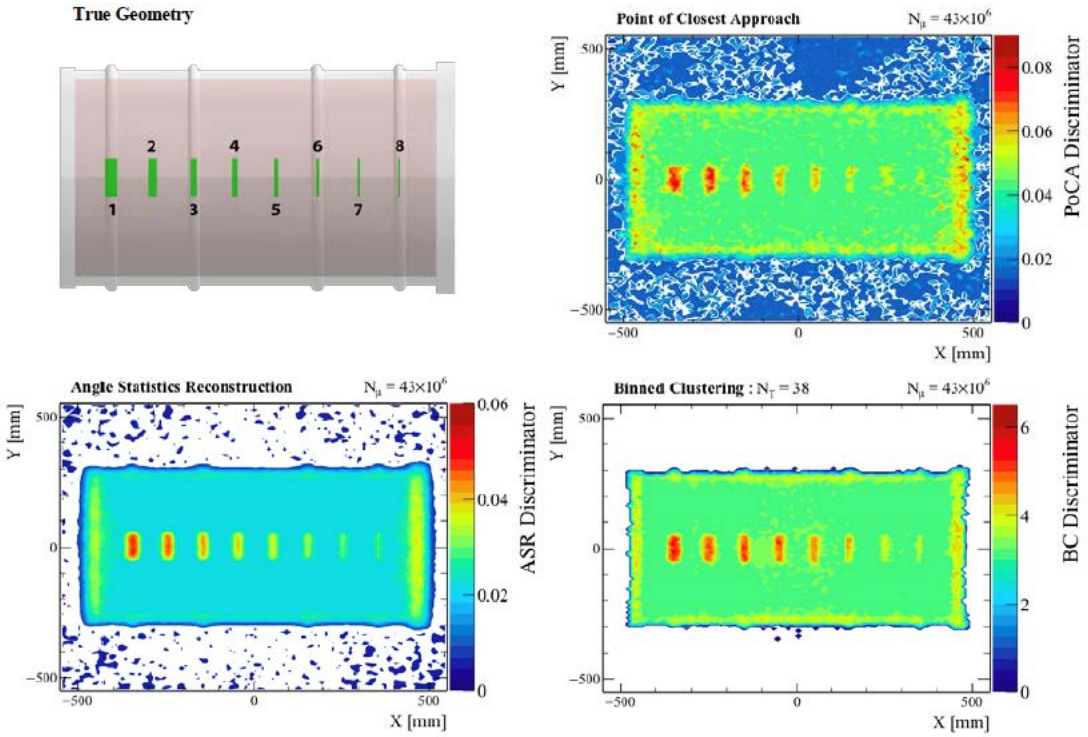

FIGURE 10: URANIUM SIZE RESOLUTION TEST IMAGES AFTER 25 DAYS OF SIMULATED COSMIC RAY EXPOSURE. THE NUMBER OF OBSERVABLE OBJECTS GIVES AN INDICATOR ON THE RESOLUTION OF EACH IMAGING TECHNIQUE. NOISE IN THE POCA ALGORITHM OUTPUTS MEANS IT IS DIFFICULT TO CLEARLY IDENTIFY THE FOUR SMALLEST TARGET OBJECTS. TAKEN FROM STOWELL ET AL. (2019)

Similarly, gas bubbles can be detected. The presence of gas bubbles in bituminized waste is a major challenge for nuclear waste storage. (Dobrowolska, *et al.,* 2018) exploited the BCA to detect gas bubbles in the framework of Chance. The scattering in the bituminized wastes is much higher than in the gas bubbles. As such, the matrix displays gaps where the bubbles occur. It is possible to precisely detect gas bubbles with a volume larger than 2 litres. The volumes of bubbles of two litres or more were measured with a relative uncertainty resolution of 1.55±0.77%. This is independent of the location and shape of the bubbles. Figure 11 shows the BCA matrix for different slices of a drum. The results for the two bubble scenarios are the same as the concrete filled drum except where the bubbles occur. Clearly two 2.2 litres bubbles can be distinguished from a single 4.4 litres bubble and the concrete scenario.

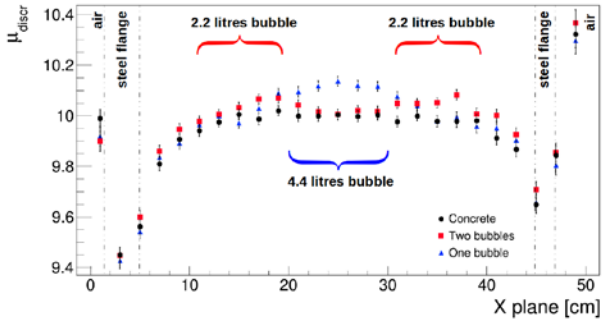

FIGURE 11: CONCRETE-FILLED DRUM WITH A 4.4 LITRES BUBBLE INSIDE (BLUE TRIANGLES) OR TWO 2.2 LITRES BUBBLES (RED SQUARES). TAKEN FROM DOBROWOLSKA ET AL. (2018)

Muon tomography is also very well suited for the imaging of large objects like CASTOR drums. There is a lot of activity in this field. The key challenge is the monitoring of dry storage casks for diversion of plutonium contained in spent reactor fuel. Several studies are published showing the differences caused by incomplete filling, i.e., missing parts of fuel rods, or replacement of the fuel rods by rods of a different material, see for example (Poulsen *et al.*, 2017), (Braunroth *et al.*, 2021) and (Durham *et al.*, 2018). Figure 12 shows a typical result, taken from (Alrheli *et al.*, 2020) acquired in the framework of Chance project. The non-standard filled baskets are behaving very different from the normally filled ones. (Poulsen *et al.*, 2017) reports that missing fuel bundles can be detected with a sensitivity of 5% missing portion of a fuel bundle.

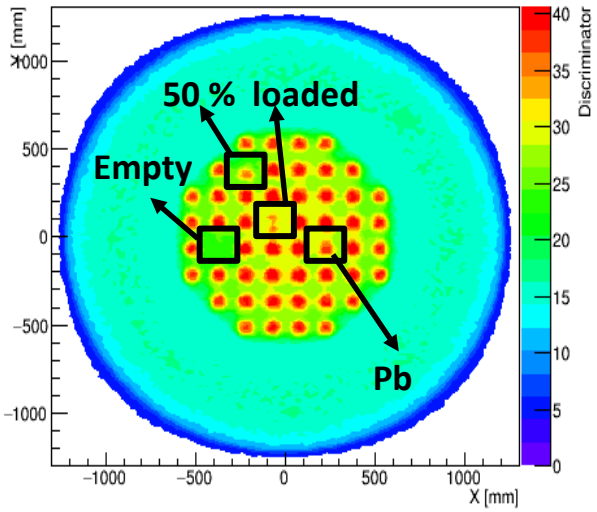

FIGURE 12: TOP VIEW OF A RECONSTRUCTION STUDY OF A CASTOR DRUM USING MUON TOMOGRAPHY. FOUR BASKETS ARE DEVIATING FROM THE OTHERS: ONE IS EMPTY, TWO ARE FILLED WITH EITHER HALF A ROD AND ONE IS FILLED WITH A FULL SIZE LEAD ROD. THESE FOUR BASKETS ARE CLEARLY DIFFERENT FROM THE BASKETS FILLED WITH RODS. TAKEN FROM ALRHELI ET AL (2020)

Many groups have been building muon tomography systems for waste characterization. Examples include (Morris *et al.*, 2008), (Checchia *et al.*, 2019), (Simpson *et al.*, 2020), (Jo *et al.*, 2015) and (Kopp *et al.*, 2020). Figure 13 shows the system developed in Chance project as published by (Kopp *et al.*, 2020). As mentioned before, for muon tomography both the incoming and outgoing muon trajectory need to be measured. This requires covering the object under inspection on both sides. As muon tomography relies on reconstruction of the scattering angle, the key parameter for the detector system is the angular resolution of the upper and lower detector system. As such, a poor hit position resolution can be compensated for by increasing the distance between the measurement planes. That typically requires large area detectors. Due to cost reasons, these detector systems are either gaseous (Morris *et al.*, 2008) and (Kopp *et al.*, 2020) or scintillation detectors like for example (Simpson *et al.*, 2020) and (Jo *et al.*, 2015). Several types of gaseous detectors are in use: resistive plate chambers (RPC), drift chambers and drift tubes are the most common. There are two types of scintillator-based detectors in common use. One uses large scintillator plates with wavelength shifting fibres attached to provide position information. A second type exploits plates of scintillating fibres. All aforementioned technologies provide large area detector systems with good performance for reasonable cost.

FIGURE 13: THE MUON SCATTERING TOMOGRAPHY DETECTOR SYSTEM OF THE CHANCE PROJECT. SHOWN ARE THE DETECTOR SYSTEMS ABOVE AND BELOW THE EMPTY SAMPLE SPACE CONSISTING OF THREE LAYERS OF DRIFT CHAMBERS AND TWO RPC LAYERS. THE TOP STACK ADDITIONALLY CONTAINS TWO LAYERS OF PLASTIC SCINTILLATORS USED AS TRIGGERS. THE DETECTORS COVER AN AREA OF APPROXIMATELY 1.8×1.8M^2

Muon tomography for nuclear waste is still a rapidly developing field. Current efforts are aimed at several main topics concerning legacy waste: monitoring smaller and smaller gas bubbles in bituminized waste, spotting small cracks in waste drums and improvement of material identification. Bubbles in bituminised waste are a major safety concern. It is important to study the development of these bubbles and how they conglomerate and grow over time. Concrete filled waste drums can display cracks. These cracks can be small and superficial or go all the way from top to bottom of a drum. Small superficial cracks are not a problem, but large and deep cracks can form a safety concern. Measuring crack depths and sizes will become an important target for muon tomography. Furthermore, there are many activities ongoing addressing the challenges of large waste drums and silos. These are large objects that are too large for tomography and radiography algorithms need to be developed or improved to extract as much information out of the data as possible. Examples include precise imaging of the contents of CASTOR drums; not only to verify that the fuel rods are present, but also their structural integrity and imaging the contents of waste silos.

3.5 Neutron radiography

Neutron radiography is, until now, not routinely applied on radioactive waste packages and results of previous R&D projects did not show convincing results (Bücherl *et al.*, 2017), probably related to both the low neutron flux used in these projects, and the low spatial resolution. To investigate the general applicability of fission neutron radiography for the non-destructive characterization of radioactive waste packages, a feasibility study was initiated with the NECTAR fission neutron facility (Figure 14) (which offers neutron fluxes up to 4.7×10^{7} $cm^{-2}s^{-1}$) of the Technical University of Munich (TUM) (Bücherl *et al.*, 2017). For this feasibility study, several mock-up drums were used bearing different typical, but non-radioactive matrices (PE grains, bitumen, concrete, supercompacted pellets, lead-shielding containers and heavy concrete – densities ranging from 1 g/cm³ up to 4.6 g/cm³), as well as a specially designed mock-up drum simulating raw waste.

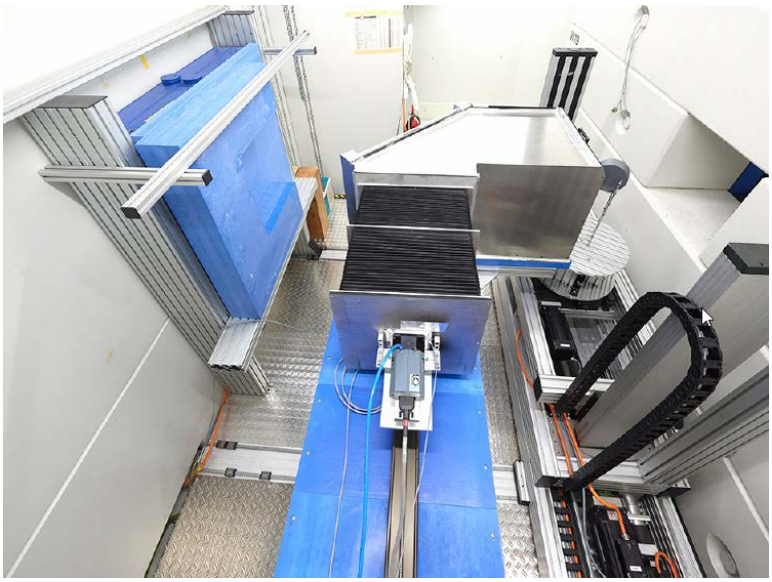

FIGURE 14: INSTRUMENT NECTAR: THE FISSION NEUTRONS ARE COMING FROM THE RIGHT, PENETRATING THE SAMPLE FIXED ON THE MANIPULATOR, AND ARE DETECTED BY A CCD-BASED SYSTEM (CENTER). A BEAMSTOP (LEFT) MINIMIZES SCATTERED RADIATION (BÜCHERL AND SÖLLRADL, 2015)

To compare neutron radiography with more currently used techniques, all samples were also measured by a tomography system using ^{60}Co (activity 2.1×10^{13} Bq) as transmission source (Bücherl *et al.*, 2017). Results showed that fission neutron radiography, and therefore fission neutron tomography too, of 200-l (radioactive) waste drums is possible, provided that a minimum neutron fluence of about 10^{7} cm^{-2} at the detector plane is achieved (Figure 15). Further improvements are needed regarding image processing and image quality.

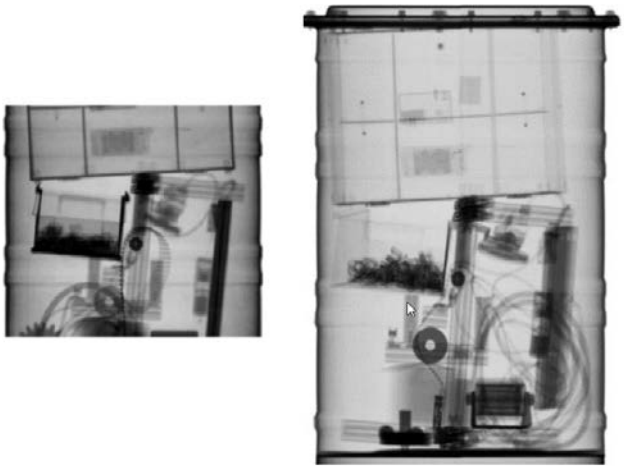

FIGURE 15: RADIOGRAPHIES OF A MOCK-UP DRUM USING FISSION NEUTRONS (LEFT) AND 60CO (RIGHT) AS TRANSMISSION SOURCE, RESPECTIVELY (BÜCHERL ET AL., 2017)

4. Passive gamma radiation measurements

For many organizations, the priority is the research and development of new non-destructive methods capable to detect the radiological (including difficult-to-measure alpha and beta emitters) and fissile mass content with an acceptable uncertainty, compatible with the waste acceptance criteria (WAC) for storage, transportation and final disposal. Ideally, these methods should be able to be applied in homogeneous and heterogeneous waste in packages of different sizes.

Passive non-destructive measurements refer to those methods consisting in measuring the radiation emitted spontaneously by the radioactive materials. In case of characterization of radioactive waste, gamma methods are effective when a measurable amount of gamma photons are able to penetrate the package to be measured (IAEA, 2007). In conditioned radioactive waste, very low energy gamma photons (or X rays) and beta and alpha emitters cannot be detected by this method (for instance long-lived radionuclides such as ^{36}Cl, ^{129}I, ^{41}Ca, ^{10}Be, but also the low energy 59.54keV gamma line of ^{241}Am). These difficult to measure radionuclides are therefore often scaled to an easily measured gamma emitter such as ^{60}Co or ^{137}Cs (see also section 6). Also radionuclides that decay by positron emission (e.g. ^{22}Na) are often detected by measuring the 511 keV annihilation photons with gamma instrumentation. If there is no measurable gamma emitter present in the wastes, then gamma measurement will not be suitable as a characterization method.

4.1 Dose rate measurements

Dose rate measurements are the simplest form of passive measurements and several types of detectors are readily available on the market, including Geiger-Müller counters, ionization chambers, and (NaI) scintillation counters. In order to convert dose rate to radiological inventory, dose conversion factors need to be determined, for example by comparing equivalent dose rate measurement to results from gamma spectrometry. Application of conversion factors can only be achieved successfully when the considered waste stream is stable in time (no change in isotopic vector), when the waste form content and activity distribution are sufficiently homogeneous, and when measurements are performed using the same procedure for all drums.

Dulama *et al*. (2010) developed a mathematical model for dose rate estimation of quasi-homogeneous batches of spent ion exchange resins and liquid radioactive wastes, to optimize quantities of waste per unit volume of conditioned waste form, in order to meet the acceptance criteria for transport and final storage. The main contributors to dose rate were gamma emitting radionuclides like Mn-54, Co-60, Co-57, Sb-124, Sb-125, Zn-65, Cs-134 and Cs-137. Model validation was performed for a set of 23 conditioned spent ion exchange waste drums which also characterized by gamma ray spectrometry (Figure 16). Dose rate was measured with a hand held device (factory set to achieve a 15% relative uncertainty in direct reading mode) at contact with the side of the waste drum. The selected representative value for the dose rate at contact was the average of readings registered at the half-height on the side of the waste drum. Main discrepancies were found due to internal inhomogeneities of the waste form which can alter both the dose rate measurement and spectrometric results.

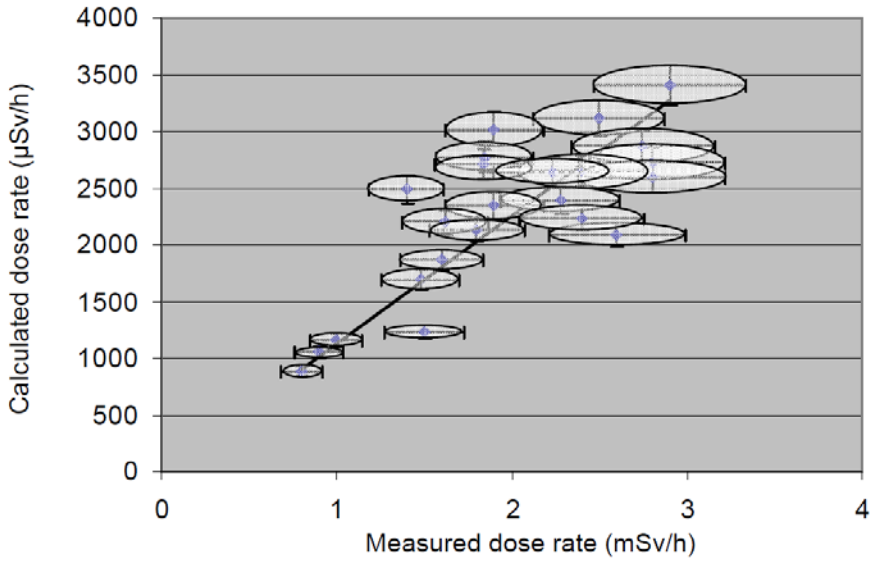

FIGURE 16: CALCULATED VERSUS MEASURED DOSE RATE WITH THEIR ASSOCIATED UNCERTAINTIES (DULAMA ET AL., 2010)

Abd *et al*. (2016) calculated the dose conversion factor for Cs-137 contaminated waste (soil) packed in metallic drums by comparison with gamma spectrometric data (figure 12). They measured the dose rate at multiple points on the drum surface and calculated the average for these measurements. In a follow-up study, Sabeeha *et al*. (2017) examined the dose rate assessment for dummy waste drums containing metallic waste (15-20%), encapsulation material and ^{137}Cs gamma point sources placed at different distances from the outer wall. The detection system was a NaI-type hand held device with 40% efficiency of gamma-ray at 0.661 MeV, in contact with the outer side of the waste package.

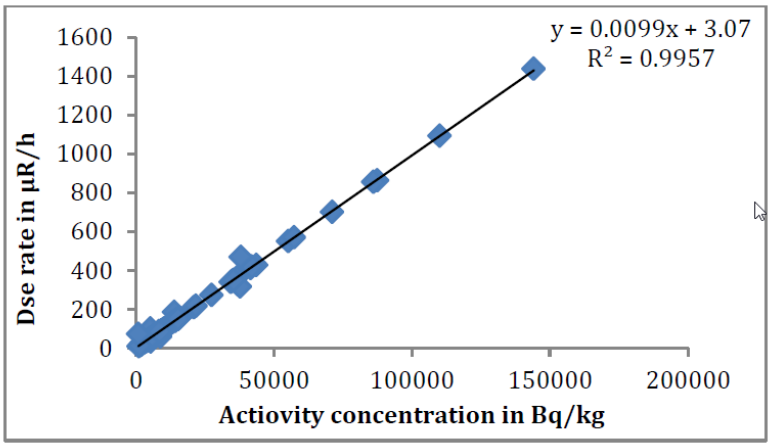

FIGURE 17: RELATION BETWEEN DOSE RATE AND ACTIVITY CONCENTRATION (ABD ET AL., 2016)

Sabeeha *et al*. (2017) report on dose rate measurements using a NaI detector for the acceptance of radioactive waste generated from decommissioning operations for transport, storage and disposal based on national regulations. They used dummy 220 L carbon steel waste drums in which metallic pieces contaminated with ^{137}Cs were conditioned with cement matrix to verify and calibrate the methodology.

4.2 Gamma ray spectroscopy

Gamma rays (γ-rays) are the highest-energy form of electromagnetic radiation due to their shorter wavelength. Because of this, the energy of γ-ray photons can be resolved individually, and a γ-ray spectrometer can measure and display the energies of the γ-ray photons detected. Gamma spectroscopy detectors are passive materials that are able to interact with incoming gamma rays. The most important interaction mechanisms are the photoelectric effect, the Compton effect, and pair production. Radionuclides commonly emit gamma rays in the energy range from a few kV to ~10 MeV, corresponding to the typical energy levels in nuclei with reasonably long lifetimes. Such sources typically produce γ-ray "line spectra" (i.e., many photons emitted at discrete energies). An example of such a spectrum is given in Figure 18.

Ideally, the recorded peaks should be very narrow but in practice, peak broadening occurs due to statistical fluctuations in the detection process and the noise added by the processing electronics (*Pérot et al., 2018*). The energy resolution mainly depends on the detector and reflects its ability to separate different gamma emitting isotopes at neighbouring energies. On the other hand, also the detection efficiency needs to be taken into account. The detection efficiency links the surface of the observed peak on the spectrum with the corresponding activity of the radionuclide in the waste, and depends on the energy of the gamma radiation, its attenuation in the measured object, the type of detector selected (material, density) and its useful volume (*Pérot et al., 2018*). Efficiency determination can be carried out by means of radioactive standards having the same size and composition of the object to be measured, or numerically with computer codes simulating the transport of X-ray and gamma photons, or by a combination of these.

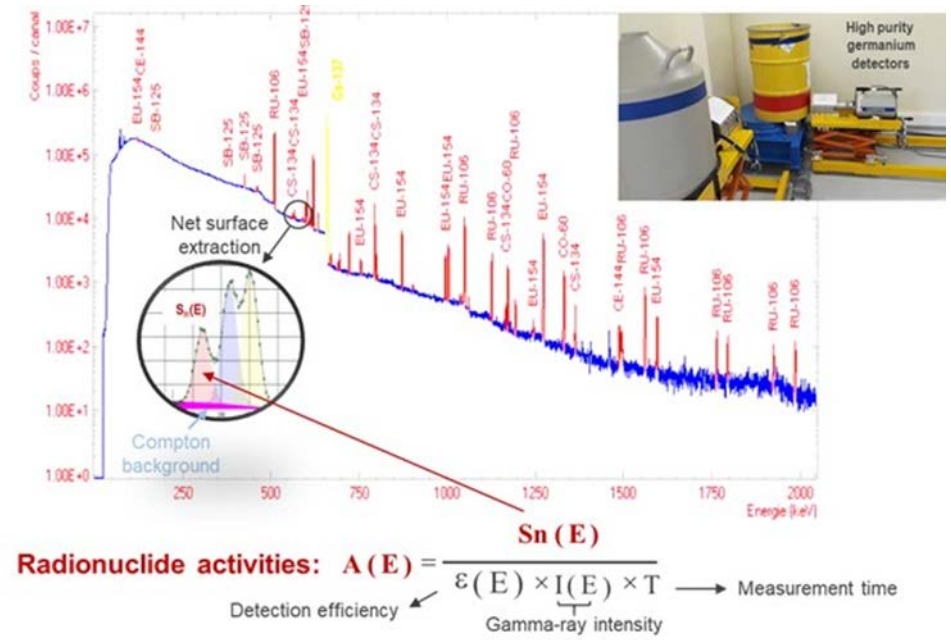

FIGURE 18 : A TYPICAL RADIOACTIVE WASTE GAMMA SPECTRUM ALLOWING NUCLIDE IDENTIFICATION (BASED ON PEAK ENERGIES) AND QUANTIFICATION (BASED ON NET AREAS). THE PICTURE SHOWS A DUAL DETECTOR GAMMA-RAY SPECTROSCOPY BENCH USED FOR "SUPER CONTROLS" IN CHICADE FACILITY, CEA CADARACHE, FRANCE

The standard system used for γ-ray spectroscopy consists of a detector which is able to measure the photons emitted by the radionuclides and delivers a signal proportional to the energy, which is then analysed and classified in the form of a histogram called a gamma spectrum (Pérot *et al*., 2018). A typical laboratory γ-ray spectroscopy setup using a Thallium-doped sodium iodide *NaI(Tl)* scintillator and a photomultiplier tube is shown in Figure 19. The scintillator converts the γ-ray photons into visible light photons, which are detected by the photomultiplier tube. The source and the detector are positioned such that most of the γ-ray photons from the source reach the scintillator. All scintillator systems are sensitive to changes in temperature, causing shifts in the spectrum on the horizontal axis. Scintillator detectors, whether inorganic (NaI, CsI, LaBr, BGO) or organic (plastic or liquid), can generally be manufactured in large volumes (notably NaI and plastics) but display generally poor energy resolution. They are therefore often used for low intensity photon flux measurements with simple gamma spectra. However, since most scintillators are very fast (signals of the order of nanoseconds), they can also be used at high counting rates or for coincidence counting (*Pérot et al., 2018*).

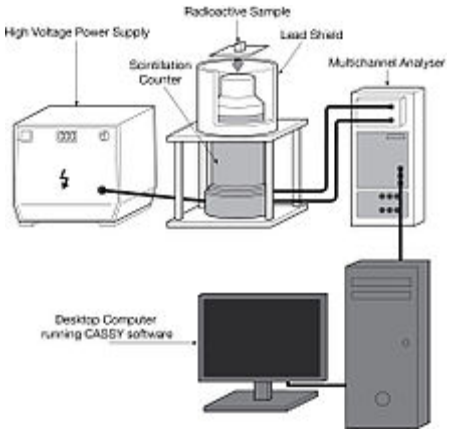

FIGURE 19 : LABORATORY EQUIPMENT FOR DETERMINATION OF Γ-RADIATION SPECTRUM WITH A SCINTILLATION COUNTER (SOURCE: WIKIPEDIA HTTPS://EN.WIKIPEDIA.ORG/WIKI/GAMMA_SPECTROSCOPY)

Semiconductor-based detectors or solid-state detectors are fundamentally different from scintillation detectors and rely on detection of the charge carriers (electrons and holes) generated in semiconductors by energy deposited by gamma ray photons. Common semiconductor-based detectors include hyper-pure germanium (HPGe), cadmium telluride (CdTe), cadmium zinc telluride (CdZnTe), silicon and GaAs. HPGe detectors provide significantly improved energy resolution in comparison to sodium iodide detectors and produce the highest resolution commonly available today. They allow to distinguish the numerous gamma and X-ray lines emitted by the nuclear material, and to deduce their isotopic composition. However, a disadvantage is the requirement of cryogenic temperatures for their operation. CdTe and CdZnTe detectors have a spectral resolution slightly better compared to scintillators, operate at room temperature and have crystals of very small size which enable them to withstand intense photon fields (*Pérot et al., 2018*).

Gamma spectroscopy is typically affected by Compton scattering. This arises because of primary gamma rays undergoing scattering within the detector, before depositing all of their energy. This leads to the presence of continuous Compton distributions in the recorded spectra, or to the recording of energies lower than those of the incident gamma ray. To reduce these effects, an anticoincidence shield can be used, which is referred to as Compton suppression.

Gamma spectrometry techniques are commonly applied to estimate the activity of Easy-To-Measure nuclides (ETM), such as Co-60 or Na-22, in waste, because their minimum detectable activity is generally below declaration thresholds for low- and intermediate-level waste (Dyrcz *et al.*, 2021). ETM are radionuclides which can be measured via non-destructive assay techniques (such as passive gamma spectrometry). Besides this, it is also relatively simple and inexpensive to use (Pérot *et al.*, 2018; Anh and Dung, 2001).

In spite of this simplicity and its wide-spread use, the determination of radioactive isotope masses by gamma ray spectrometry is often flawed due to the unknown waste matrix gamma ray attenuation, self-absorption due to the radioactive material itself, the drum-to-detector distance, and sensitivity to isotopes positions (Carasco, 2021; Anh and Dung, 2001). These large uncertainties frequently are translated into conservative approaches to estimate and declare isotope masses in order to stay on the safe side regarding waste acceptance criteria. However, such overestimations might also lead to non-optimal waste management routes, higher costs or even over-designed waste repositories.

4.2.1 Global measurement of waste containers

Gamma spectrometry is frequently used to measure waste packages because it can meet the characterization requirements for a wide range of very different types of containers (bins, drums, concrete packages), physico-chemical properties, volume, activity level, isotopic spectrum and localization of radioelements (Pérot *et al*., 2018). However, the measurement technique may also suffer from the attenuation of the radiation in the material, as well as from the (activity) heterogeneity of inspected packages or objects. For dense materials like concrete (2-3 g/cm³), the measurable depth of matrix is only a few cm for the gamma emissions of the major radioactive isotopes (50 keV to 2 MeV).

Done *et al*. (2014) describe the use of gamma spectrometry for the characterization of the radiological content of conditioned radioactive waste drums before final disposal. They employ gamma spectrometry with a HPGe detector to characterize the final conditioned steel drums, which consist of a 100 L drum placed in a concrete shielded 200 L drum. Efficiency calibration on this type of drum was performed using different geometrical configurations of cylindrical standard Eu-152 sources distributed in different positions in a dummy concrete matrix drum in order to simulate situations as close as possible to real waste container configurations. Measurements were accompanied by activity calculations considering a homogeneous distribution of activity in the 100 L drum, the remaining volume of 200 l being considered as concrete shield. Results showed that, depending on the actual configuration of the sources, efficiencies between ~ 40 and 100% were obtained. The biggest deviation was observed for a geometrical case in which the Eu-152 sources were all concentrated in one (central) hole, while the activity calculations considered a homogeneous distribution.

Several recent papers describe the use of gamma spectroscopy measurements to characterize (low level) waste stemming from accelerator facilities, and the particular steps taken to overcome difficulties and uncertainties associated with the analysis of such materials. Rimlinger *et al*. (2020) report on the qualification of gamma spectrometry measurement for the radiological characterization of mixed VLLW cables in particle accelerators. Due to the different types of cables used in terms of material composition, source distribution and density, the variations in efficiency calibration curves necessitated the development of a new qualification methodology to establish more accurate activity values with their corresponding uncertainties. Dyrcz *et al*. (2021) reported on the qualification of a gamma spectroscopy measurement calibration (HPGe detector) of LILW waste stemming from activation mechanisms in accelerator machines. Because of their origin, this waste is typified by non-regular shapes and heterogeneous activation patterns (“hot spots”), which can lead to underestimation of radionuclide activities (Frosio *et al*., 2020). Therefore, Dyrcz *et al*. (2021) studied different geometry models for four faces of a particularly shaped sample to quantify the impact of assuming homogeneous distribution (figure 15). Mirion Technologies’ ISOCS (In Situ Object Counting System) and LabSOCS (Laboratory Sourceless Calibration Software) software (incorporating MNCP Monte Carlo simulations) were applied for creating efficiency calibrations. The ISOCS Uncertainty Estimator (IUE) developed equally by Mirion Technologies was used to improve the quality of the gamma spectrometry uncertainty estimate. In order to estimate the impact of heterogeneous source distribution contrast on the activity results, geometry models are simulated by varying the hot spots dimensions, locations, and source relative concentrations. From this set of geometry models, an uncertainty analysis is performed using the GURU (Geometry Uncertainty Reduction Utility) data analyser framework (Frosio *et al*., 2020). Results showed that using detector average results of multiple faces was recommended over limiting to one side gamma spectrometry measurement.

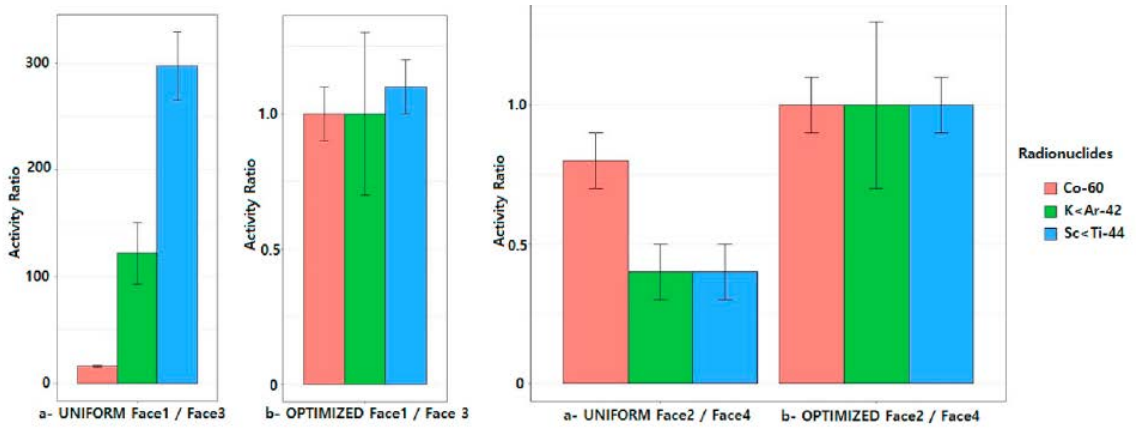

FIGURE 20 : ACTIVITY RATIO FOR PAIR OF DETECTORS FACES 1 AND 3, AND FACES 2 AND 4, BEFORE AND AFTER GEOMETRY OPTIMIZATION (DYRCZ *ET AL.*, 2021)

Exercises such as reported by Done *et* al. (2014) and Dyrcz *et al*. (2021) demonstrate that there is a need to optimize global gamma measurements. For optimization, the detector height and distance between the germanium crystal and the waste package can be adjusted according to the physical characteristics of the package determined by high-energy photon imaging (height, dimension and position of the waste within the matrix) and of its contact dose rate previously measured (Pérot *et al*., 2018).

Different commercial installations (both mobile and static) are available on the market, by suppliers such as ORTEC (www.ortec-online.com), NUKEM Technologies (https://www.nukemtechnologies.de/en/) or Mirion Technologies (www.mirion.com). These systems also frequently come with their own software for spectrum acquisition and analysis.

4.2.2 Segmented measurements

By means of a collimator reducing the field of view of the detector, the determination of activity can be perfected. In these focused measurements, the package can be scanned by means of a system of movement (translation, rotation, elevation) of the package or the detector. In gamma scanning measurements, the collimator has an opening angle that allows the measurement of a complete slice in the width of package which is scanned vertically (Pérot *et al*., 2018).

Segmented gamma scanners (SGS) are relatively widely available within nuclear facilities worldwide (Metz and Hogenbirk, 2017). They are now considered as a traditional technique and has been used in a lot of practical cases (Anh and Dung, 2001).

Bai *et al*. (2009) report on an improved method to quantify the activity of spatially concentrated gamma-emitting isotopes (“hot spots”) in heterogeneous waste drums measured by segmented gamma scanning. Indeed, generally it is assumed that the matrix and activity are uniformly distributed in each measured drum segment. Corrections for gamma attenuation are performed by estimations of density by drum weighing or by calculated corrective factors based on assumptions for average density and activity distribution. Because uncertainties related to the heterogeneity of waste drums, both in terms of matrix composition and activity distribution, are introduced using such standard correction procedures, Bai *et al*. (2009) developed a new method based on numerical simulations of the measured angular dependent count rate distribution during drum rotation. This method was then validated through the measurement of Cs-137 and Co-60 activities in 13 real waste drums and by comparing the method with conventional measuring methods.

To improve the reliability and accuracy of the calculation of isotope specific activities in SGS, Krings and Mauerhofer (2012) describe an improved method to quantify the activity of spatially concentrated gamma-emitting isotopes (point sources or hot spots) in heterogeneous waste drums containing internal shielding structures, based on numerical simulations and fits of the angular dependent count rate distribution recorded during a rotation in SGS (Figure 21). The segmented gamma scanning methodology used for a 200L drum (height of 80 cm and radius of 28 cm) consists of scanning in 20 segments of 4 cm height; each segment is scanned while rotating in steps of 30°, leading to 12 sectors per segment. The counting time per segment is about 12 s, leading to a total scan time of about 1 h.

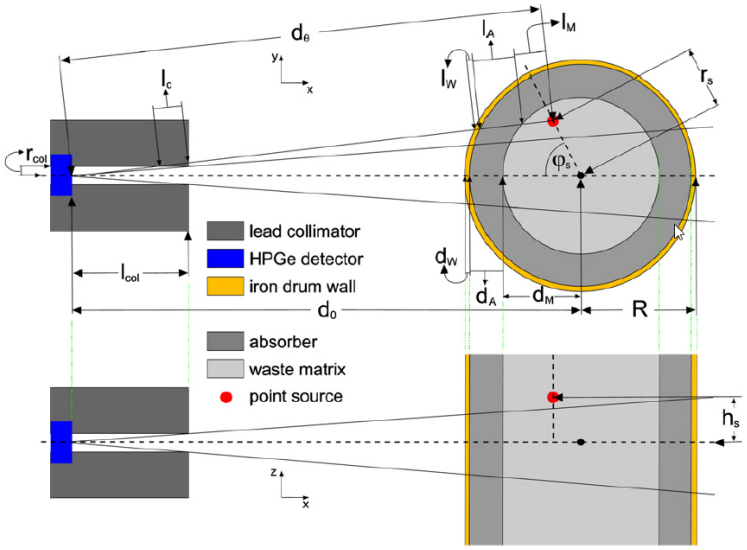

FIGURE 21 : GEOMETRIC MODEL OF THE EXPERIMENTAL SETUP USED FOR SEGMENTED GAMMA SCANNING. THE UPPER PART SHOWS THE TOP VIEW AND THE LOWER PART SHOWS THE SIDE VIEW OF THE COLLIMATED DETECTOR WITH A DRUM SEGMENT CONTAINING AN ACTIVITY POINT SOURCE (KRINGS AND MAUERHOFER, 2012)

Patra *et al*. (2019) developed a methodology for performing SGS of low/intermediate alpha activity-containing 200 L waste drums without the use of a standard drum of identical geometry, which is difficult in the case of lab-generated waste which is inherently inhomogeneous by nature. The methodology relies on the full energy peak (FEP) efficiency, determined using a standard ^{152}Eu point source of 1 mCi (Figure 22). The point source was placed at various radial positions during the scanning, allowing to obtain the efficiency at each radial arrangement. FEP efficiency was seen to depend both on general matrix attenuation and on lump attenuation. An infinite energy extrapolation of apparent mass approach has been adopted to resolve the problem of inaccurate attenuation correction.

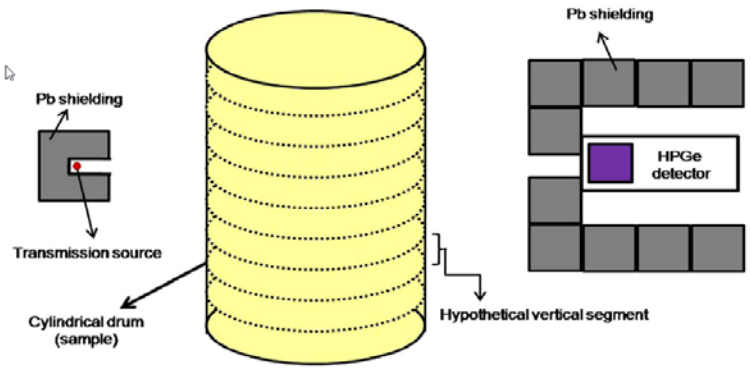

FIGURE 22 : SCHEMATIC DRAWING OF THE SGS SET-UP (PATRA *ET AL.*, 2019)

4.2.3 Emission and gamma tomography

Emission tomography relies on a collimation reduced to a segment of the package and requires a horizontal scan coupled with angular acquisitions, making it possible to reconstitute the spatial distribution of the activity in the tomographic section (Figure 23). This operation can be repeated in different sections to reconstruct the 3D activity of the waste. The tomographic reconstruction step requires knowledge of the gamma attenuation by the materials in the waste container and therefore complementary photon transmission measurements.

Tomographic gamma scanning (TGS) was developed to measure residues containing special nuclear material and transuranic waste (Hansen). Because a wide range of arbitrarily distributed isotopes must be quantified and the composition and distribution of matrix materials are generally unknown, these materials are extremely difficult to assay. TGS systems have been portrayed as the ideal tool for non-destructive measurement of heterogeneous radioactivity distributions (Croft *et* al., 2006; Venialgo *et al*., 2012). A TGS system combines high resolution gamma ray spectroscopy, a low spatial resolution collimator, a transmission source, and an image reconstruction algorithm to characterize radioisotope distributions. In this kind of scanner, a three-dimensional image of activity distribution for a selected photo peak is produced. The difference between TGS and a segmented gamma-ray scanner (SGS) is the addition of a translation axis that allows the detector to view the sample along all possible lines that pass through it rather than just through the radial centreline as in the SGS technology (Hansen). There is always a trade-off between improved accuracy and sensitivity (higher image spatial resolution), and throughput.

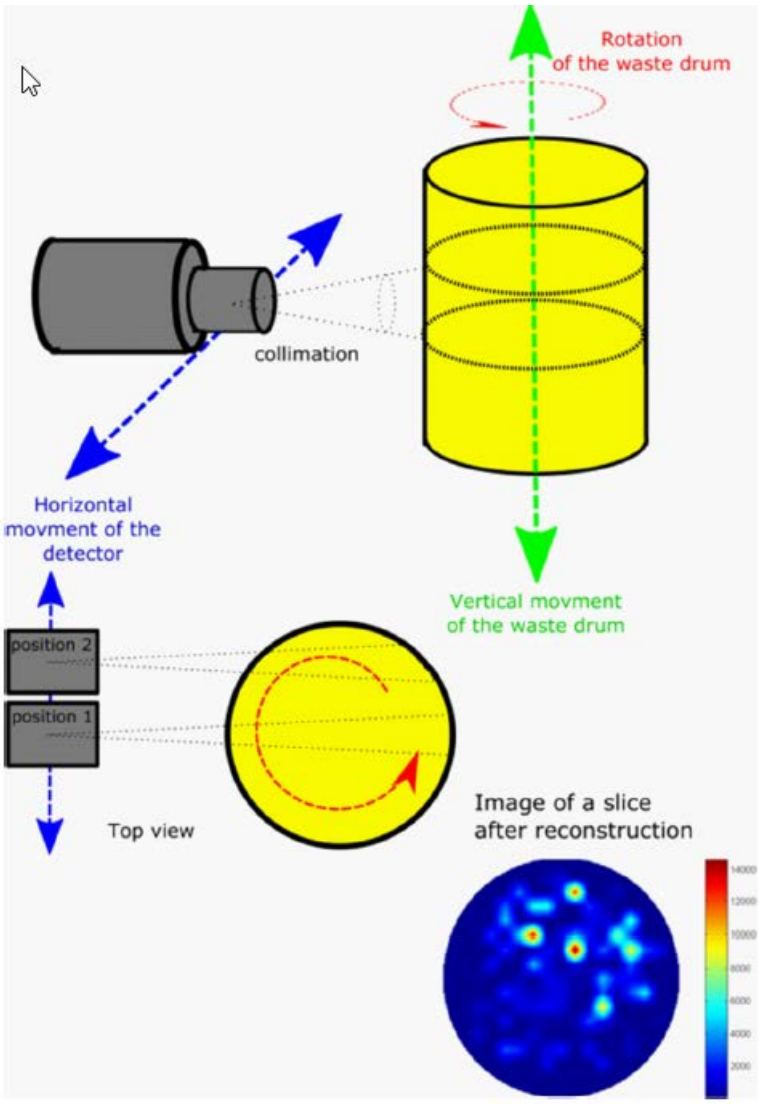

FIGURE 23 : PRINCIPLE OF GAMMA EMISSION TOMOGRAPHY (PÉROT *ET AL.*, 2018)

Development of TGS technology began in the early 1990's (Hansen, Martz *et al.*, 1996). At LLNL, an active & passive (A&PCT) system was developed that enabled to identify all detectable radioisotopes present in a container and measure their activity, allowing to certify radioactive or mixed wastes when they are below the TRU threshold, determine if they meet regulations for LLW, and certify TRU wastes[2] for final disposal (Martz *et al.*, 1996). The objective from the onset was to improve the accuracy of the assay by exploiting imaging technology (Croft *et al.*, 2006). The LLNL system utilized an active ^{166m}Ho isotope source and a well-collimated single high-purity Germanium (HPGe) detector system, as well as a three-axis drum manipulator capable of

[2] TRU (Transuranic) Waste as defined by WIPP is waste containing radioactive constituents with an atomic number greater than 92, a half-life greater than 20 years and concentrations exceeding 100 nano-curies per gram of waste (Hansen)

translating and elevating a waste drum as well as rotating it through 360 degrees. Other gamma sources (such as ^{75}Se) can be used as well (Hansen).

The A&PCT system produces two- and three-dimensional internal images of containers contents nonintrusively. It requires an active CT measurement using gamma-rays at different energies to map the unknown waste matrix in a drum, revealing the attenuating objects. A passive CT measurement locates and identifies any detectable radioisotopes present within the drum. Using a combination of the two measurements, it is possible to correct the measured radioactive intensities for attenuation caused by the drum contents. These corrected passive intensities provide an accurate quantitative absolute measure of the source strength of all detected internal radionuclides (Martz *et al.*, 1996). TGS allows to view the sample as a composite of small volumes combined with a means of estimating the mass of the target isotopes within each small volume.

(Venialgo *et al*., 2012) examined the resolution and sensitivity of three collimator shapes utilizing a Monte Carlo application. The influence of the energy resolution of HPGe, CZT, NaI(Tl) detectors in the radioisotopes discrimination was also studied. An exhaustive bibliography of tomographic gamma scanning methods applied to waste assay and nuclear fuel measurements can be found in Croft *et al*. (2006).

4.2.4 Innovations in gamma-ray spectroscopy

We mention below just a few examples of ongoing R&D topics but as gamma-ray spectroscopy is the most widely used non-destructive technique, this technology (detectors, electronics, and data processing) is in continuous improvement, allowing higher energy resolution, higher count rates, higher detection efficiency or very compact detectors, etc. The consequences of these performance improvements is the possibility to develop new spectroscopic systems and methods.

4.2.4.1 Compton Suppression Spectrometer

In the frame of the UTM project related to the characterization of radioactive bituminized waste packages (Artaud *et al*., 2001), the CEA has studied an HPGe detector equipped with an optimized Compton Suppression Spectrometer (CSS). A BGO veto detector surrounding the germanium crystal allows detecting escaping photons following Compton scattering, and thus to reject such events from the HPGe gamma spectrum with an anti-coincidence electronics. This CSS was optimized to improve the measurement of low energy rays, especially those of ^{241}Am at 59.5 keV, as shown in Figure 24: the large Compton continuum due to the scattering of ^{137}Cs gamma rays (661.7 keV) is divided by a factor of 6 at 59.5 keV, which greatly improves the detection of the ^{241}Am gamma ray.

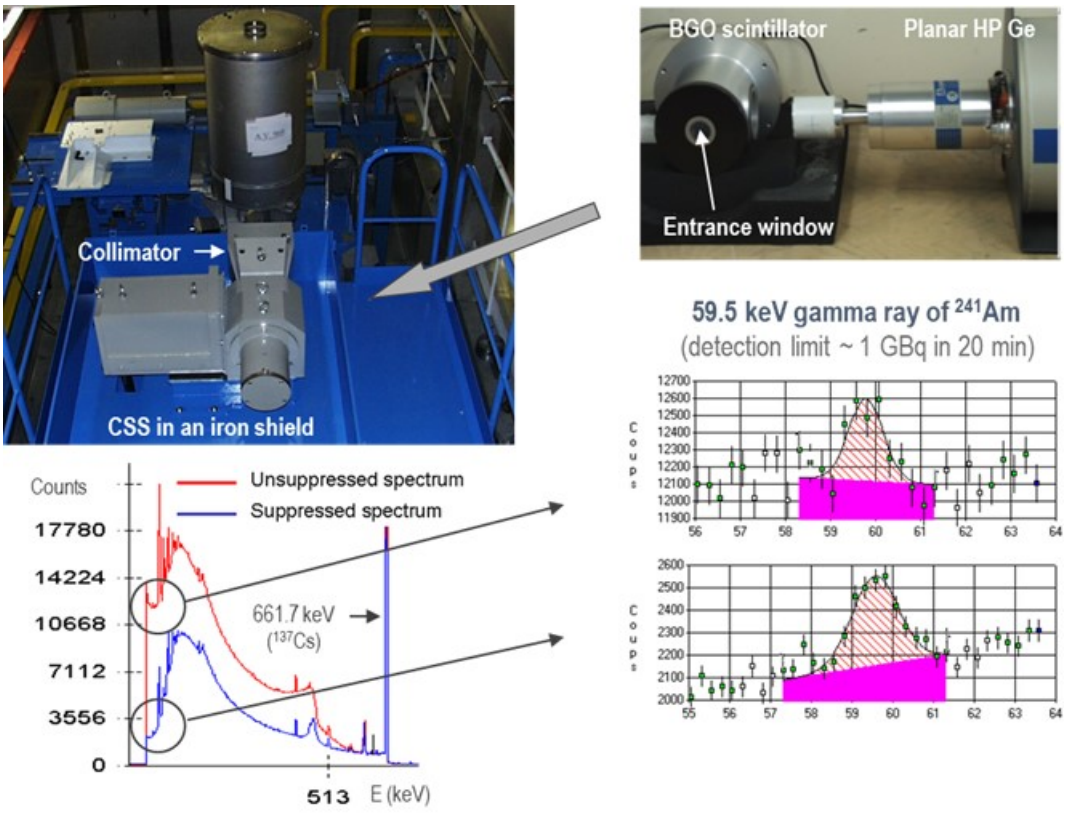

FIGURE 24 : COMPTON SUPPRESSION SPECTROMETER OPTIMIZED FOR ^{241}AM DETECTION IN BITUMINIZED WASTE DRUMS WITH A PREDOMINANT ^{137}CS ACTIVITY (ARTAUD *ET AL.*, 2001)

4.2.4.2 Radium and uranium mining waste

In the frame of CEA - ORANO Mining collaboration aimed at improving the sensitivity and precision of radiometric uranium measurements for mining exploration and exploitation, innovative patent-pending low- and high-resolution gamma spectroscopy methods have been developed allowing the characterization of uranium ores in short measurement times. These methods based on HPGe (high resolution) or NaI (low resolution) detectors could easily be adapted to the measurement of radium bearing waste or for uranium mining residues (samples, conveyor belt, canisters, or bulk dump).

The new proposed methods exploit uranium X-ray fluorescence in order to reduce measurement time and improve accuracy (Marchais *et al.*, 2018). Gamma radiation from radioactive isotopes of the natural uranium decay chain, such as ^{214}Pb and ^{214}Bi, create a large Compton scattering continuum beyond the K-absorption discontinuity at 115.6 keV, resulting in a large photoelectric absorption rate and, subsequently, in the emission of uranium fluorescence X-rays. Uranium fluorescence K lines, in the 100 keV region, are representative of the uranium concentration up to a depth of a few centimetres, which is particularly interesting for small samples and drill cores. The intensity of self-fluorescence depends on the activity of the radioactive isotopes present in the ore, which can be directly quantified by gamma spectrometry from their characteristic lines, and on the density and mineralogy of the ore. In addition to uranium content, it is possible to detect a heterogeneity, for instance a uranium nugget, by comparing the ^{234}Th passive emission line at 92 keV and the uranium $X_{K\alpha 1}$ fluorescence line at 98 keV (Marchais *et al.*, 2018). In parallel to high resolution gamma spectroscopy, another low-resolution approach with a NaI(Tl) scintillator is used to characterize the uranium content and potential imbalances between uranium and its radioactive daughters, such as the main gamma emitters ^{214}Pb and ^{214}Bi. This second

approach is based on the analysis of broad energy areas of the NaI gamma spectrum, instead of narrow peaks with HPGe, see Figure 25.

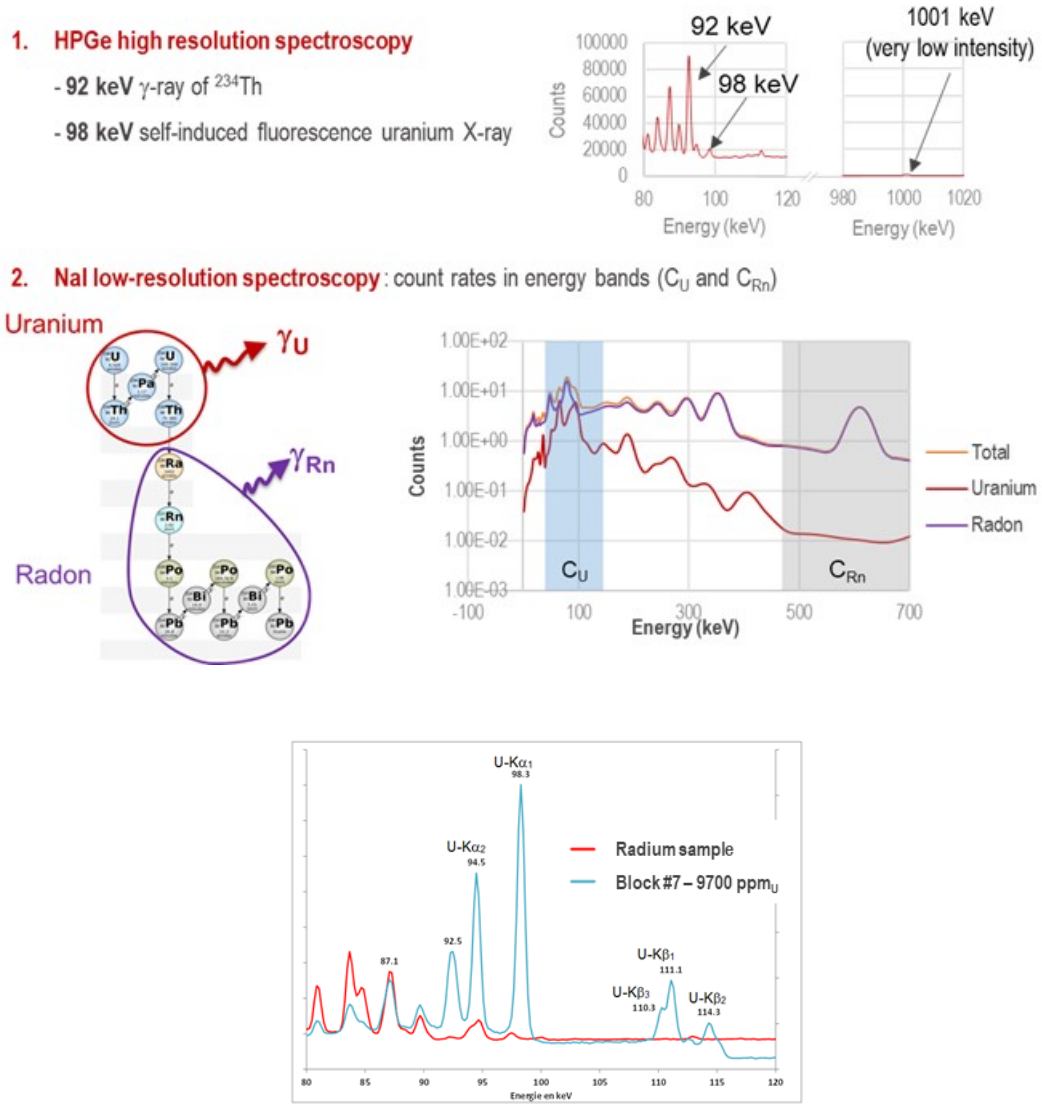

FIGURE 25 : HIGH- AND LOW-RESOLUTION GAMMA SPECTROSCOPY APPROACHES FOR URANIUM ORE CHARACTERIZATION. THE BOTTOM SPECTRUM SHOWS SELF-INDUCED FLUORESCENCE X-RAYS OF URANIUM, IN COMPARISON WITH A PURE RADIUM SAMPLE (MARCHAIS *ET AL.*, 2018)

4.2.4.3 HPGe spectra analysis based on a probabilistic approach

Many software are commercially available to analyse HPGe gamma spectra. However, some difficulties remain when full energy peaks are folded together with a high ratio between their amplitudes, when the Compton background is much larger compared to the signal of a single peak and when spectra are composed of a great number of peaks. Therefore, Rohée *et al.* (2015) has developed a new probabilistic approach called SINBAD. Contrary to conventional methods based on peak fitting (e.g. with Gaussian functions), SINBAD uses

nonparametric Bayesian inference to process the gamma spectrum data to improve peak centroid estimation (for radionuclides identification) and net peak area determination (for activity estimation) (figure 15).

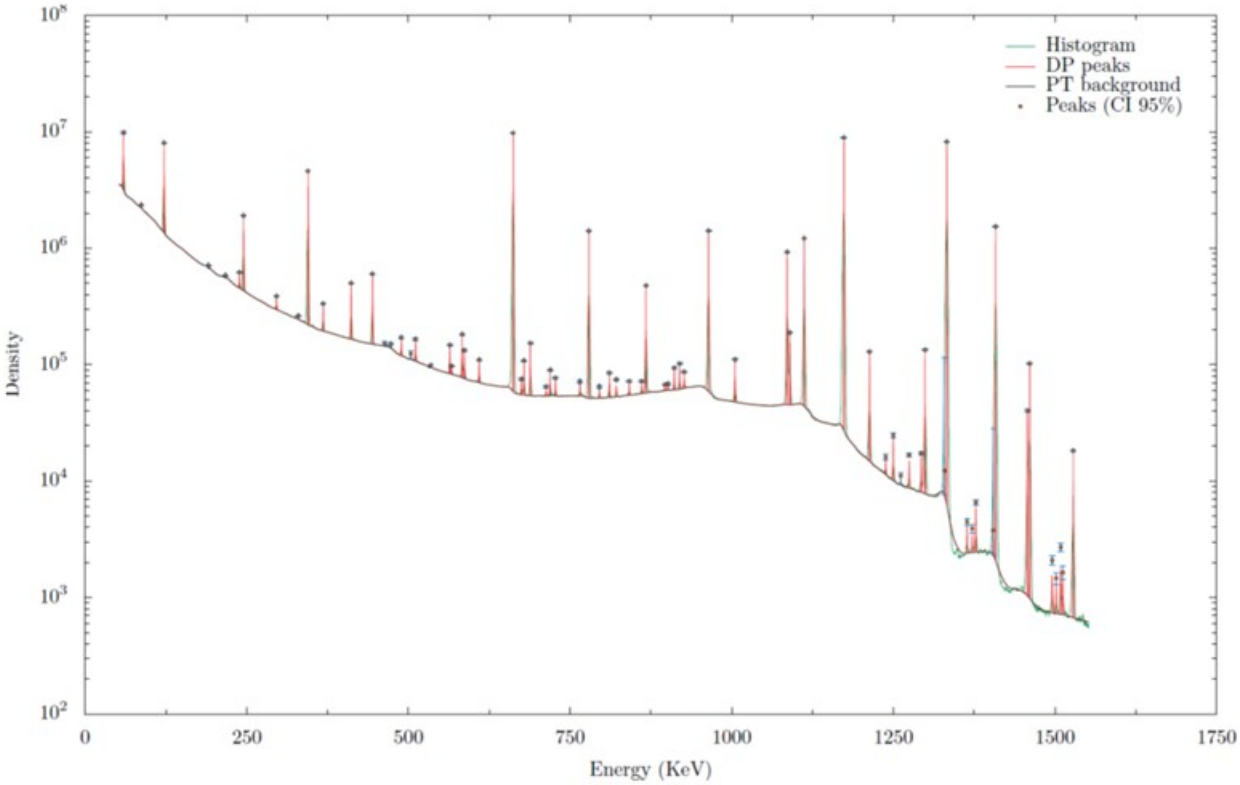

FIGURE 26 : GAMMA SPECTRUM OF ^{60}CO, ^{137}CS, ^{152}EU AND ^{241}AM SOURCES ANALYSED WITH SINBAD: IN GREEN THE MEASURED SPECTRUM, IN BLACK THE CONTINUUM FIT BY SINBAD, IN RED THE DIRAC PEAKS CORRESPONDING TO GAMMA RAYS FOUND BY SINBAD, WITH HEIGHTS (POINTS) CORRESPONDING TO THE NET PEAK AREAS AND ERROR BARS CORRESPONDING TO 95 % CONFIDENCE INTERVALS (I.E. 2σ UNCERTAINTIES) (ROHÉE *ET AL.*, 2015)

4.2.4.4 Radiological analysis for radioactivity depth distribution

During decommissioning of reactors and accelerator facilities, concrete structures form a substantial part of the generated radioactive waste. Radioactive concrete is divided into contaminated concrete and activated concrete.

Lee *et al*. (2021) analysed radioactivity depth distribution in activated concrete by measuring ^{152}Eu using the Peak to Compton (PTC) method by means of a high-purity germanium (HPGe) detector. The PTC method compares the full energy peak of the spectrum and the count rate of the Compton continuum. Experimental results on activated concrete in cyclotron facilities agreed within a 3% relative error with results of MCNP simulations, and within 20% relative error or less compared with sample analysis.

4.2.4.5 Applicability of other detectors than HPGe

The identification and quantification of radionuclides by means of (segmented) gamma scanning relies on the separation of their characteristic gamma peaks in measured spectra. The detectors used in such a setup therefore need to exhibit sufficient energy resolution to identify the key radionuclides expected in radioactive wastes. Currently, most systems are equipped with high purity germanium (HPGe) semiconductor detectors. However, other detectors might provide similar energy resolution while also improving higher detection efficiencies and better timing properties (reduction of dead time) than HPGe detectors. Göbbels *et al*. (2015) studied the applicability of cerium doped lanthanum bromide ($LaBr_3$(Ce)) detectors in the non-destructive characterization of radioactive waste drums and came to positive results. The avoidance of a cooling system (as is required for HPGe detectors) in such detectors would also economize maintenance costs as well as reduce the size and weight of the detection system, allowing the construction of mobile detection systems.

5 Neutron counting

Neutron counting is sometimes necessary particularly in characterizing nuclear materials whose gamma emission is masked by that of more intense emitters such as fission or activation products, or for the purpose of obtaining complementary information and reducing measurement uncertainties, such as those linked to the attenuation of gamma and neutron radiation in packages (Pérot *et al*., 2018).

A synopsis of (passive) neutron assay systems was performed as part of the ENTRAP (European network of testing facilities for the quality checking of radioactive waste packages) project (Bücherl and Lierse von Gostomski, 2001), summarizing the basic principles of operation, the required equipment and the layout of a system.

5.1 Principle of neutron measurements

The main objective of passive neutron assay is to prove the presence of neutron emitters within a waste package. Since neutron emission spectra of different isotopes measured outside the waste package do not show characteristic differences, an isotope specific identification and quantification is generally not possible and quantification is performed in terms of $^{240}Pu_{equiv}$ mass (Bücherl and Lierse von Gostomski, 2001). However, using time correlation methods (TCM) a general distinction and quantification between spontaneous (sf) and (α, n)-reaction neutron sources is possible. The design of a passive neutron assay system and the choice of the most appropriate equipment must be adapted to the type and size of the waste packages to be characterized.

Neutrons cannot be detected directly and therefore nuclear reactions are used to convert neutrons in energetic charged particles like photons, α-particles, etc. These secondary particles then can be detected using conventional radiation detectors. For the neutron assay of waste packages, conventionally thermal neutron detectors are used. Neutron detectors can be simple counting tubes or one- or two-dimensional position sensitive detectors, typically using ^{3}He as conversion material. Position sensitive detectors offer the possibility of segmented neutron counting. In most current operating systems, ^{3}He-counting tubes are used, although BF_3-counting tubes, fission chambers and Gd- or B-loaded scintillation detectors can also be applied.

Apart from a neutron detector system, a neutron assay system also consists of:

- a moderator, typically polyethylene, which slows down the neutrons allowing more effective detection using thermal neutron detectors ;
- background shielding, to eliminate background signals;
- a manipulator, allowing, e.g., segmented neutron counting;

- a control unit, controlling both the movements of the manipulator system and the measuring process;
- a data evaluation unit, allowing to perform the quantification of the neutron emitting material present in the waste package;
- optional additional equipment (e.g., turntable, transmission source, time correlation method systems, etc.)

The reader is referred to (Bücherl and Lierse von Gostomski, 2001) for more information on these aspects.

The results of passive neutron measurements are count-rates, their quantification conventionally based on the assumption of a homogeneous distribution of the neutron emitters and of the matrix. This conventionally applied procedure usually results in a conservative calculation of the $^{240}Pu_{equiv}$ mass. In order to convert the net count rate to the $^{240}Pu_{equiv}$ mass, a transfer or correlation factor is determined, either experimentally or by mathematical calculations.

To calibrate neutron assay systems, dummy waste packages with well-defined compositions and activity contents (preferably similar to the waste packages to be characterized), are measured and evaluated.

5.2 Total neutron counting

Total neutron counting is an integral measurement and the simplest measuring mode in passive neutron assay, summing up the signals of all individual detectors. During the measurement, the waste package may be rotated to increase the fraction of waste package surface "observed" by the neutron detectors. This manipulation also levels out small inhomogeneities of the neutron emission-rate distribution on the surface of the waste package.

The evaluation of this type of data is only representative and reliable for a nearly homogeneous distribution of the neutron emitters within the waste package and a nearly homogeneous matrix (Bücherl and Lierse von Gostomski, 2001).

5.3 Segmented neutron counting

Segmented neutron scanning (SNS) allows to determine the distribution of the neutron emission-rates on the surface of the waste package. For this purpose, the waste package surface is subdivided into equidistant segments, and each segment subdivided into sectors. For each sector, the neutron emission rate is determined by either (2-dimensional) position sensitive detectors, or by a special arrangement of vertical and horizontal neutron detector tubes in combination with an appropriate manipulation (rotation) of the waste package. A subsequent deconvolution of the measured data results then in a set of data giving information on the distribution of the neutron emission rate on the waste package surface (Bücherl and Lierse von Gostomski, 2001).

The application of this configuration allows to verify the assumption of homogeneity required for applying the total neutron counting evaluation procedure, and the detection of hot spots.

5.4 Time correlation methods

To separate the neutron emission rates from sf- and (α, n)-reactions, time correlation methods need to be applied. In these methods, the signals of all individual detectors are summed up and fed into a special time correlation method system. Several methods are known for this like, e.g., the shift register method, neutron coincidence counting (NCC) and neutron multiplicity counting (NMC). The shift-register method has proven to be acceptable for low-density material waste packages, but often fails for dense matrices. NCC, which needs information on the matrix properties, and NMC have shown their applicability both for light and dense matrices.

Passive NCCs assay nuclear materials that contain spontaneously fissioning isotopes: the assays are based on coincident neutrons that are naturally emitted by these materials. NCCs are well suited for measuring dense materials containing ^{238}Pu, ^{240}Pu, and ^{242}Pu, often in the form of fuel plates and pins, powder, pellets, scrap and waste. NCCs are also suitable for mixtures of uranium and plutonium oxide and kilogram quantities of ^{238}U. NCCs work well in areas with a high neutron background because background neutrons are not coincident.

While NMC is self-calibrating and, hence, does not require a priori information on the matrix properties, its application is limited to $^{240}Pu_{equiv}$-masses of at least 100 mg, and is furthermore strongly sensitive to background effects. During measurement, the waste package may be rotated to level out inhomogeneities of the neutron emission-rate distribution on the surface of the waste package (Bücherl and Lierse von Gostomski, 2001).

6 Activation calculations, scaling factor, isotope vector

The scaling factor (SF) method is an experimental method (IAEA, 2009) used to quantify the activity of difficult-to-measure (DTM) radionuclides (IAEA, 2007) such as pure beta-emitters, in radioactive waste packages. The method relies on the collection of a representative sample from the waste population, the measurement of the activities of the DTM radionuclides and the major easy-to-measure (ETM) radionuclide (IAEA, 2007), called key nuclide (KN), and the establishment of a correlation function between those activities. If such a function exists, it is possible to evaluate the activity of the DTM radionuclides on a waste package by scaling the measured activity of the key nuclide via a so-called scaling factor (Zaffora *et al*., 2020). However, the uncertainties on the isotopic vector or scaling factor could be important and induce a major uncertainty on the inferred activity of non-measurable radionuclides. Measurement methods for tracers include dose rate measurements and gamma spectrometry.

In the simplest case, the scaling factor is a scalar. However, the characteristics of a waste population can change over time. For instance, this happens when new radioactive waste is produced with different radiological properties, or when the half-lives of DTM and KN are different (Zaffora *et al*., 2020). A number of statistical methods are available for taking into account the time dependence of the scaling factors as well as for updating them when new data is available. Zaffora *et al*. (2020) present a Bayesian framework to update and control scaling factors based on new data sets showing time evolutions of the waste population.

Computer simulations based on Monte Carlo methods can be used to obtain information on activation of structures inside nuclear facilities by using the facility floor plan and operation information. Although this method has few restrictions, it requires a variety of input values, which can reduce accuracy due to input value errors (Cha *et al*., 2016).

Jang *et al*. (2017) report on activation calculations for the concrete shielding of a cyclotron facility that is used for radiopharmaceutical isotopes production. Their calculations highlight the importance of impurities in the concrete matrix. The presence of (small, ppm-level) impurities caused an approximately 98% higher exposure dose compared to calculations which did not take such impurities into account. Also the main contributing isotopes to the dose were completely different.

Frosio *et al*. (2020B) report on the development of a software package which allows characterizing waste packages from different waste types originating at CERN, directly from gamma spectroscopy reports without needing anymore hand-made calculations. The waste involves mostly activated cables and activated metallic waste (as VLLW in the French waste classification scheme). The radioactive waste is generally conditioned in 1.35 or 2.77 m^3 packages and shipped to the repository in 20 feet containers half-height (Figure 27). The characterization process is performed by means of gamma spectroscopy measurements (Figure 28) and scaling factors. The list of predicted radionuclides and scaling factors are estimated and radiochemical analyses performed on representative random samples. More than 1500 possible activation scenarios were analysed using Monte Carlo simulations. Two lists of predicted radionuclides and scaling factors sets are computed in order to better describe the waste containing short- or long-lived radionuclides:

- One set used for the characterization of waste with decay times from 6 months to 3 years, to characterize waste at exit of accelerators,
- The other set used for the characterization of wastes with decay time from 3 years to 30 years, to characterize historical waste.

The paper further describes the entire process to eliminate the VLLW from the side (covering waste treatment, traceability, radiological characterization, as well as the quality control program) in order to meet the acceptance criteria of the final repository, and to fulfil the ANDRA requirements for the acceptance of the waste.

FIGURE 27 : CONTAINER 20 FEET HALF HEIGHT LOADED WITH ACTIVATED CABLES (LEFT) AND ACTIVATED METALLIC (RIGHT) WASTE (FROSIO *ET AL.*, 2020B)

FIGURE 28 : GAMMA SPECTROSCOPY PERFORMED IN A DEDICATED AREA FOR IN-SITU MEASUREMENTS. THE WHITE MARKS ON THE FLOOR REPRESENT THE LOCATION OF THE 1.35 M³ PACKAGE. TWO HPGE DETECTORS ARE USED TO EVALUATE THE GAMMA EMITTERS RADIONUCLIDES IN THE PACKAGE (FROSIO *ET AL.*, 2020B)

For reasons of occupational exposure, but also in view of the management of radioactive waste, the complete spectrum of radioactive isotopes expected to be present in certain facilities needs to be accurately assessed. Hajdu *et al*. (2021) studied the activation of concrete to be used as a shielding material in the European Spallation Source (ESS) by means of both MCNP simulations and experimental studies. In this study, the importance of knowledge on trace element concentrations inside the concrete materials is highlighted in order to obtain realistic input data for the simulations. Indeed, certain of these trace elements can be expected to be the dominant source of neutron induced radiation due to their particularly high cross sections for neutron activation (Tesse *et al*., 2018; Hajdu *et al*. (2021)). To this end, concrete compositions were determined via an array of different techniques including X-ray fluorescence (XRF), prompt gamma activation analysis (PGAA) and neutron activation analysis (NAA).

7 Calorimetry

Calorimetry is an experimental technique employed in the measurement of the thermal power generated by heat-producing substances (Mason, 1982). This technique finds application in a variety of fields including scientific research, medicine, industry, military research and microbiology.

Calorimetry has been successfully applied in the nuclear industry for the accurate quantification of nuclear matter contained in drums for inventory or classification purposes. It is a Non-Destructive Assay (NDA) technique that consists in precisely measuring the thermal power generated by the nuclear decays within the radioactive matter and relate it to the specific power of the isotope to deduce the mass of the assayed matter.

Several prototypical or commercial instruments are currently in operation in different research centres around the world (CEA-France, Lawrence Livermore National Laboratory – USA, AWE-UK, BARC-India).

7.1 Characteristics of calorimetry

Calorimetry is suited for nuclear materials that generates heat by alpha and beta particle decays in the range of thermal power spanning from 0.001 W to 135 W. It is mainly used for the assay of Plutonium and ^{241}Am (either as a single isotope or mixed with Plutonium). Calorimetry can be coupled with a spectroscopic technique when the sample contains different isotopes.

Calorimetry measurement technology is characterized by the following advantages compared to other NDA techniques **(**Bracken, 2002**)**:

- Very high precision (from ~0.5% for low power items (≤0.2 W) to ~0.1% for items dissipating more than 1 W). Higher precision is attainable when the isotopic composition of the item can be determined with another NDA technique.
- Measurement is performed on the entire mass (low dependency on the spatial distribution of the source).
- Impossibility to shield the power generation. Once a steady state condition is reached, the whole power generated by the item under test is completely evacuated by the measurement chamber, regardless of the packaging of the item.
- Measurement result is independent from material matrix composition and geometry (only assay time is affected).
- Answer is not affected by self-attenuation effects.
- The calibration of the instrument is standardized and can be verified when necessary.

On the other hand, the calorimetric method is affected by the following limitations:

- The measurement accuracy can be degraded in case of materials with inhomogeneous isotopic composition, because of the uncertainty in the determination of the effective specific power.
- The calorimetric assay features longer measurement time compared to other NDA techniques. Even if the packaging of the source does not affect the measurement accuracy, it can though affect the measurement time.
- It usually requires a very large equipment for accurate measurement results. Because of the relatively low power rates of nuclear samples and the large volume under test, usually the overall dimensions of a standard equipment can be important.
- If heat is produced by reactions others than nuclear, this cannot be discriminated by the calorimeter and this will affect the measurement accuracy.

In its very basic configuration, a calorimeter is composed by the following components (Figure 29):

- **The measurement chamber**: where the sample is placed for measurement
- **A temperature sensor**: for the continuous monitoring of the temperature inside the measurement chamber
- **Thermostated heat sink**: this part of the calorimeter represents the reference temperature for the measuring system. It can be furnace, a thermostatic bath, a combination of both or a different solution. The heat sink is maintained at a certain temperature TF, set by the user and measured by a suitable temperature sensor. Ideally, the heat sink will maintain a uniform temperature TF throughout its volume no matter the value of thermal energy exchanged by the sample.

- **Thermal resistance**: this is the resistance of thermal path connecting the measuring chamber to the heat sink. The thermal resistance is one of the main characteristics to distinguish the operation of the different types of instruments.
- **Environment**: this is the part of the world that accommodate the instrument. It must be taken into account in the design and operation of the calorimeter for obtaining the best performance.

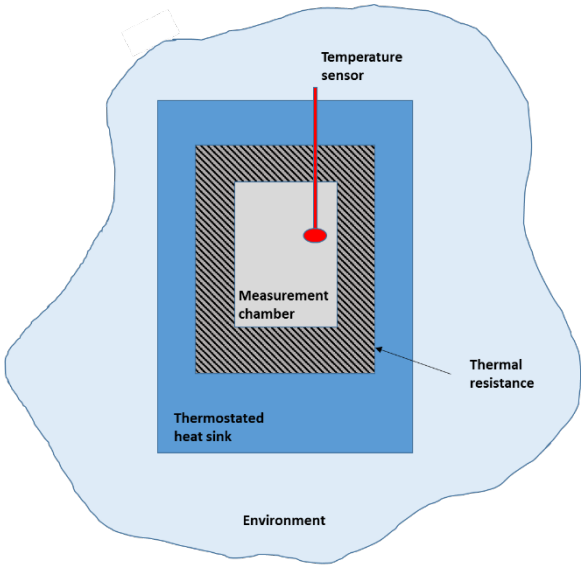

FIGURE 29 : SCHEMATIC DESIGN OF A CALORIMETER

7.2 Types of calorimeters

Instruments for calorimetry can be subdivided according to the principle of heat measurement adopted (Kemp, 1988). In the ideal **adiabatic calorimeter**, the measurement chamber is surrounded by a perfect thermal insulation, thus the heat flow between the measurement chamber and the heat sink is zero. The thermal power generated by the sample under assessment is contained within the measurement chamber, increasing the temperature of the chamber. The final temperature of the sample in the measurement chamber can be related to the thermal power generated through a calibration factor (the apparent heat capacity of the sample).

This instrument is adapted for sample generating finite amount of thermal power. For samples with continuous thermal power generation (e.g. radioactive samples), the temperature increase would be indefinite. This setup is thus not adapted for nuclear applications.

In the **compensation calorimeter**, the measurement chamber is maintained at a constant temperature (isothermal operation). In order to achieve this, the power exchanged by the samples must be promptly compensated to avoid any temperature increase within the sample. The most used technique nowadays is the compensation of the power produced by the sample by electric means. If thermopiles are used for this, endothermic effects can also be compensated by reversing the current in the same thermopile.

In the heat conduction calorimeter, a continuous and stable heat flow is maintained between the measurement chamber and the heat sink by keeping the measurement chamber at a temperature higher than the heat sink. This heat flow is continuously monitored by measuring the temperature difference between the measurement

chamber and the heat sink for example using thermopiles installed between the sample and the heat sink but other techniques may also be employed.

For nuclear applications, the heat conduction calorimeter is usually operated in the Isoperibol mode, where the temperature of the heat sink is kept constant, but other operations mode are also possible (scanning mode, modulated mode).

The thermal power generated by the samples is detected as a change in the heat flow between the measurement chamber and the heat sink.

The output of the heat flow sensors is first measured without any heat producing sample: the output curve obtained in this configuration is called baseline. Once an active sample is introduced in the measurement chamber, the output of the sensors changes in an exponential fashion until it reaches a plateau (Figure 30). The output voltage difference between the baseline and the new stabilization plateau is proportional to the thermal power generated by the sample via the instrument calibration factor, which is experimentally obtained during the qualification of the equipment.

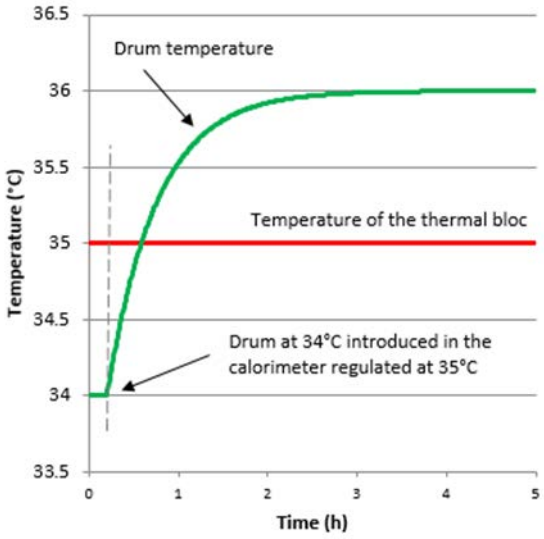

FIGURE 30 : TYPICAL OUTPUT SIGNAL OF A HEAT-FLOW CALORIMETER

The heat-flow calorimeter configuration is one of the most used techniques for the characterization of radioactive samples with calorimetric techniques.

An example of a heat flow calorimeter for large volume nuclear applications is KEP Technologies LVC 1380 calorimeter (Jossens, 2015), based on the Calvet design **(**Calvet, 1948**)**. The measurement cell is completely surrounded by thermoelectric modules that measure the heat flow from the measurement chamber to the external heat sink.

7.2.1 The twin-cell design

The twin-cell design is adopted in calorimetry with the aim of reducing the measurement errors caused by the thermal noise produced by the heat sink and the surrounding environment.

In the twin-cell design, two identical measurement cells are installed inside the same heat sink. One cell houses the sample to be measured while the other cell remain empty or houses an inert reference sample. Being inside the same heat sink, the two cells experience the same thermal noise. The noise can be eliminated by operating the two cells according to the difference principle. In this way, any fluctuation of the thermal block is automatically eliminated in the output signal, thus reducing the detection limit of the instrument and minimizing the thermal noise affecting the baseline (see Figure 31).

When thermoelectric modules are used as temperature sensors, the modules realize the thermal contact between the measurement cells and the heat sink. The thermoelectric modules are connected in such way to give as output the differential signal between the two cells, where the thermal noise is already eliminated.

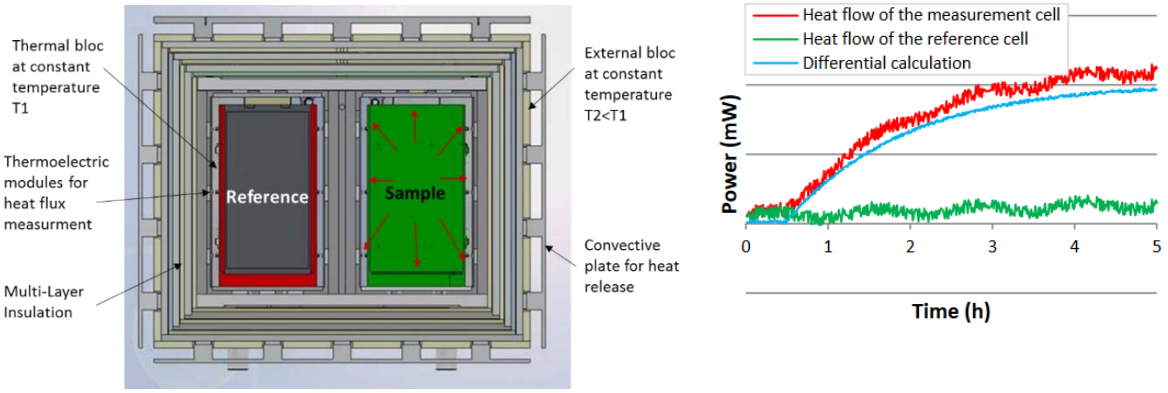

FIGURE 31 : TWIN-CELL CALORIMETER (LEFT) AND DIFFERENTIAL HEAT FLOW OUTPUT (RIGHT)

The twin cell design features the best precision and accuracy thanks to the reduction of the thermal noise. However, the construction of the two cells must be identical and avoid any minimal difference in order to accurately cancel the thermal noise.

Some major drawbacks of the twin cell design include the weight increase, the augmented space consumption and the longer measurement time. For large measurement chambers (>100 L) the twin design could become impractical or very difficult to implement.

With the aim of benefiting from the noise reduction of the twin cell design also in large volume calorimetry, Setaram introduced the innovative concept of the ghost reference cell (Jossens, 2018). In this concept, the reference cell is embedded into the measurement cell by providing:

- a reference plate replicating the mass of the measurement plate
- a compact reference sample placed below the measurement sample and with the same thermal capacity.

This solution allows the minimization of the distance between the measurement cell and the reference cell, thus providing that the two elements experience exactly the same thermal noise.

Thanks to this innovation, a large volume calorimeter can benefit from the thermal noise reduction deriving from the twin cell design within the dimensions of a single cell calorimeter.

7.3 Activities in the frame of the CHANCE Project

In the frame of the Task 3.2 of the CHANCE Project "Experimental investigation", a 200 litres calorimeter with low detection limit was developed, manufactured and tested by KEP Nuclear. This calorimeter was conceived for measuring plutonium and other possibly hidden RN in realistic nuclear waste drums. Measurements were carried out with mock-up waste drums at CEA Cadarache. SCK-CEN will also perform measurements with mock-up waste drums and with a 200 L real unconditioned waste drum.

The calorimeter developed in the frame of the CHANCE Project can assess cylindrical samples (industrial drums) with a volume up to 260 litres. It can measures thermal power ranging from 100 to 3500 mW with a measurement accuracy lower than 2.5% and a precision better than 2% in the whole measurement range.

Based on an established design, the measurement chamber is easy to access thanks to the opening in two half-shells (Fig. 4). This facilitates loading/unloading of the sample in the measurement chamber.

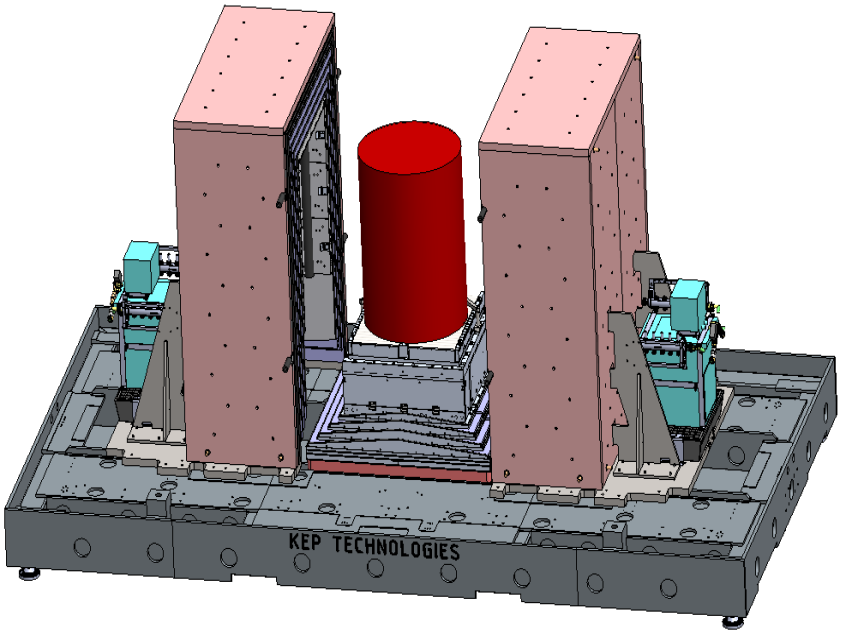

FIGURE 32 : MODEL OF THE CHANCE LVC CALORIMETER WITHOUT THE EXTERNAL CASING SHOWING THE HALF-SHELL DESIGN

This new calorimeter is based on the Kep Technologies LVC 1380 proven design but includes some innovative features:

- the geometry of measurement chamber is optimized to assess the drums of interest for the CHANCE project. This optimizes the performance of the instrument and the measurement time.

- in addition to the Peltier modules surrounding the measurement chamber and providing the measurement of the thermal power released by the sample, the measurement chamber is also surrounded by temperature probes. They are used to create a 3D map of the temperature distribution in the measurement cell for monitoring and diagnostics purposes.
- the measurement cell is equipped with compliant copper braids creating a preferential thermal path between the sample and the measurement plates. The aim of this feature is to reduce the thermal resistance surrounding the samples improving the precision of the measurement and reducing the measurement time.
- The calorimeter is equipped with an embedded liquid-based cooling system for the stabilization of the external plates. Each half-shell is equipped with an independent cooling circuit for an optimized thermal regulation. The cooling plates are realized in an innovative way with the cooling circuit fully embedded inside the plate for improved performance.

7.3.1 Monte Carlo modelling of the calorimeter

As calorimetry is not bias-free. Source position, material density distribution, chemical reactions, phase changes and also radiation leakage can influence the final result. In order to evaluate how the leakage impacts on the result and how the radiation behaves within the volume of the calorimeter (i.e. how the energy is deposited inside the system and to estimate the amount of escaping flux) Monte Carlo modelling of the KEP-LVC calorimeter was realized, using the MCNP6 code and ENDFB-7.1 cross sections library.

Two kinds of generic radiation sources were used in the modelling. In this study, the most conservative source was limited to only one pin in the center of the assembly with only one container in the middle of the pin. In this scenario emerging particles have the longest possible pathway to leave the system.

A second generic source, called the “homogeneous" source, was a sand filled drum and air on top. The particle starting points were sampled inside the whole section filled with sand. The amount of escaping radiation is of course higher in this case, as the particles may appear nearby the wall of the drum.

Depending on the source configuration and particle types, between 4% - ~13% of the energy escaped the system and 73% - 87% was detected. The amount of deposited energy in the reference element was no bigger than 1.5%. This deposited energy is not measured by the Peltier elements, and the final result would be reduced by this value. The maximum bias caused by this phenomenon is <3%. The percentage of the total energy deposited depends on the source energy, i.e. low-energy emitters are less biased than high-energy ones.

MCNP simulations were performed for generic source and matrix compositions to quantify the percentage of particles (mainly gamma and neutrons) leaving the waste drum. While escaping radiation can be largely hampered with these matrices, the heat flux is unaffected, thus demonstrating the usefulness and complementarity of calorimetry in these cases and in general.

MCNP simulations of the calorimeter suggest that the uncertainty related to the energy deposition, based on uncertainty on the distribution of activities within a drum, is smaller than the two orders of magnitude. Therefore, we also demonstrated the usefulness of calorimetry in cases with unknown distribution of activities within drum.

Some experimental measurements with the calorimeter are under progress to confirm those results.

8. Active interrogation methods

Non-destructive active methods (fast neutron activation, active neutron or photon interrogation) were designed, tested and proved to be particularly useful to overcome limitations of non-destructive passive methods (for instance, the quantification of actinide masses in high neutron or gamma background) (Carrel *et al*., 2014).

8.1. Active neutron interrogation

Active neutron interrogation is based on the detection of neutrons emitted as a result of fission induced by a pulsed neutron generator. The extraction of the useful signal due to prompt and delayed fission neutrons, embedded in the interrogating neutron generator flux which is several orders of magnitude higher, uses techniques of time and energy discrimination. The prompt neutron measurement is based on the Differential Die-Away Technique (Caldwell *et al.*, 1986) called DDT (or sometimes DDA):

- the neutron generator emits a short pulse (typically a few dozen to hundred µs) of neutrons of 14 MeV, during which fissions induced by fast neutrons are produced whose prompt neutrons cannot be used because it is impossible to distinguish them from the interrogating neutrons;
- the fast neutrons of the generator slowdown in the constituent materials of the measuring device (notably graphite, see Figure 33) and in the object to be characterized;
- when the interrogating flux is essentially thermal (a few hundred µs after the end of the neutron pulse), it becomes possible to discriminate energy between the interrogating neutrons (thermal) and the prompt fission neutrons (fast). This is accomplished with blocks of ^{3}He detectors surrounded by polyethylene, coated with cadmium and / or B_4C to absorb the interrogating thermal neutrons that will nevertheless let the fast prompt fission neutrons through, the latter being then thermalized by the polyethylene and detected by the ^{3}He counters.

The prompt fission neutron signal, after subtraction of the active background visible in Figure 34, is proportional to the amount of fissile material. The coefficient of proportionality, called the calibration coefficient, or sensitivity (in $s^{-1}.g^{-1}$ or fissile isotope: ^{235}U, ^{239}Pu or ^{241}Pu), is estimated for the different waste matrices likely to be measured. It is important to underline that this prompt neutron signal allows a direct assessment of the fissile mass, without necessarily knowing its isotopic composition (uranium, plutonium, U/Pu ratio).

Measurement of delayed neutrons involves two phases, first an irradiation of the package intended to cause fissions (with fast, epithermal and thermal neutrons) and then a counting of the delayed neutrons resulting from induced fissions. Since each of these phases lasts for several seconds or minutes, the emission of the generator is not necessarily pulsed and the use of an isotopic source of neutrons is possible. However, the delayed neutron signal can be observed more efficiently online, between the pulses of the neutron generator, after the disappearing of the prompt neutron signal, see Figure 34.

The use of both prompt and delayed fission neutron signals allows disentangling U and Pu contributions in nuclear materials (Raoux *et al*., 2003).

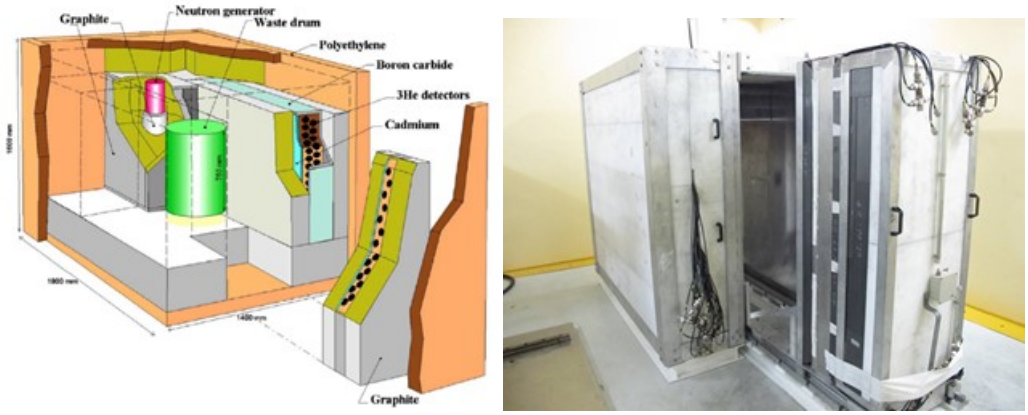

FIGURE 33 : "PROMETHEE 6" ACTIVE NEUTRON INTERROGATION R&D CELL IN CHICADE NUCLEAR FACILITY, AT CEA CADARACHE, FRANCE

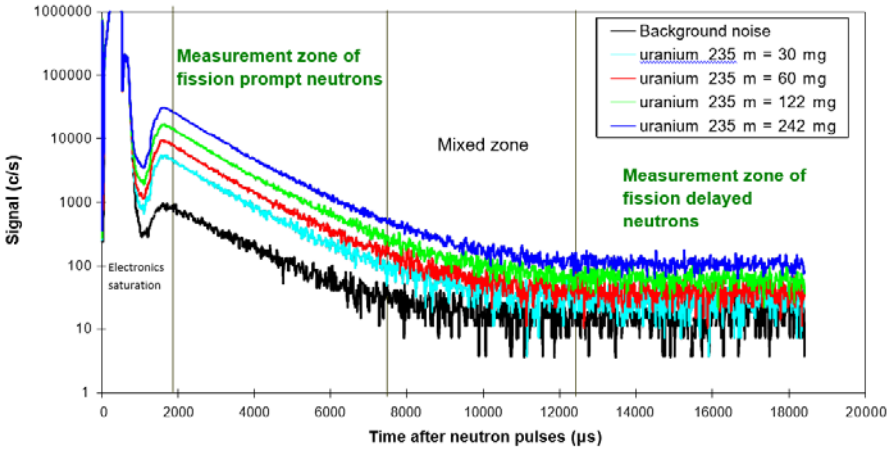

FIGURE 34 : DDT TIME SPECTRUM OF THE PULSED MEASUREMENT OF PROMPT AND DELAYED FISSION NEUTRONS

The neutron interrogation method essentially makes it possible to characterize fissile nuclei (^{235}U, ^{239}Pu and ^{241}Pu). The signal due to fertile nuclei (^{238}U and ^{240}Pu) may nevertheless be significant for some measurements of delayed neutrons when the neutron interrogating flux is relatively hard (limited thermalization). Whatever the mode of interrogation (isotopic source, neutron generator), they allow an overall characterization of the waste package, but they are sensitive to the nature of the matrix (its density and chemical composition), to the position of the contaminant in the package and to self-shielding effect in fissile materials. These penalties may be extensive but when these effects are controlled, the method is very sensitive and detection limits can reach a few tens of milligrams of fissile materials in less than 30 min measurements. Beyond fissile mass estimation which does not absolutely requires to know the isotopic composition, for the determination of the alpha activity however it is necessary to distinguish the contributions of the different isotopes. In such instance, the isotopic composition needs to be known a priori or determined by complementary methods like gamma spectroscopy.

Several active neutron interrogation systems are in operation, both for R&D and industrial purpose. For instance, the cell of Figure 35 is used to perform Super Controls in France for ANDRA. On the other hand, four industrial systems are in operation at ORANO La Hague to determine the residual fissile mass in hulls and end pieces after shearing and dissolution of spent fuels, or before and after compaction of these metallic residues (Toubon *et al.*, 2001). In passive mode, i.e. when the neutron generators are turned off or far from their pulses (in the delayed neutron area of Figure 34), the measurement of passive neutron emission also allows assessing the curium activity in these high-activity metallic waste drums, by detecting its dominant spontaneous fission neutron emission. In such waste, fission delayed neutrons are negligible.

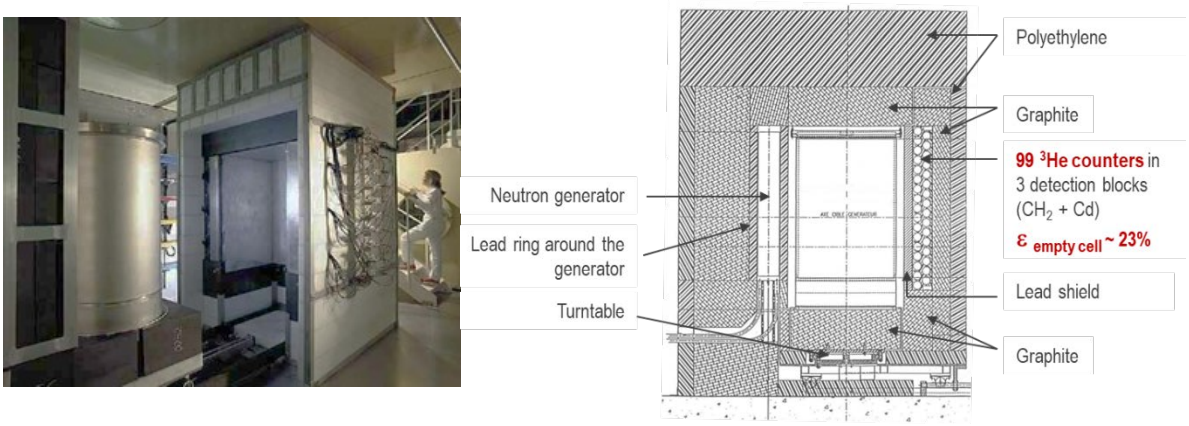

FIGURE 35 : SYMETRIC EXPERTISE CELL USED FOR SUPER CONTROLS IN CHICADE FACILITY, AT CEA CADARACHE, FRANCE

R&D is underway to reduce matrix and localization effects, which are even more stringent in active neutron interrogation than in passive neutron counting. Indeed, a high attenuation of the interrogating neutron flux is observed in matrices containing neutron absorbers like chlorine, iron, boron, etc. Correction methods based on internal flux monitors (i.e. detectors sensitive to the thermal neutron flux in the matrix, like ^{3}He counters collimated with cadmium) are being investigated, as illustrated in Figure 36. Based on a number of Monte Carlo calculations and a multi-linear regression, a correlation was established between the calibration coefficients of fissile isotopes (e.g. ^{239}Pu) and the internal flux monitor (Antoni *et al.*, 2014). Beyond these monitors sensitive to thermal interrogating neutron absorption, an additional "moderation indicator" can also be used, based on fast neutron transmission or scattering (like the "Add A Source" method used in passive neutron counting) to further improve matrix effect corrections.

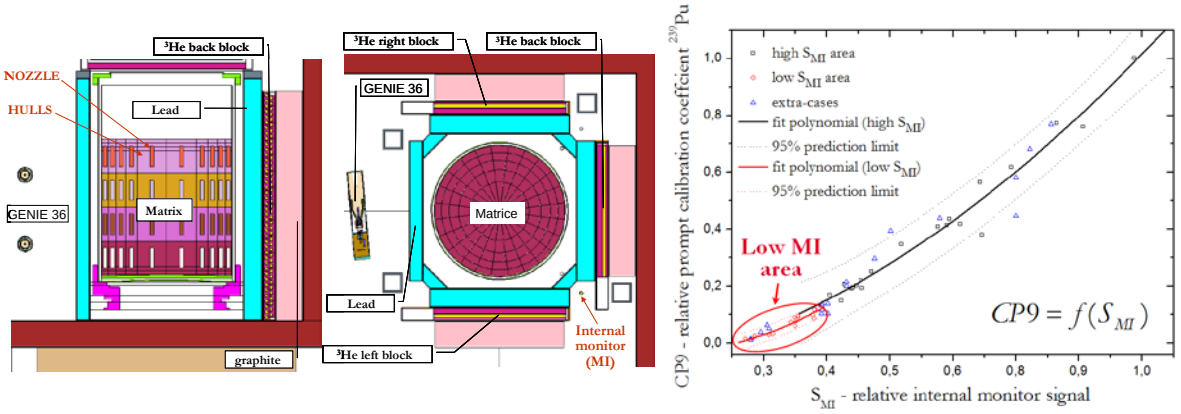

FIGURE 36 : MCNP MODEL OF AN INDUSTRIAL NEUTRON CELL FOR 800 L WASTE DRUMS FILLED WITH HULLS AND NOZZLES, BEFORE THEIR COMPACTION AT ORANO LA HAGUE, SEE THE TEXT FOR DETAILS

8.2. Active photon interrogation (photofission) for the identification of nuclear materials

In the past years, CEA has reported on numerous advances to use active interrogation methods for the detection of actinides in radioactive waste packages. In this respect, many experiments have been performed in the SAPHIR (Active Photon and Irradiation System) facility operated at CEA Saclay, and more recently at CEA Cadarache. Non-destructive active methods, based on the detection of delayed particles emitted after a photon interrogation, have been shown to enable locating, identifying and quantifying actinides contained inside both medium size waste (220 L) as well as bulky (up to 870 L) concrete waste packages (Gmar *et* al., 2005; Carrel *et al.*, 2011; Simon *et al.,* 2016; De Stefano *et al.*, 2019). The advantage of measuring delayed neutrons and high energy delayed gammas is that they can together overcome the limitations due to heavy shielding. Even though the fission interaction cross sections are lower for photon activation compared to neutron activation, it has some added benefits such as availability of higher intensity beam, high penetrability in the shield matrix, good collimation and lower self- induced activation background (Dighe *et al.*, 2014). On the other hand, photofission data in literature at the beam energies used (e.g., 10 MeV) are scarce and therefore data need to be generated in order to allow non-destructive analysis of actinides (Delarue et al, 2021).

The method consisting in using high-energy photons to induce reactions of photofission on heavy nuclei (actinides) present in the waste is described, for instance, by Gmar *et al*. (2005) (Figure 379). As a result of photofission, fission products are created which emit delayed neutrons that are counted between each pulse of photons. As the mean number of neutrons emitted per fission depends on the actinide species, the temporal evolution of delayed neutrons can be used to calculate the mass of actinide inside the waste package. Simulations or calibrations with a mock-up package are needed to eliminate effects related to the geometry and the matrix of the package. Gmar *et al*. (2005) also present the first measurements on a 870 L concrete mock-up and on two real ~200 L waste drums. In order to improve the accuracy of the method, Gmar *et al*. (2006) carried out a tomographic measurement allowing to compute the three-dimensional spatial distribution of the actinide mass inside the nuclear waste package. Such a measurement allows to overcome the limitation with respect to the assumption of the actinides localization inside the waste package.

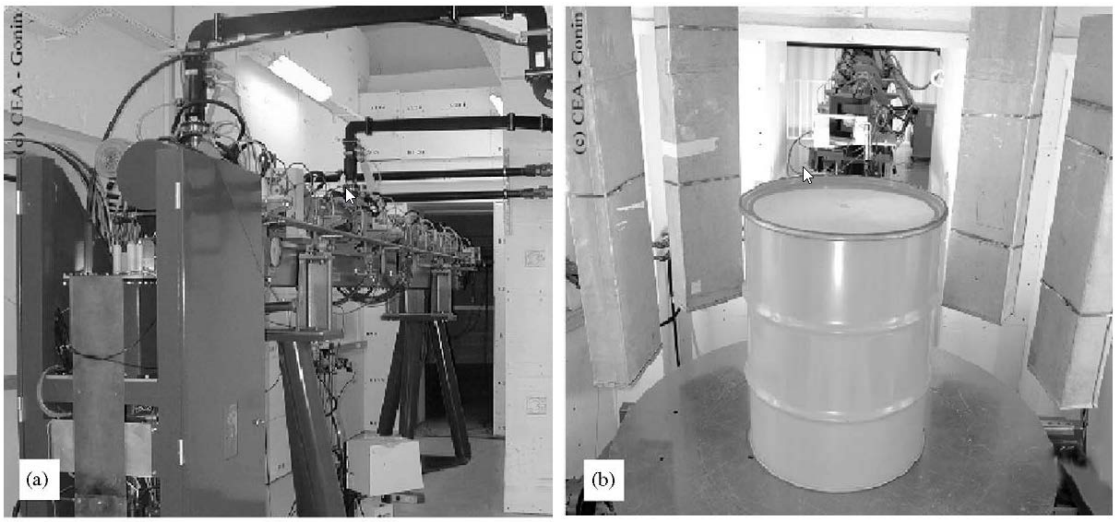

FIGURE 37 : SAPHIR INSTALLATION (A) ELECTRON ACCELERATOR; (B) A WASTE PACKAGE PLACED ON THE CONVEYOR SURROUNDED BY NEUTRON DETECTORS (GMAR *ET AL.*, 2005)

Carrel *et al*. (2006) report on a method to identify (mixtures of) actinides (^{235}U, ^{238}U, ^{239}Pu) inside nuclear waste packages based on the detection of delayed gammas emitted by fission products after neutron or photon interrogation. The considered fission reactions were exclusively due to thermal neutrons. After fission of fertile (photon activation analysis) or fissile (neutron activation analysis and photon activation analysis) actinides, fission processes occurred leading to specific distributions of fission products directly depending on the nature of actinides. The qualitative and quantitative analysis of peaks in the delayed gamma spectrum then allows the identification of each of the actinides present in the package. The method was experimentally tested using mixtures of ^{235}U and ^{239}Pu (in fission), and of ^{235}U and ^{238}U (in photofission). The experimental protocol used for the detection of the delayed gammas consists of three steps: 1) pulsed irradiation period to create fission products of interest; 2) cooling period to decrease the active background; 3) counting period for the acquisition of the delayed gamma spectrum (Carrel *et al*., 2006).

In Carrel *et al*. (2010) the photofission process and detection of delayed particles (delayed neutrons and delayed gamma rays) is used in the characterization of actinides (U and Pu) inside a concrete waste package (CBFC2 type). The high-energy photons required to induce photofission reactions are produced using a linear accelerator (LINAC). The use of the LINAC allows to combine photon activation analysis methods and high-energy radiography (see also section 10). Figure 39 shows an example of a photofission tomography carried out for a hot spot in the sample. However, in such concrete packages, the dense, hydrogenated matrix cannot be accurately examined by neutron interrogation followed by the detection of fission neutrons because of unacceptable uncertainties related to the high and variable attenuation (Simon *et al*., 2016). Therefore, CEA started investigating the use of an incident high energy proton beam to produce photofission in actinides, and to measure delayed gamma rays.

The detection of high-energy (β-)delayed gamma particles (above a given threshold, usually 2-3 MeV) versus delayed neutrons following photofission has been shown to be interesting for two main reasons (Norman *et al.*, 2004; Carrel *et al.*, 2011): 1) high emission yield (compared to the poor neutron emission yield of in particular the photofission of ^{239}Pu, see also Figure 38), and 2) poor sensitivity to the presence of hydrogenous materials. Simon *et al*. (2016) contributed further to the feasibility assessment of fissile mass quantification using photofission delayed gamma rays by using the Monte Carlo code MCNPX and found that the achievable detection limit would be lower than the expected uranium mass in large, long-lived medium activity radioactive waste packages. In their paper, Simon *et al*. (2016) also compared different materials (tungsten and silica) that could be used as Bremsstrahlung breaking target. Su-Ping *et al*. (2014) showed that the effective half-life of the delayed high-energy gamma ray method can be used as a complementary evidence to confirm the presence of nuclear materials, on the precondition that a "clear" spectral region of interest can be settled upon.

	^{238}U—0.7%	^{235}U—85%	^{239}Pu—94%
HEDG/DN	0.638 ± 0.015	1.395 ± 0.019	2.497 ± 0.124

FIGURE 38 : HIGH-ENERGY DELAYED GAMMA SIGNAL (HEDG) DIVIDED BY THE DELAYED NEUTRON SIGNAL (DN), ACCORDING TO THE NATURE OF THE IRRADIATED ACTINIDE, HERE FOR NATURAL (0.7%) OR HIGHLY ENRICHED (85%) URANIUM, OR LOW BURNUP (94% OF ^{239}PU) PLUTONIUM (CARREL *ET AL.*, 2011)

In Carrel *et al.* (2011) the results of active interrogation techniques based on high-energy delayed gamma detection on an 870 l mock-up package are described. The possibility to use measurement of delayed gamma rays following neutron-induced fission for the characterization of fissile mass in larger (870 L) radioactive waste drums was further explored by De Stefano *et al*. (2019). In their simulations, they used the MCNP model of the MEDINA cell located at FZJ in Jülich, Germany (Mauerhofer and Havenith, 2014). The calculated results were encouraging for homogeneously distributed fissile materials in the waste, with detection limits in the range of 10s of grammes for ^{235}U and ^{239}Pu for the main high energy delayed gamma rays of interest.

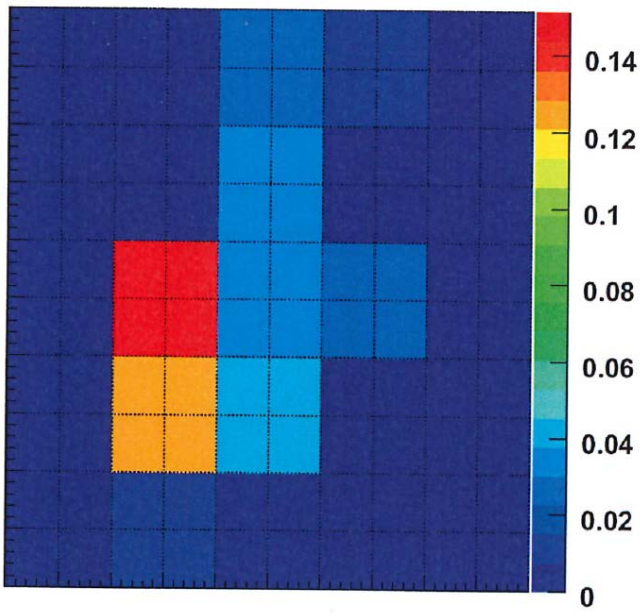

FIGURE 39 : RESULT OF PHOTOFISSION TOMOGRAPHY CARRIED OUT FOR A HOT SPOT IN THE INVESTIGATED CONCRETE WASTE DRUM. THE COLOUR SCALE INDICATES THE MASS OF ACTINIDES CONTAINED IN EACH VOXEL (CARREL *ET AL.*, 2010)

The use of photofission for quantification of actinides was also investigated by Dighe *et al.* (2014) and Dighe *et al.* (2019). In Dighe *et al.* (2014) an industrial 10 MeV LINAC equipped with a tantalum target was used to analyse delayed neutron and delayed gamma decay data produced after photofission to quantify natural uranium (^{238}U) and thorium (^{232}Th) in cm-sized samples both in pure and mixed forms. In their setup (Figure 40), they were able to reach a maximum error in estimation of less than 40% for actinides in mixed state. Dighe *et al.* (2019) expanded on this concept by investigating a mock-up drum of 50 cm diameter and 100 cm length, equipped with 20 hollow tubes to place experimental fissile material samples. The drum was placed horizontally and irradiated with high-energy photons axially (Figure 40). In this set-up, only delayed neutrons were measured and results allowed to obtain minimum detection limits as well as photofission delayed neutron yield/100 fissions for ^{232}Th.

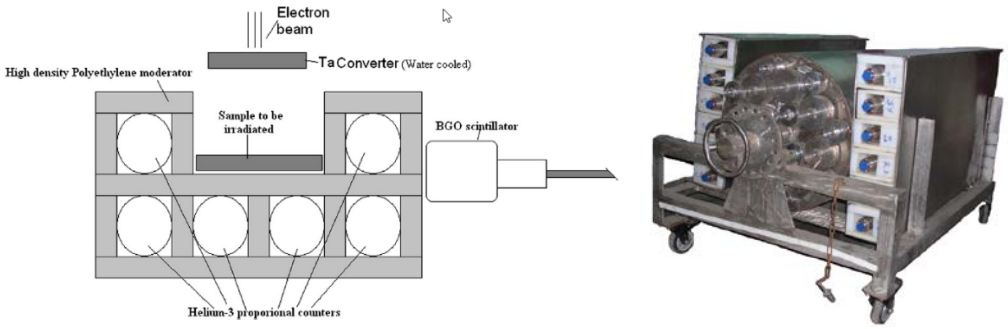

FIGURE 40 : LEFT SCHEMATIC DIAGRAM OF THE EXPERIMENTAL SET-UP USED. IN EXPERIMENTS THE ELECTRON BEAM IS IMPINGED DOWNWARD PARALLEL TO THE PLANE OF THE PAPER AND SCANS THE SAMPLES AXIALLY PERPENDICULAR TO THE PLANE OF THE PAPER (DIGHE *ET AL.* (2014)); RIGHT: PICTURE OF THE MOCK-UP DRUM WITH HE-3 NEUTRON DETECTORS (DIGHE *ET AL.* (2019)

On the other hand, it is interesting to mention that active methods have been readily deployed in situ to prevent illegal traffic of special nuclear materials (e.g., uranium-238, uranium-235 and plutonium-239 – associated with weapons of mass destruction) inside cargo (shipping) containers at borders, especially sea ports. The method, which is sometimes referred to as "the nuclear car wash" (Slaughter *et al*. (2007)) consists of the interrogation of a container by high-energy photon and the subsequent detection of particles (delayed neutrons and gamma rays) emitted after the fission (Norman *et* al., 2004; Jones *et* al., 2005; Agelou *et al*., 2009). Such methods overcome the disadvantage of passive measurements of photons or neutrons in that such nuclear materials can be undetectable because of shielding inside the container. In the Figure 41, the high energy photon beam is created by a pulsed electron linear accelerator (LINAC). The accelerated electrons impinge a tungsten or copper target and produce photons via the bremsstrahlung process. It is mentioned here as well that Micklich *et al*. (2003) proposed to use the very efficient $^{19}F(p,\alpha\gamma)\,^{16}O$ reaction (in a technique called FIGARO, Fissile Interrogation using Gamma Rays from Oxygen) instead of a LINAC, but, to our understanding, this method is rarely used in practice.

For all actinides, photofission reactions occur above an energy threshold of around 6 MeV (Carrel *et al*., 2006). Since the higher photon energies enable both increased cargo penetration as well as increased photonuclear source generation, higher energy pulsed electron accelerators are more desirable. Detection systems have been tested and used for prompt and delayed photon-induced neutron emissions and for gamma particles. Delayed neutron detection is a clear indication of the presence of nuclear material and additional data analysis and interrogations enable material identification (Jones *et al*., 2005; Kinlaw and Hunt, 2006). In (Agelou *et al*., 2009) it is described that delayed neutrons are counted between accelerator pulses, while delayed gammas are counted only after stopping irradiation. Practical limitations to the use of this technique in this context are set by regulatory constraints, e.g., the maximum photon energy that can be used in a public environment, and the maximum dose per inspection (Agelou *et al*., 2009).

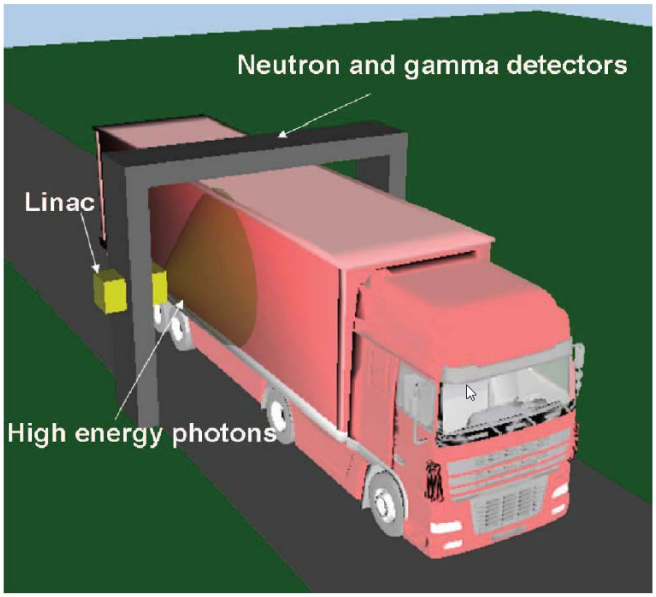

FIGURE 41 : ILLUSTRATION OF THE PRINCIPLE OF ACTIVE INTERROGATION OF CONTAINERS (AGELOU *ET AL.*, 2009)

8.3. Neutron Activation analysis

Another application of active interrogation is related to the characterization of the amount of toxic elements present in (long-lived and medium activity) radioactive waste packages. Typically, this amount also needs to be assessed before such packages can be accepted in repository facilities. Neutron activation analysis (NAA) refers to a method for the qualitative and quantitative determination of elements based on the measurement of characteristic radiation from radionuclides formed by irradiating materials by neutrons. Neutron activation analysis can be performed in a variety of ways. This depends on the element and the corresponding radiation levels to be measured, as well as on the nature and the extent of interference from other elements present in the sample. Most of the methods used are non-destructive, based on the detection of gamma radiation emitted by the irradiated material after or during the irradiation (https://www.iaea.org/topics/neutron-activation-analysis). The most suitable source of neutrons for such an application is usually a research reactor. Several research reactors, such as the BR1 reactor in SCK CEN (Figure 42), can provide sufficient neutron flux to irradiate samples.

FIGURE 42 : BR1 reactor at SCK CEN, used for neutron activation analysis

But NAA can also be performed in neutron activation cells instead of a reactor. An R&D program was started between the CEA, ANDRA and FZ Jülich to study the performance of Prompt Gamma Neutron Activation Analysis (PGNAA) for elements showing large capture cross sections such as mercury, cadmium, boron and chromium (Ma *et al.*, 2012; Nicol *et al.*, 2016). Feasibility measurements have been performed on both 50 cm^3 liquid or powder samples, and on a 20 kg concrete sample (1.53 g cm^{-3} density) containing homogeneously distributed toxic elements (Ma *et al.*, 2012).

The R&D program also resulted in the installation of a new analytical facility called MEDINA (Multi Element Determination based on Instrumental Neutron Activation) at the Forschungszentrum Jülich (Mauerhofer and Havenith, 2014). In this facility (Figure 43), prompt and delayed gamma neutron activation analysis (P&DGNAA) using a 14 MeV neutron generator is used for the determination of non-radioactive elements and substances in 200-l radioactive waste drums in the view of acceptability of such drums to the KONRAD repository. Amongst others, the facility and technique was tested through the analysis of a steel drum homogeneously filled with concrete blocks, in order to obtain the elemental composition of the concrete and to verify the presence of toxic elements like cadmium and mercury. The limits of detection for these two elements, were, respectively 4 and 145 mg/kg for an assay time of 2000s (Mauerhofer *et al.*, 2016). In further studies, also the influence of heterogeneous compositions and the impact of the presence of neutron moderating and absorbing elements, as well as gamma absorbing elements (like lead), on the accuracy of the analytical results were studied (Mildenberger and Mauerhofer, 2016; Mildenberger and Mauerhofer, 2017).

FIGURE 43 : THE FACILITY MEDINA FOR THE ASSAY OF 200-L DRUMS WITH THE HPGE-DETECTOR IN FOREGROUND AND THE 14 MEV NEUTRON GENERATOR ON THE RIGHT (MAUERHOFER AND HAVENITH, 2014)

The MEDINA facility was further tested using MCNPX simulations for the ^{235}U and ^{239}Pu characterization in 225L bituminized waste drums based on the detection of fission delayed gamma rays (Nicol *et al.*, 2014; Nicol *et al.*, 2016B). However, the detectability and performance in the bituminized drums were found to be strongly limited by the high gamma count rate due to ^{137}Cs, making the detection of the weak delayed gamma signal impossible. However, promising results were obtained in lower-activity cemented waste drums.

The same PGNAA methodology was used by Naqvi and co-workers (Naqvi *et* al., 2009; Naqvi *et* al., 2010; Naqvi *et al.*, 2011) to estimate the chlorine concentration in concretes. Several fly ash cement concrete specimens containing between 0.8 and 3.5 wt.% chlorine were analysed (Figure 44). They could reach minimum detectable concentrations of chlorine in blast furnace slag (BFS) and fly ash (FA) cement concrete in the order of 0.03-0.04wt%.

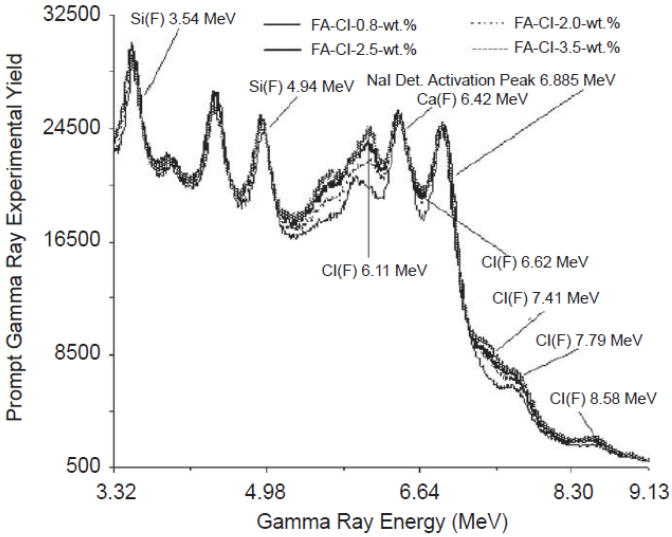

FIGURE 44 : PROMPT GAMMA-RAY SPECTRA FROM FOUR CHLORIDE-CONTAMINATED FLY ASH CEMENT CONCRETE SPECIMENS CONTAINING BETWEEN 0.8 AND 3.5 WT.% CHLORINE WITH ENERGIES IN EXCESS OF 3 MEV (NAQVI *ET AL.*, 2009)

8.4. Quantification of fissile isotopes for nuclear fuel safeguards

The identification of fissile isotopes and quantification of their relative concentration are the goals of non-destructive assay in nuclear fuel safeguards, and a number of techniques have been explored for this objective. Kinlaw and Hunt (2006) examined delayed neutron emission decay rates following photofission in a U-238 target to detect and identify fissionable isotopes. Campbell *et al.* (2011) and Mozin *et* al. (2012) investigated through simulations the use of delayed gamma rays from fission-product nuclei to directly measure the relative concentrations of U-235, Pu-239 and Pu-241 in irradiated fuel assemblies. Their "high-energy delayed gamma spectroscopy" (HEDGS) method is based on the unique distribution of fission-product nuclei produced from fission in each of these fissile isotopes (Figure 45). Before, assay methods relied on passive measurements (of, e.g., Cs-137 and Cm-244) combined with computational predictions based on initial fuel composition and reactor operating history. The new active method, however, would allow to directly measure the mass of key fissile isotopes, which is impossible by means of passive techniques because of the intense gamma-ray and neutron emissions from long-lived fission products and actinides. Campbell *et al*. (2011) complemented the numerical simulations with benchmarking measurements performed at the prompt gamma neutron activation analysis (PGNAA) facility at Oregon State University, consisting of an HPGe spectrometer viewing a sample in the path of a collimated neutron beam from the University's TRIGA reactor.

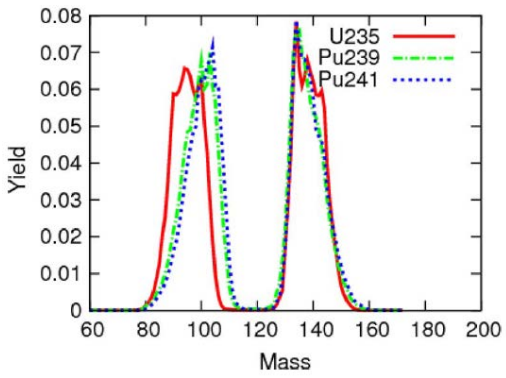

FIGURE 45 : THERMAL NEUTRON FISSION-PRODUCT YIELD DISTRIBUTION FOR U-235, PU-239 AND PU-241 (CAMPBELL *ET AL.*, 2011)

DeSimone *et al*. (2010) discussed and reviewed several different active interrogation techniques (mainly concentrated on uranium) along with their strengths and weaknesses, within the framework of an attribute measurement system with an information barrier (such a system can be used to confirm a declaration concerning the characteristics of a sensitive, special nuclear materials item, without revealing any sensitive information). Important attributes for measuring uranium are enrichment and mass. Due to the low spontaneous fission rate of uranium, passive neutron techniques are not considered suitable for determining uranium properties. Also, the gamma rays emitted from ^{235}U are easily attenuated by the container and its packaging, making passive measurement of the enrichment impossible. The active interrogation techniques developed for the measurement of uranium use active neutron (either a random source or a spontaneous fission source such as ^{252}Cf) and photon (bremsstrahlung source) systems, either inducing fission and measuring the corresponding coincidence, or measuring the gamma rays emitted (DeSimone *et al*., 2010).

- In photofission using high-energy gamma rays (energies ranging from 6 to 10 MeV), fission signatures are observed with suitable detectors. During interrogation, the detectors are saturated from the bremsstrahlung source and cannot observe the prompt signals from fission; therefore, delayed fission signals can be observed after detector recovery (in the order of milliseconds).
- In nuclear resonance fluorescence (NRF), gamma rays excite the isotopes of interest at lower energies (e.g., for ^{235}U within the energy range of 1.0 to 2.5 MeV), leading to de-excitement by re-emitting gamma ray radiation at discrete energies characteristic of the nucleus.
- In active well coincidence counting (AWCC) a random neutron source (such as americium-lithium, producing 0.4 MeV neutrons) is used and induced fission reaction neutrons on ^{235}U are counted using coincidence techniques. The interaction of random source neutrons with the uranium (called "coupling") makes AWCC more complex than passive multiplicity counting.
- As alternative to the AWCC, a Californium Shuffler uses ^{252}Cf to induce fissions (2.2 MeV neutron energy). Because of the higher emission rates of this source, the system counts the delayed neutrons seconds to minutes are fissions (after removal of the source).
- In the differential die-away technique (DDA), a deuterium-tritium (D-T) neutron generator produces repetitive pules of neutrons that are thermalized in the item matrix and absorbed on the surface of the nuclear material, generating fission neutrons with an epithermal spectrum. The epithermal signal can be differentiated from the thermal interrogating signal by using shielded and bare detectors.
- Since a D-T generator generates also alpha particles travelling in a direction opposite to the neutron, measurement of the alpha particle allows the detection of correlations with events captured in different fast neutron detectors following interrogation of the item. This method is called the Associated Particle Technique.

- In the delayed neutron reinterrogation technique, delayed neutrons emitted upon induced fission of the uranium sample are detected. Generally, a pulsed source is used to perform repetitive interrogations generating a uniform distribution of fission products throughout the fissile material. The yield per fission of each delayed neutron precursor is dependent on the fissioning isotope and the particle inducing fission.

9. Detection of radioactive gas

Detection of radioactive gaseous emissions originating from nuclear facilities and waste is challenging. Those emissions mostly consist of tritium and radiocarbon, mainly emitted in the form of water vapour (HTO), carbon dioxide ($^{14}CO_2$) and methane ($^{14}CH_4$). $H^{36}Cl$ is also of interest in the particular case of irradiated graphite waste. Those radionuclides are long-lived and often diluted in an atmospheric matrix making them particularly difficult to detect. They are problematic because they have a high residence time in the environment, can easily be assimilated into living matter, and, due to their long half-life require long-term monitoring (IAEA 2004). They are particularly challenging to detect on-site, as current methods are based on laboratory-based detection techniques. New methods for rapid continuous in-situ analysis are therefore needed, for example for the characterization of nuclear waste outgassing, which is essential to ensure safe disposal of nuclear waste.

In recent years, optical detection of radionuclide has been successfully demonstrated for radiocarbon (Galli 2011, Genoud 2015, McCartt 2016, Fleisher 2017, Sonnenschein 2018, Galli 2016) and tritium (Bray 2015), and low detection limits were achieved. In particular, laser spectroscopy can be used to provide selective and sensitive detection of molecules directly in the gas phase. Optical detection offers several advantages over conventionally used techniques for nuclear applications, such as Liquid scintillation counting (LSC), which is commonly used for laboratory analysis in nuclear facilities. LSC requires sample collection and off-line analysis and in most cases is not suitable for on-site monitoring. Gaseous samples must be trapped in liquid form and bound to the medium, which will produce additional radioactive waste. Additionally, scintillation peaks of different radionuclides typically overlap in LSC spectra, thus limiting its sensitivity and often requiring time-consuming radiochemistry methods to separate the different beta emitters.

Laser spectroscopy can circumvent most of these issues. It analyses directly gaseous samples, thus producing no additional waste. The use of an optical technique also enables compact (footprint of around 45 cm x 60 cm), automated, and cost-effective instruments to be built, ideal for online in-situ monitoring. The method is selective and will only be sensitive to one radionuclide, meaning that the concentration of the radionuclide of interest can easily be determined even if the sample contains other radionuclides. The method also detects only one molecular form and thus provides a means to determine its speciation. In the case of radiocarbon, $^{14}CO_2$ is detected while other organic species such as $^{14}CH_4$ are not. Tritium can be detected in the form of tritiated water (HTO) and ^{36}Cl in the form of $H^{36}Cl$.

One of the most sensitive laser spectroscopy technique is cavity ring-down spectroscopy (CRDS) (O'Keefe1988, Romanini 1997), which is used for trace gas detection for a variety of applications, e.g. in industrial and environmental monitoring or medicine (Berden 2000), easily delivering sensitivities in the range ppt-ppm.

9.1 Cavity ring down spectroscopy

The CRDS can provide the sensitivity required to detect fugitive radioactive emissions from nuclear waste outgassing. In CRDS, the gas sample is placed inside an external resonant optical cavity consisting of high-reflectivity mirrors with an effective path length of several kilometres. A laser beam is coupled into the cavity, and the light exiting the cavity is focussed onto a detector, as shown in Figure 46. The laser coupling is suddenly switched off and the light decaying out of the cavity recorded. The signal is fitted with an exponential curve and the decay time, also called ring- down time (τ) determined. Additional losses due to analyte absorption result in a shorter ring-down time. Spectra are recorded at low pressure (~ 10 mbar) such that the absorption features are narrow and the peaks of the different molecules and isotopologues are well separated. Quantum cascade lasers (QCLs) are ideal to probe molecules, as they emit light in the mid-infrared region, where strong molecular vibrational levels are present. They are compact and relatively low cost, and high resolution can be achieved, as they typically have a linewidth of a few tens of MHz. The recent rise of commercial QCLs has paved the way for a field deployable CRDS system for radionuclide detection. For the highest sensitivity, the strongest absorption feature of the target isotopes must be identified. Interferences from other molecules and isotopes should also be taken into account as well as availability of lasers and other optical components. For instance, one of the strongest lines of $^{14}CO_2$, with minimum interference from other isotopologues of CO_2 and molecules, is situated at 2209.1 cm^{-1} (4.52 µm). This line has been used for highly sensitive detection of radiocarbon with CRDS below ppb levels (Galli 2011, Genoud 2015, McCartt 2016, Fleisher 2017, Sonnenschein 2018), with detection levels as low a few ppq (Galli 2016). An example of a spectrum of tritiated water recorded with a CRDS system is shown in Figure 478 where it is seen that in this case the central wavelength of the targeted absorption line is at 4596.48 cm^{-1} or 2.175 µm.

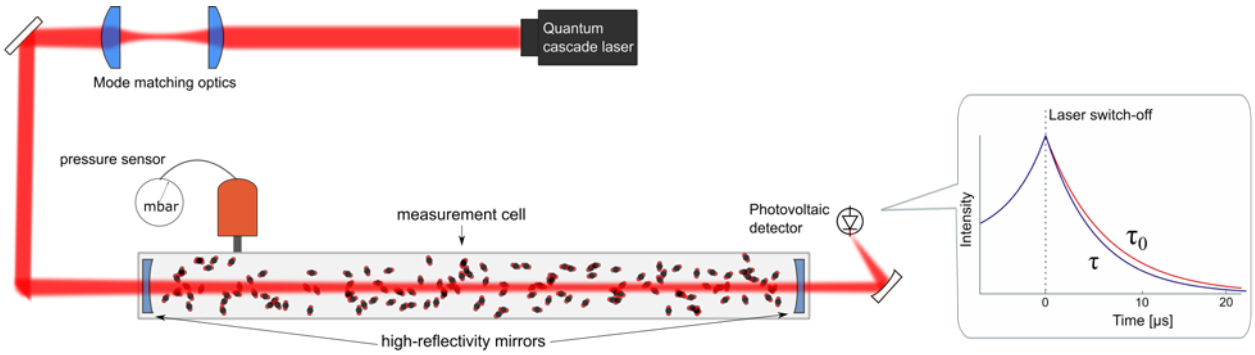

FIGURE 46 : PRINCIPLE OF THE CRDS TECHNIQUE. A QUANTUM CASCADE LASER IS COUPLED INTO A HIGH FINESSE CAVITY, AND THE LIGHT EXITING THE CAVITY IS DETECTED BY A PHOTOVOLTAIC DETECTOR. THE ABSORPTION SPECTRUM IS RECORDED BY COMPARING THE RING-DOWN TIME (τ) TO THE VACUUM RING-DOWN TIME (τ_0) AS FUNCTION OF WAVELENGTH

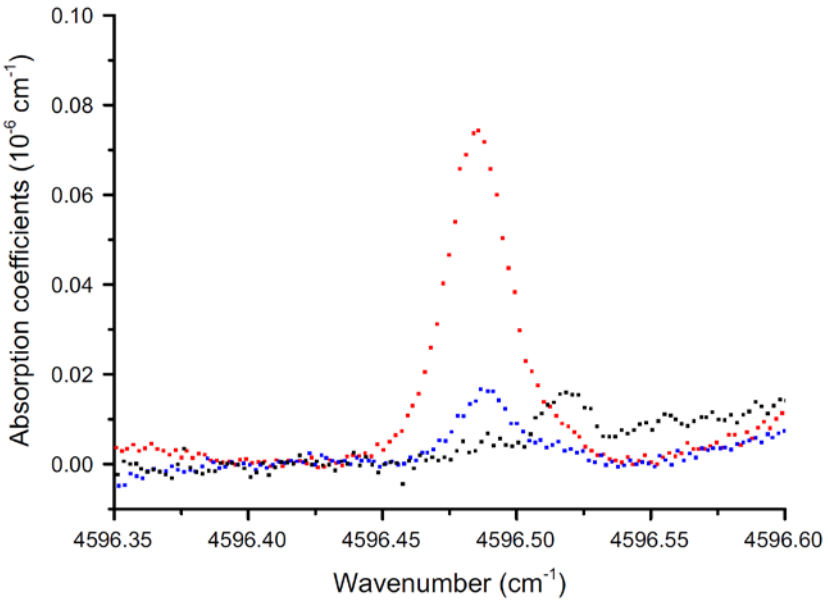

FIGURE 47 : EXPERIMENTAL ABSORPTION SPECTRA OF THREE WATER SAMPLES: A TRITIATED WATER STANDARD WITH AN ACTIVITY CONCENTRATION OF 340 MBQ/G OR HTO/H2O=5.4 PPM (RED LINE), ANOTHER STANDARD OF TRITIATED WATER WITH AN ACTIVITY CONCENTRATION OF 72.21 MBQ/G OR HTO/H2O=1.14 PPM (BLUE LINE), AND DISTILLED WATER (BLACK LINE). FIGURE ADAPTED FROM (BRAY 2015)

For many applications, including nuclear waste outgassing monitoring, the direct detection of the target radionuclide by CRDS is not feasible, as the molecular species is diluted in an atmospheric matrix. It is therefore necessary to first trap the molecules of interest (CO_2, H_2O…) and then release an almost pure sample into the CRDS cell. In this manner the highest sensitivity can be achieved, and trace amount of the radionuclide can be detected. It is however crucial to maintain the advantages of using an optical method to enable in situ measurements. The sampling method must be automated and performed on-line and should for example not result in trapping the gas in a liquid medium. This way, no complex sampling preparation is needed. There are several options to trap the gaseous molecules. A cryogenic trap, with a "freeze-and-release" method or cryofocusing can be used to trap CO_2 and has been previously explored. However, the relative slow cooling and heating cycle and the cost of a cryogenic unit is not ideal. Selective CO_2 trapping can be achieved using an adsorbent. A weak anion exchange resin can for example efficiently trap CO_2 while instantaneously releasing CO_2 at only 100°C, making them ideal for in situ monitoring[39]. For detection of tritium in the form in tritiated water, water vapour can easily be trapped using a standard cold trap. If rapid sampling is necessary, several sampling modules in parallel can be used, as illustrated in Figure 48. A catalytic converter can be added in order to convert other molecular forms of the radionuclide of interest into the molecular form used for the measurements (e.g., $^{14}CH_4$ can be converted in $^{14}CO_2$ or HT into HTO).

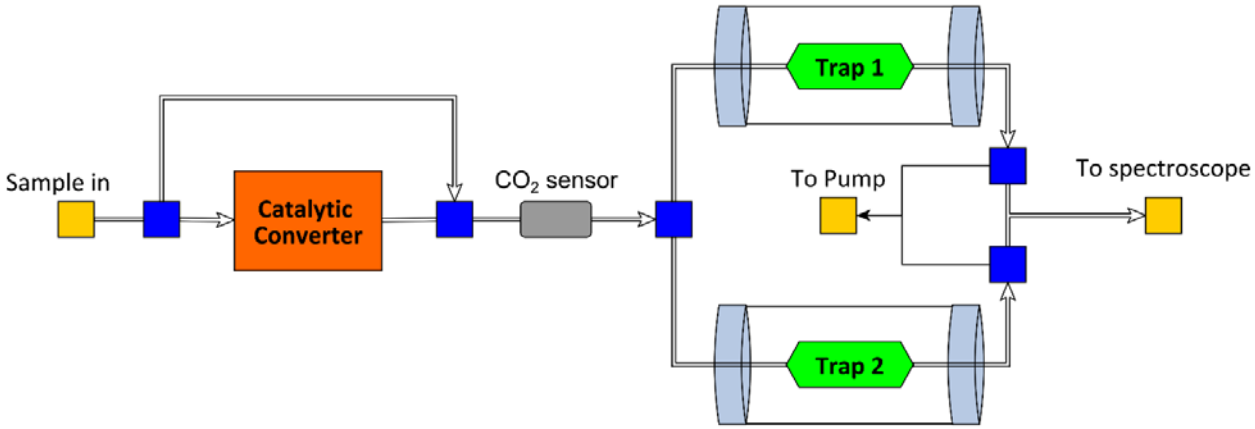

FIGURE 48 : POSSIBLE CONFIGURATION OF A SAMPLING SYSTEM TO BE USED IN COMBINATION WITH CRDS. THE SYSTEM MAINTAINS THE SAMPLES IN GAS FORM AND CAN EASILY BE AUTOMATED USING SOLENOID VALVES (BLUE SQUARE)

This approach of combining on-line sampling with CRDS has been successfully used to monitor the radiocarbon emissions from a nuclear power plant stack (Lehmuskoski 2021). High sensitivity was achieved as well as a measurement time of only 50 min, which is an order of magnitude faster than conventional techniques currently used, such as LSC. An example of such measurements is shown in Figure 49. The same method is currently being used in CHANCE for characterisation and monitoring of nuclear waste outgassing. A CRDS instrument for the detection of radiocarbon compounds will be used to study in detail their outgassing rate on various types of waste. A novel instrument for the detection of $H^{36}Cl$ based on CRDS is also being developed. This is the first time that CRDS is used to detect this molecule, which is highly relevant in the case of outgassing from graphite waste. This will advance the use of CRDS as an innovative technique to characterize outgassing of radioactive waste. It will result in a major step forward in the development of the use of CRDS to detect radioactive gas emissions, with the demonstration of its use for a new application.

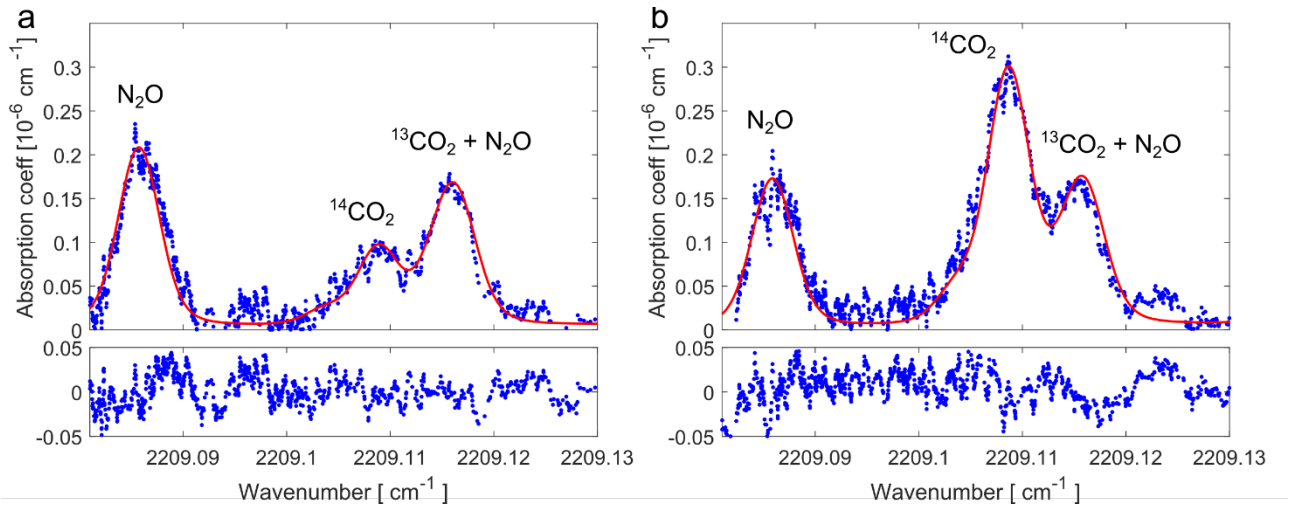

FIGURE 49 : TWO ABSORPTION SPECTRA RECORDED FROM A NUCLEAR POWER PLANT STACK EMISSIONS AT TWO DIFFERENT DATES. THE RING-DOWN DATA IS SHOWN IN BLUE. THE RED LINES REPRESENT THE FITTED SPECTRA AND THE CORRESPONDING RESIDUALS ARE SHOWN BELOW. A CLEAR DIFFERENCE IN THE INTENSITY OF THE $^{14}CO_2$ PEAK AT 2209.109 CM^{-1} IS VISIBLE. FROM THE FITS, THE RADIOCARBON CONCENTRATION CAN BE INFERRED. IN (A) THE CONCENTRATION OF WAS 1.3 PPB WHILE IN (B) IT WAS 4.8 PPB. ABSORPTION LINES OF N_2O ARE ALSO VISIBLE IN THE SPECTRA, ORIGINATING FROM THE TRAPPING PROCEDURE WHICH PRODUCES TRACE AMOUNTS OF THIS MOLECULE

10. Coupling of different techniques

As discussed before, in case of historic waste (in some cases produced more than 50 years ago…), the available information is often incomplete and insufficient information is available for key parameters (like package materials content, alpha-activity, fissile mass …) in order to allow them to enter a final disposal facility.

As discussed in previous sections, a large panel of characterization techniques is available and can be used to characterize radioactive waste. Recent developments show that, instead of handling information from these techniques separately, it could be advantageous to combine them within a coherent description of the waste characteristics, to take advantage of possible correlations between the different types of information (Carasco, 2021). The Euratom H2020 project MICADO also investigates if combinations of different characterization techniques might lead to reducing uncertainties on the radiological inventory of a radioactive waste drum (https://www.micado-project.eu/). In other cases, applying a combination of different techniques could allow reducing uncertainties. Within CHANCE WP3, calorimetry, gamma spectroscopy and neutron measurements are combined to evaluate their mutual synergetic effect on reducing overall measurement uncertainty in waste drums containing Pu sources.

The application of this formalism has been tested mostly in a combination of tomography and gamma spectrometry techniques. Indeed, tomographic information can be used to discretize a given waste package into areas with different densities, allowing to correct for photon attenuation. In standard gamma spectrometry application, the handling of the unknown chemical composition in waste is often problematic and it is commonly assumed that (sections of) the waste drum is homogeneous.

Anh and Dung (2001) presented a model based on tomographic technique that allows correcting for the self-attenuation (lump effect) when performing gamma spectrometry of a waste drum containing a lump of Pu metal. Biard (2013) developed and employed specific computational tools and methods to compute the self-attenuation of a degraded irradiated fuel rod and to automate the processing of gamma spectra in order to analyse the quantitative activity profile of fission products along the bundle. In his study, Biard (2013) relied on the coupling of X-ray tomograms to locate and identify materials and estimate their density, with gamma emission tomograms to locate the fission product distribution inside the bundle.

On the other hand, Jallu *et al.* (2000) used simultaneous active neutron interrogation and induced photofission measurements to quantify fissile (^{235}U, $^{239, 241}$Pu …) and non-fissile ($^{236, 238}$U, $^{238, 240}$Pu …) elements separately in only one (combined) measurement (called SIMPHONIE). The probing source of the SIMPHONIE method is built up by a mixed source of high-energy neutrons and high-energy photons (above the 6 MeV photofission threshold). This is achieved by the combination of an electron accelerator and two targets (Bremsstralung and (γ,n)) (Figure 50). Because of the time difference between photofission and thermal neutron fission, prompt and delayed neutrons released as a result of both processes are not detected at the same time, resulting in a specific shape of the detected signal.

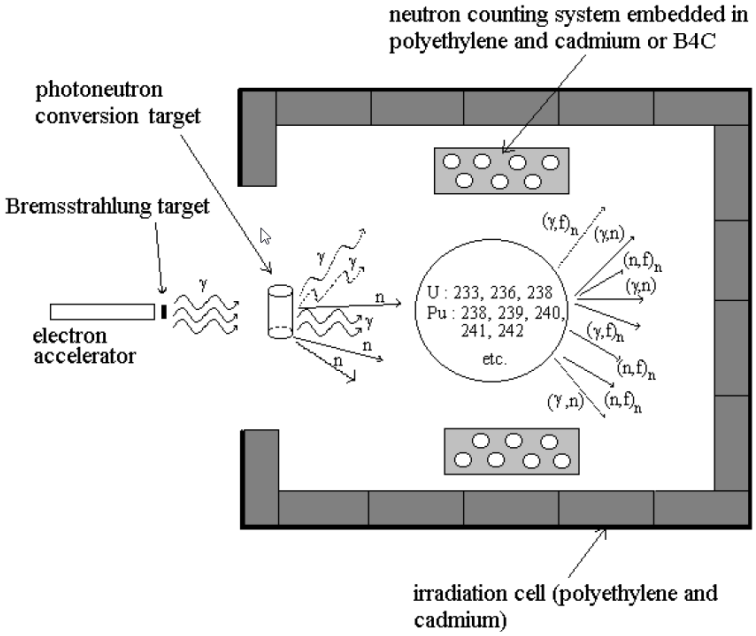

FIGURE 50 : EXPERIMENTAL PRINCIPLE OF THE SIMPHONIE METHOD (JALLU *ET AL.*, 2000)

Carrel *et al.* (2010) reports that coupling between passive and active non-destructive methods allows reducing uncertainties associated to the characterization of waste packages and uses a combination of several non-destructive methods (passive gamma-ray spectrometry, high-energy radiography) with traditional photon activation analysis techniques (altitude scan to detect hot spots, global photofission, photofission tomography) to optimize the quantification of actinide (^{238}U and ^{239}Pu) masses in bulky concrete waste packages (CBFC2-type). Figure 51 shows the results of high-energy radiography of the CBFC2 package. In the case of Pu, good results were obtained between the calculated Pu mass and the declared content. However, regarding the uranium mass, the measured uranium mass was roughly ten times larger than the declared one. In Carrel *et al.* (2014) a combination of active and passive non-destructive methods was used to characterize a nuclear waste package (TE 1060 package of 4.4 tons containing a 220 liter barrel surrounded by a concrete wall) from the 1960s (Figure 52). For historical waste, available information is often incomplete and key parameters (content of the package, alpha activity, fissile mass, …) for further management steps (including transport, storage and disposal) are

frequently lacking. The techniques used included traditional passive (gamma-ray spectrometry, passive neutron counting), high-energy radiography and photon activation analysis methods. The results clearly showed the added value of using non-destructive active methods based on a LINAC in the frame of this characterization. Indeed, in large concrete packages, passive neutron counting and gamma spectroscopy generally suffer from high uncertainties due to large neutron and gamma attenuation effects. LINAC tomography provides density mapping, which is useful for improving the interpretation of gamma or neutron measurements (active or passive) and reducing uncertainties. In addition, High energy X-ray imaging allows determining the areas of interest in the package (objects suspected to contain nuclear materials for instance, which can be confirmed by a passive gamma scanning or a gamma camera) and then focussing a photofission inspection owing to the directional X-ray beam of the LINAC. This approach generally improves the signal (compared to passive measurements) and reduces measurement uncertainties, for instance by detecting the high energy delayed gamma rays emitted by photofission products as described in Delarue et al. 2021 (second reference).

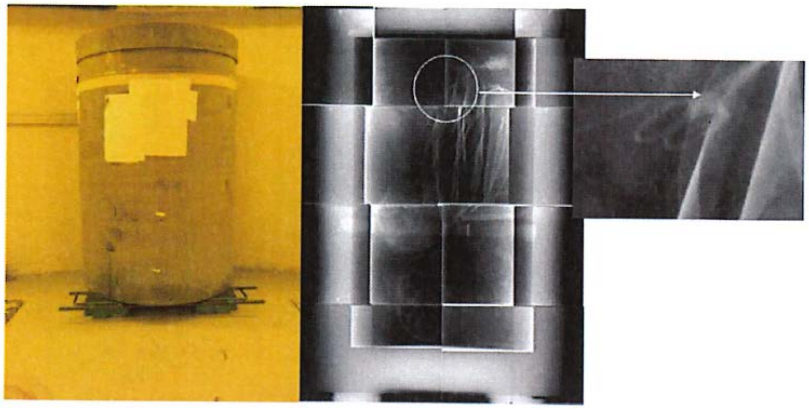

FIGURE 51 : HIGH-ENERGY RADIOGRAPHY OF THE CBFC2 PACKAGE CARRIED OUT IN THE SAPHIR FACILITY (CARREL *ET AL.*, 2010)

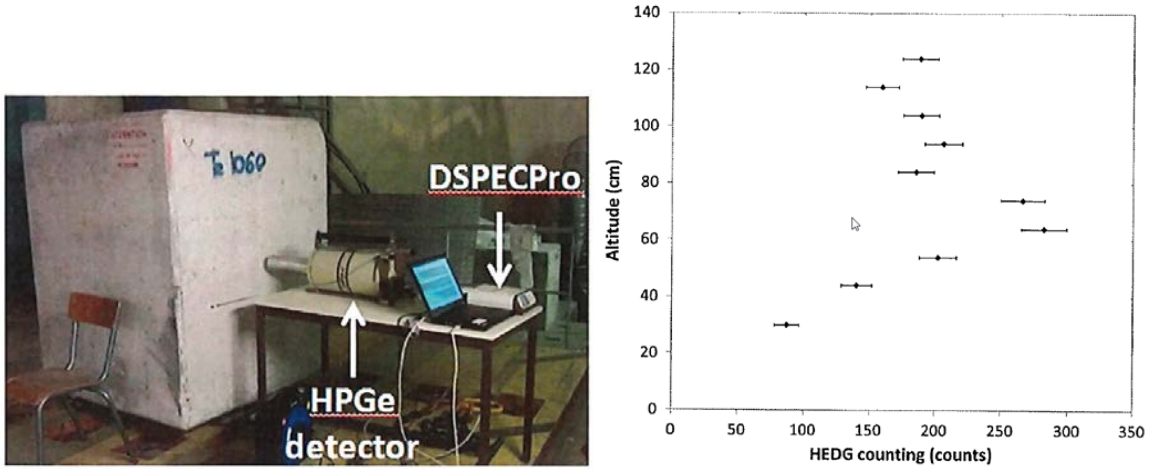

FIGURE 52 : (LEFT) PICTURE OF THE TE 1060 PACKAGE IN EXPERIMENTAL CONFIGURATION FOR GAMMA-RAY SPECTROMETRY ACQUISITION; (RIGHT) RESULTS OF THE ALTITUDE SCAN ANALYSIS BASED ON HIGH-ENERGY DELAYED GAMMA COUNTING (CARREL *ET AL.*, 2014)

11. Bayesian approaches

Carasco (2021) introduced a Bayesian formalism to couple gamma-ray spectrometry and tomographic scans in order to characterize radioactive wastes using available (prior) information and data measurements in a coherent frame. The approach is illustrated numerically for a virtual 200 L waste drum containing a $^{239}PuO_2$ sphere using gamma ray spectrometry with four HPGe detectors placed around the waste and scanning 2 cm thick slices in scanning mode, together with a density map obtained after a tomographic scan to identify drum matrix density and possible heterogeneities. The Pu mass is then inferred by Markov chain Monte Carlo (MCMC) sampling using the random walk Metropolis (RWM) algorithm. Results showed that the use of the density prior information allowed to reduce the Pu mass uncertainty by up to a factor 3, depending on the sphere position.

Researchers from SCK CEN also recently proposed a Bayesian approach to probabilistically infer vertical activity profiles within a radioactive waste drum from segmented gamma scanning (SGS) measurements (Laloy et al., 2021). This approach also resorts to MCMC sampling but using the state-of-the-art Hamiltonian Monte Carlo (HMC) technique and, more importantly, accounts for two important sources of uncertainty: the measurement uncertainty and the uncertainty in the source distribution within the drum. The approach requires calculation of the detector's efficiency for a limited number of extreme cases (point-source and fully homogeneous source for different source locations) and then interpolates between them using a vector of weighting factors that is jointly inferred with the other unknown variables. In addition, the considered efficiency model simulates the contributions of all considered segments (that is, drum sub-volumes) to each count measurement. The approach was demonstrated both synthetically and for a real waste drum package for which the vertical activity distribution of 5 nuclides was resolved. The SCK CEN Bayesian approach is currently being extended to:

1. account for the uncertainties in the vertical density and matrix composition distributions of the considered drum using a similar interpolation approach as for the uncertainty in the source distribution type;
2. combine different measurements techniques (various types of gamma measurements, passive neutron measurements and calorimetry) for a more accurate inference of the vertical activity profile and total activity within the drum.

Another recent development in the field of Bayesian uncertainty quantification of waste drums is the study by Buchërl et al. (2021). Buchërl and co-workers proposed an MCMC-based methodology to infer the 2D activity distribution of a given radionuclide within horizontal drum slices, from SGS data, detailed efficiency calculations and prior information about the waste matrix obtained from transmission measurements done beforehand. Although quite encouraging, the results by Buchërl et al. (2021) show that (1) the derived activity uncertainty is likely to be significantly underestimated if all relevant sources of uncertainty are not accounted for within the Bayesian inversion, and (2) finding a proper regularization for the derived 2D activity fields is an open issue.

Lastly, Clément et al. (2021) developed an MCMC-based approach to determine the total activity of gamma-emitting radionuclides in a waste drum from gamma spectrometry measurements. To alleviate the burden of running a computationally-heavy simulation of the efficiency of the used detector with an MC-based transport code for each waste package for which the mass of a given radionuclide is sought, Clément and co-authors constructed beforehand a surrogate model of the detector's efficiency by means of the Gaussian processes (GP) method for nonlinear regression. This requires running computationally-demanding efficiency calculations for selected waste drum configurations and the chosen detector, to create a sufficiently large training set. After the GP surrogate model has been trained with these data, it can be fed with the known characteristics of the sensed object to get the estimated detector's efficiency, before launching the MCMC inference of the mass of the considered radionuclide. It is worth noting, however, that if the required characteristics of the sensed objects are not known in advance, they can in principle be jointly estimated by MCMC together with the radionuclide mass or activity.

This handful of very recent examples in literature illustrates that Bayesian approaches are very natural to apply in the context of radioactive waste characterization. The main challenges and corresponding R&D needs are in the area of 1) translating computationally demanding process model outputs to efficient and effective surrogates to use in state-of-the-art probabilistic programming languages, 2) finding effective ways to represent and infer the contents of a waste package in high resolution and 3) making the approach accessible to end users, so Bayesian inference can be applied at industrial scale.

12. Mobile measurement systems

The transport of radioactive waste packages, in particular those with high activity or limited knowledge of their radiological, physical and chemical characteristics, is very complex: obtaining the necessary authorizations is time-consuming. In this context, bringing the characterization system to production or storage sites is, therefore, often easier. The mobile measurement system can then increase the processing rates and characterize a large number of objects, such as, for example, the legacy waste packages before their recovery, or nuclear components before cleanup and dismantling operations.

Gamma spectroscopy, which is an easily transportable technique, is already in common use for in situ radioactive waste characterization, but heavier measurement systems (neutron cells, gamma or X-ray imaging) require specific developments, as illustrated by the following examples.

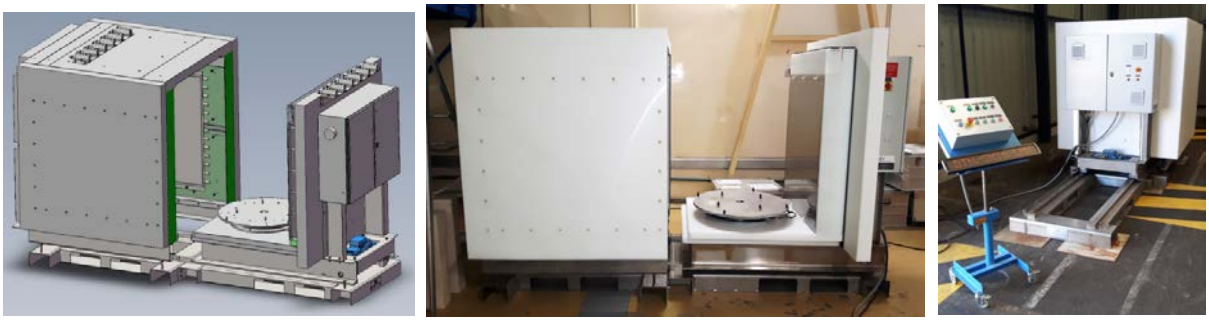

FIGURE 53 TRANSPORTABLE PASSIVE NEUTRON MEASUREMENT SYSTEM USED AT CEA CADARACHE FOR THE CHARACTERIZATION OF LEGACY WASTE

FIGURE 54 PACCMAN, COQUINA, ACTIVE NEUTRON INTERROGATION SYSTEMS PLUGGABLE TO HOT CELLS IN ORDER TO ASSESS URANIUM AND PLUTONIUM IN DIFFICULT TO TRANSPORT HIGH LEVEL WASTES

In the framework of H2020 MICADO project, a transportable passive and active neutron system is being developed to characterize radioactive waste drums up to 400 L.

FIGURE 55 TOMIS, A HIGH-ENERGY X-RAY TOMOGRAPHIC SYSTEM UNDER DEVELOPMENT FOR IN SITU CHARACTERIZATION OF LEGACY WASTE[3]

In the context of the French "PIA ANDRA" Framework, a transportable tomographic imaging system is developed to characterize radioactive waste drums. With the high energy and dose rate of the LINAC (9 MeV and 30 Gy/min at 1 meter from the target), radiographic and 3D tomographic pictures of large concrete drums (up to 500 L) will be performed with millimetre precision and a measurement time of 30 min. This prototype is planned to be operational in 2023 in Cadarache.

TOMIS (low-dose and multi-energy TOMograph In Situ) project aims at:

- developing a powerful tomography tool that can be implemented in situ, for the physical characterization of historic waste, decommissioning waste, as well as possible parts of structures and equipment;
- constituting a non-destructive tool to supplement radiological characterization, by combining X-ray imaging with measurement methods such as gamma spectrometry and neutron measurement.

The particularity of TOMIS is its mobile and adaptable nature, so that it can be used directly on nuclear and nonnuclear sites (storage, disposal, dismantling, etc). The TOMIS tomographic system can thus be moved as close as possible to containers, which are sometimes difficult to transport. In particular, the mobility of TOMIS system requires a reduction in its dose impact, linked to the use of a specific self-shielded linear electron accelerator.

[3] French "PIA ANDRA" Framework, TOMIS Project, CEA and THALES Parners
https://www.andra.fr/sites/default/files/2018-06/Fiche%20projet%20TOMIS%20VF.pdf

Alpha, beta, gamma and neutron cameras or autoradiography systems used in D&D applications are not illustrated here because they are not used (or just qualitatively) to characterize radioactive waste packages. However, techniques used in cleaning and D&D operations are detailed in ref. (CEA, 2018).

In a consortium with other companies, Belgian firm DSI is developing a mobile unit (Figure 56) for radioactive waste analysis which will combine for the first time X-ray imagery and radioactive isotopes characterization using gamma spectroscopy ("SYSCADE" project, https://mobile-radiography.com/). The unit targets specifically (non-conditioned) historical/legacy waste and combines a 320 kV (450 kV as an option) X-ray source and a digital linear detector for real-time digital radiography with a high-resolution gamma spectrometry systems with HPGe detector that can be used in 3 modes: "in situ" measurement mode to estimate the total activity content in each drum, SGS mode, and SGS mode combined with angular measurement to localize hot spots in waste drums.

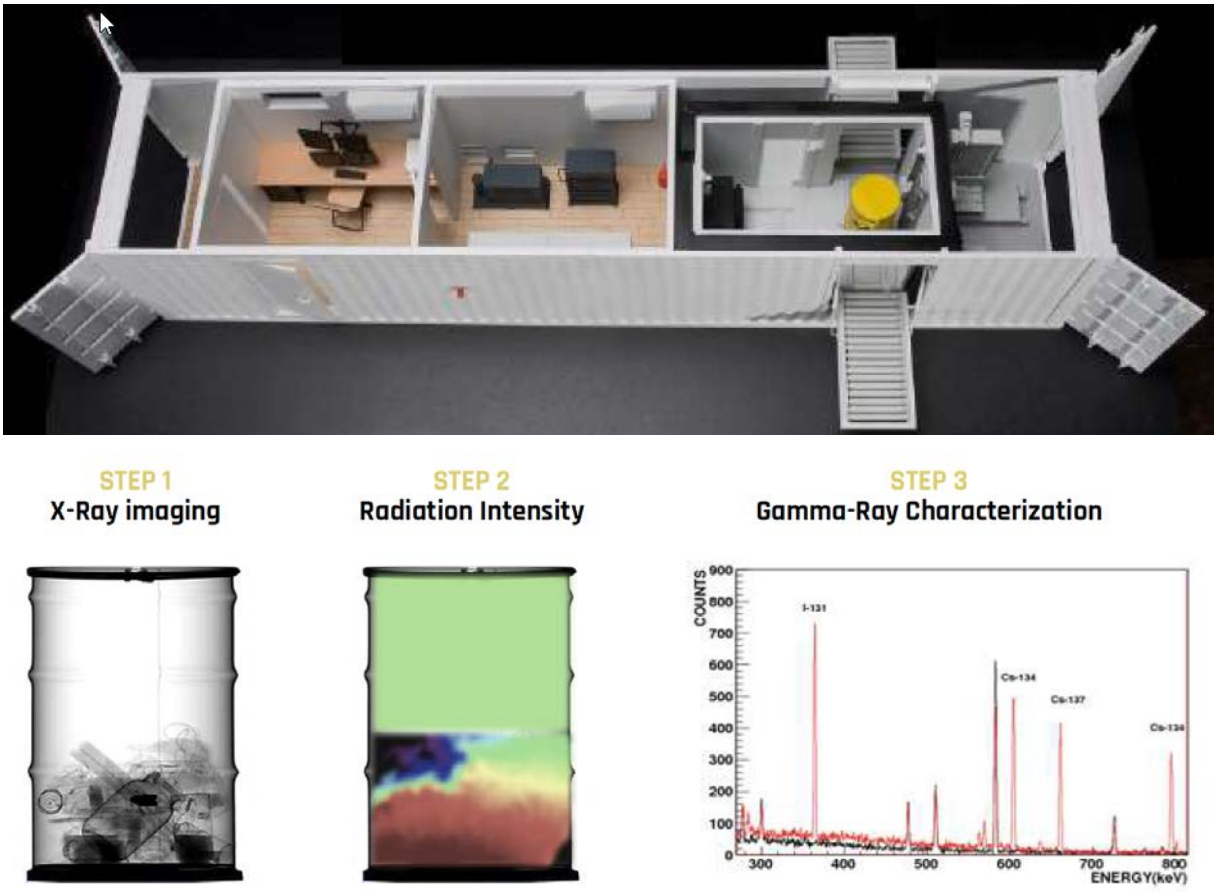

FIGURE 56 : SYSCADE mobile radioactive waste inspection and characterization unit (https://mobile-radiography.com/)

14. Conclusion

The R&D needs in nondestructive nuclear measurements and in radio-chemical analyses are constantly increasing to address waste management challenges:

- legacy radioactive waste characterization to transport them from their interim storage to a final safe repository,
- radioactive waste categorization in the view of acceptance into an appropriate final repository (surface vs. geological),
- regulatory radioactive waste examinations (super-controls),
- criticality control before transportation, storage or repository,
- characterization of D&D wastes,

The main characterization needs concern:

- radiological content for handling (recovery, transportation), interim storage and long-term repository: short, medium and long life isotopes, high gamma or neutron emitters, dose rate, fissile mass for criticality purpose, thermal power, etc.
- chemical properties: presence of toxic chemicals, reactive products, corrosion, complexing molecules, forbidden substances, etc.
- physical properties of the waste packages: mechanical resistance, containment properties of the containers and matrices, conformity of the packaging, presence of voids, swelling, etc.
- mobile systems to perform non-destructive (and even radio-chemical analyses) onsite, in legacy waste interim storages or D&D sites.

This report summarizes the state-of-the-art in non-destructive waste characterization addressing many of these needs. Distinction can be made between passive and active measurements allowing to obtain insights into the inventory of easy-to-measure and difficult-to-measure radioisotopes and, in the case of active measurements, also of toxic elements, and imaging techniques based on low-energy (for non-conditioned, raw waste) or high-energy (for conditioned waste) X-rays to allow visualization of the inner contents of a waste drum or waste package. These techniques are complemented by recent developments which tackle specific characterization challenges frequently associated with specific waste forms. Examples were highlighted related to calorimetry, muon tomography and cavity ring-down spectroscopy, three techniques which are further developed within the CHANCE project. Finally, new developments include combination of techniques and Bayesian approaches which aim to reduce typical uncertainties frequently encountered when dealing with heterogeneous wastes or wastes with unknown physico-chemical content.

Still, new developments are underway and are still needed to overcome problems encountered with currently available techniques. To this end, important R&D challenges include:

- high energy and dual energy X-ray imaging to characterize the physico-chemical content and structure of large and dense waste packages;
- photofission (active photon interrogation with high energy X-rays) to measure and identify nuclear materials in large and dense packages;
- neutron coincidence counting with alternatives to ^{3}He detectors (now too expensive);
- active neutron interrogation to measure the fissile mass in high-level waste (high gamma irradiation and high neutron emitters like curium isotopes);

- neutron activation analysis to characterize the chemical elements (including toxic chemicals) or the long-lived isotopes that are difficult or impossible to measure by gamma-ray spectroscopy;
- attenuation corrections (combined matrix and localization effects) based on Machine Learning techniques and intensive calculations (e.g. Monte Carlo simulations) to establish predictive models of the searched parameters (activity, position of the radionuclides, etc.);
- bayesian approaches to take advantage of all the available information (measurements, expert knowledge, X-ray radiographic or tomographic pictures, etc.) in view to iteratively adjust the prior distributions of the activity, radionuclide location, matrix density and composition, etc. until the model fits as well as possible the available measured data: for instance the different net peak areas of a radionuclide in a gamma-ray spectroscopy (e.g. ^{239}Pu), the neutron counts of individual detection blocks distributed all around the package, the signals measured with different angles, different fields of view, or at different heights with respect to the package, etc.
- mobile measurement systems: The transport of radioactive waste packages, in particular those with high activity or limited knowledge of their radiological, physical and chemical characteristics, is very complex and obtaining the necessary authorizations is time-consuming, with unguaranteed success. In this context, bringing the characterization device to production or storage sites is often easier. The mobile measurement system can significantly increase the number of waste package characterizations.

For the techniques studied in the framework of the Chance project, great improvements has been done in the development, in the date acquisition and in modelling but future needs remains namely:

- For Muon tomography:
    - development of algorithms for the monitoring of smaller gas bubbles in bituminized waste to study the formation and behaviour of the gas bubbles and assess the safety risks of the bubbles;
    - development of algorithms for spotting small cracks in concrete filled waste drums to evaluate the depth and width of these and assess the safety risks;
    - improvements in the algorithms for material identification for objects inside the waste drums to limit the data taking time and identify smaller objects;
    - imaging of the contents of CASTOR drums; not only to verify that the fuel rods are present, but also their structural integrity and imaging the contents of waste silos;
- For calorimetry:
    - developments to improve insulation of the calorimeter to measure smaller effect and be able to work in facility with important room temperature fluctuation
    - developments to decrease measurement time and to increase accuracy in the quantification of radioelements emitting high gamma ray
- For CRDS for outgassing monitoring, future developments will focus on validating the method in real industrial conditions. Characterization of the method in different gas matrices will also be needed to ensure that the CRDS works in all situations. Finally, simultaneous detection of different radionuclides of interest (e.g. C-14, tritium, Cl-36) will be implemented in order to have a single system capable of detecting all relevant radioactive species present in outgasses;

15. Glossary

A&PCT: active & passive computed tomography

AWCC: active well coincidence counting

CASTOR®: Cask for storage and transport of radioactive material

CRDS: cavity ring-down spectroscopy

CRT: cathode ray tube

CSS: Compton Suppression Spectrometer

CT: Computed Tomography

DA: Destructive analysis

DDT or DDA: Differential Die-Away Technique

DN: delayed neutron signal

DR: digital radiography

D-T: deuterium-tritium

DTM: difficult-to-measure

ENTRAP: European network of testing facilities for the quality checking of radioactive waste packages

ESS: European Spallation Source

ETM: easy-to-measure nuclides

FEP: full energy peak

FIGARO: Fissile Interrogation using Gamma Rays from Oxygen

GP: Gaussian processes

GURU: geometry uncertainty reduction utility

HEDG: high-energy delayed gamma signal

HPGe: high-purity Germanium

HTO: tritiated water

ISOCS: in situ counting object system

IUE: ISOCS uncertainty estimator

KN: key nuclide

LabSOCS: laboratory sourceless calibration software

Linac: linear accelerator of electrons

LSC: Liquid scintillation counting

MEDINA: multi element determination based on instrumental neutron activation

MNCP: Monte Carlo N-Particle code

NAA: neutron activation analysis

NCC: neutron coincidence counting

NDA: nondestructive assay

NDE: nondestructive examination

NMC: neutron multiplicity counting

NORM: naturally occurring radioactive materials

NRF: nuclear resonance fluorescence

PGAA: prompt gamma activation analysis

P&DGNAA: prompt and delayed gamma neutron activation analysis

PoCA: point of closest approach

PTC: peak to Compton

QCLs: Quantum cascade lasers

RWM: random walk Metropolis algorithm

RPC: resistive plate chambers

SAPHIR: Active Photon and Irradiation System

SF: scaling factor

SGS: Segmented gamma scanners

SNMs: special nuclear materials

SNS: segmented neutron scanning

TCM: time correlation methods

TGS: Tomographic gamma scanning

WAC: waste acceptance criteria

VLLW: very low-level waste

XRF: X-ray fluorescence

Z: atomic number

16. References

Abd, S.M., Al-Musawi, I.H., Hussein, J.N. (2016) Calculating dose conversion factor experimentally for Cs-137 radionuclide for radioactive waste in metallic drums, *International Journal of Current Engineering and Technology*, **6 (6)**, 2091-2093.

Agelou, M., Doré, D., Dupont, E., Carrel, F., Gmar, M., Ledoux, X., Poumarède, B., Pérot, B., Bernard, P. (2009) Detection special nuclear materials inside cargo containers using photofission, *IEEE Nuclear Science Symposium Conference Record*, N13-234, 936-939.

Anh, T. H., Dung, T. Q. (2001) Evaluation of performance of gamma tomographic technique for correcting lump effect in radioactive waste assay, *Annals of Nuclear Energy*, **28**, 265-273.

Antoni R., Passard C., Loridon J., Perot B., et al. (2014) Matrix effect correction with internal flux monitor in radiation waste characterization with the Differential Die-away Technique, *IEEE Transactions on Nuclear Science*, **61 (4)**, 2155-2160.

Artaud J-L., Pérot B. et al., (2021) Compton suppression detector dedicated to the measurement of bituminized waste drums from the Marcoule reprocessing plant using gamma spectrometry, Proceedings of the ASME 2001 8th International Conference on Radioactive Waste Management and Environmental Remediation, Bruges, Belgium. September 30–October 4, 2001, 949-953.

Bai, Y.F., Mauerhofer, E., Wang, D.Z., Odoj, R. (2009) An improved method for the non-destructive characterization of radioactive waste by gamma scanning, *Appl. Rad. Isot.*, **67**, 1897-1903.

Berden, G., Peeters, R. & Meijer, G. (2000) Cavity ring-down spectroscopy: Experimental schemes and applications. *Int. Rev. Phys. Chem.* **19**, 565 -607.

Bernardi R.T., Martz H.E. (1995) Nuclear waste drum characterization with 2 MeV x-ray and gamma-ray tomography, *Proc. SPIE 2519, X-ray and ultraviolet sensors and applications,* SPIE's 1995 International Symposium on Optical Science, Engineering and Instrumentation, 1995, San Diego, CA, USA, doi: 10.1117/12.211897.

Biard, B. (2013) Quantitative analysis of the fission product distribution in a damaged fuel assembly using gamma-spectrometry and computed tomography for the Phébus FPT3 test, *Nuclear Engineering and Design*, **262**, 469-483.

Bracken D.S., Biddle R. S., Carrillo L. A., Hypes P. A., Rudy C. R., Schneider C. M., Smith M. K. (2002) Application guide to safeguards calorimetry, Los Alamos National Laboratory Manual LA-13867-M.

Bray C., Pailloux A., Plumeri, S. (2015) Tritiated water detection in the 2.17µM spectral region by cavity ring down spectroscopy. *Nucl. Instruments Methods Phys. Res. Sect. A Accel. Spectrometers, Detect. Assoc. Equip.* **789**, 43–49.

Braunroth T., Berner N., Rowold F., Péridis M., Stuke M. (2021) Muon radiography to visualise individual fuel rods in sealed casks, *EPJ Nuclear Sci. Technol.* **7** , 12.

Bücherl T., Lierse von Gostomski Ch. (2001) Synopsis of neutron assay systems. Comparison of neutron determining systems and measuring procedures for radioactive waste packages. Report WG-A-02, European network of testing facilities for the quality checking of radioactive waste packages – Working Group A.

Bücherl T., Kalthoff O., Lierse von Gostomski Ch. (2017) A feasibility study on reactor based fission neutron radiography of 200-l waste packages, *Physics Procedia*, **88**, 64-72.

Bücherl T., Söllradl S. (2015) NECTAR: Radiography and tomography station using fission neutrons, *Journal of large-scale research facilities*, 1, A19, https://jlsrf.org/index.php/lsf/article/view/45

Bücherl T., Rummel S., Kalthoff O. (2021) A Bayesian method for the evaluation of segmented gamma scanning measurements – Description of the principle, *Nucl. Instrum. Methods Phys. Res. A.*, **1019**, 165887.

Caldwell J.T., Hast R.D., Herrera G.C., Kunz W.E., Shunk E.R. (1986) The Los Alamos Second-Generation System for Passive and Active Neutron Assays of Drum-Size Containers, LA-10774-MS.

Calvet E. (1948) Nouveau microcalorimètre différentiel et à compensation, C. R. Hebd. Séances Acad. Sci., **226**, 1702-1704.

Campbell L.W., Smith L.E., Misner A.C. (2011) High-energy delayed gamma spectroscopy for spent nuclear fuel assay, *IEEE Transactions on Nuclear Science*, **58 (1)**, 231-240.

Carasco C. (2021) Coupling gamma ray spectrometry and tomography in a Bayesian frame, *Nucl. Instrum. Methods Phys. Res. A.*, **990**, 164985.

Carrel F., Gmar M., Lainé F., Loridon J., Ma J-L., Passard C. (2006) Identification of actinides inside nuclear waste packages by measurement of fission delayed gammas, *IEEE Nuclear Science Symposium Conference Record,* **28-1**, 909-913.

Carrel F., Agelou M., Gmar M., Lainé F., Poumaréde B., Rattoni B. (2010) Measurement of plutonium in large concrete radioactive waste packages by photon activation analysis, *IEEE Transactions on Nuclear Science,* **57 (6)**, 3687-3693.

Carrel F., Agelou M., Gmar M., Lainé F. (2011) Detection of high-energy delayed gammas for nuclear waste packages characterisation, *Nucl. Instrum. Methods Phys. Res. A.*, **652**, 137-139.

Carrel F., Charbonnier B., Coulon R., Lainé F., Normand, S., Salmon, C., Sari, A. (2014) Characterization of old nuclear waste packages coupling photon activation analysis and complementary non-destructive techniques, *IEEE Transactions on Nuclear Science,* **61 (4)**, 2137-2143.

CEA Nuclear Energy Division Monograph (2018) Cleanup and dismantling of nuclear facilities, ISSN 1950-2672 http://www.cea.fr/english/Documents/scientific-and-economic-publications/clean-up-dismantling-nuclear-facilities-monograph.pdf

Cha G.Y., Kim S.Y., Lee J.M., Kim Y.S. (2016) The effects of impurity composition and concentration in reactor structure material on neutron activation inventory in pressurized water reactor, *JNFCWT*, **14 (2)**, 91-100 http://www.jnfcwt.or.kr/journal/article.php?code=41704

Checchia P, Benettoni M., Bettella G., Conti E., Cossutta L., Furlan M., Gonella F., Klinger J., Montecassiano F., Nebbia G., Pegoraro M., Pesente S., Rigoni Garola A., Urbani M., Viesti G., Vanini S., Zumerle G. (2019) INFN muon tomography demonstrator: past and recent results with an eye to near-future activities., *Phil. Trans. R. Soc. A*, **377** (2137) 20180065.

Clément A., Saurel N., Perrin G., Gombert N. (2021) Bayesian approach for multigamma radionuclide quantification applied on weakly attenuating nuclear waste drums, *IEEE Transactions on Nuclear Science*, **68**(9), 2342-2349.

Croft S., Bracken D.S., Kane S.C., Venkataraman R., Estep R.J. (2006) Bibliography of tomographic gamma scanning methods applied to waste assay and nuclear fuel measurements, *Conference: 47th annual meeting of the institute of nuclear materials management, Nashville, TN, USA.*

Dobrowolska M., Velthuis J., Frazão L. , Kikoła D. (2018) A novel technique for finding gas bubbles in the nuclear waste containers using Muon Scattering Tomography, *Journal of Instrumentation*, **13**, P05015.

Delarue M., Simon E., Pérot B. et al. (2021) Measurement of cumulative photofission yields of 235U and 238U with a 16 MeV Bremsstrahlung photon beam, *Nuclear Inst. and Methods in Physics Research A,* **1011,** 165598, https://doi.org/10.1016/j.nima.2021.165598

Delarue M., Simon E., Pérot B., et al., (2021) Localization of nuclear materials in large concrete radioactive waste packages using photofission delayed gamma rays, ANIMMA 2021 International Conference, June 2021, Prague, Czech Republic, EPJ Web of Conferences 253, 08003.

De Simone D., Favalli A., MacArthur D., Moss C., Thron J. (2010) Review of active interrogation techniques and considerations for their use behind an information barrier, Los Alamos National Laboratory, LA-UR-10-06958.

De Stefano R., Carasco C., Pérot B., Simon E., Nicol T., Mauerhofer E. (2019) Feasibility study of fissile mass detection in 870 L radioactive waste drums using delayed gamma rays from neutron-induced fission, *J. Radioanal. Nucl. Chem.*, **322**, 1185-1194.

Dighe P.M., Goswami A., Das D., Mittal K.C., Pithawa C.K. (2014) Quantification of fissionable materials in pure and mixed form using photofission, *Nucl. Instrum. Methods Phys. Res. A.*, **737**, 242-247.

Dighe P.M., Vinod M., Thombare S.G., Prafulla S., Kamble N.R., Kamble L.P., Bhatnagar P.V., Das D. (2019) Photofission method for quantification of fissile material in large drums, *Nucl. Instrum. Methods Phys. Res. A.*, **946**, 162624.

Done L., Tugulan L.C., Dragolici F., Alexandru C. (2014) Gamma-ray spectrometry method used for radioactive waste drums characterization for final disposal at National Repository for Low and Intermediate Radioactive Waste – Baita, Romania, *Applied Radiation and Isotopes*, **87**, 380-383.

Dulama C.N., Dulama M., Dobrin R., Pavelescu M. (2010) Estimation of the gamma dose rate for homogeneous waste containers, *Rom. Journ. Phys.*, **56** (9-10), 1136-1142.

Durham J. M., Poulson D., Bacon J., Chichester D. L., Guardincerri E., Morris C. L., Plaud-Ramos K., Schwendiman W., Tolman J. D., Winston P. (2018) Verification of Spent Nuclear Fuel in Sealed Dry Storage Casks via Measurements of Cosmic-Ray Muon Scattering, *Phys. Rev. Applied,* **9**, 044013.

Dyrcz P., Frosio Th., Menaa N., Magistris M., Theis C. (2021) Qualification of the activities measured by gamma spectrometry on unitary items of intermediate-level radioactive waste from particle accelerators, *Appl. Rad. Isot.*, **167**, 109431.

Engelberg D., Pattrick R.A.D., Wilson C., McCrae R., Withers P.J. (2012) Three-dimensional imaging of inhomogeneous lithologies using x-ray computed tomography: characterization of drill core from the Borrowdale Volcanic Group, *Mineralogical Magazine,* **76 (8)**, 2931-2938.

Estre N., Eck D., Pettier J.-L., Payan E., Roure C., Simon E. (2015) High-energy X-ray imaging applied to nondestructive characterization of large nuclear waste drums, *IEEE Transactions on Nuclear Science*, **62 (6)**, 3104-3109.

Estre N., Eck D., Eleon C., Kistler M., Payan E., Tamagno L., Tisseur D. (2018) Design of a very efficient detector for High Energy Tomography*, NSS 2018, 10-17 November 2018, Sydney, Australia.*

Fleisher A. J., Long D. A., Liu Q., Gameson L., Hodges, J. T. (2017) Optical Measurement of Radiocarbon below Unity Fraction Modern by Linear Absorption Spectroscopy. *J. Phys. Chem. Lett.* **0**, 4550-4556.

Frazão L., Velthuis J., Thomay C., Steer C. (2016) Discrimination of high-Z materials in concrete-filled containers using muon scattering Tomography, Journal of Instrumentation, **11**, 07020.

Frosio Th., Menaa N., Duchemin C., Riggaz N., Theis C. (2020) A new gamma spectroscopy methodology based on probabilistic uncertainty estimation and conservative approach, *Appl. Rad. Isot.*, **155**, 108929.

Frosio Th., Bertreix P., Magistris M., Menaa N., Michaud R., Rimlinger M., Theis C., Ulrici L., Zaffora B. (2020B) An enhanced characterization process for the elimination of very low level radioactive waste in particle accelerators, *Appl. Rad. Isot.*, **166**, 109312.

Galli I., Bartalini S., Borri S., Cancio P., Mazzotti D., De Natale P., Giusfredi G. (2011) Molecular Gas Sensing Below Parts Per Trillion: Radiocarbon-Dioxide Optical Detection. *Phys. Rev. Lett.* **107**, 270802.

Galli, I. *et al.* (2016) Spectroscopic detection of radiocarbon dioxide at parts-per-quadrillion sensitivity. *Optica* **3**, 385-388.

Genoud G., Vainio M., Phillips H., Dean J., Merimaa M. (2015) Radiocarbon dioxide detection based on cavity ring-down spectroscopy and a quantum cascade laser. *Opt. Lett.* **40**, 1342-1345.

Gmar M., Jeanneau F., Lainé F., Makil H., Poumarède B., Tola F. (2005) Assessment of actinide mass embedded in large concrete waste packages by photon interrogation and photofission, *Appl. Rad. Isot.*, **63**, 613-619.

Gmar M., Jeanneau F., Lainé F., Poumarède B. (2006) Photofission tomography of nuclear waste packages, *Nucl. Instrum. Methods Phys. Res. A.*, **562**, 1089-1092.

Göbbels C., Krings T., Mauerhofer E. (2015) On the applicability of $LaBr_3$ detectors in the non-destructive characterization of radioactive waste drums, *J. Radioanal. Nucl. Chem.*, **303**, 2399-2405.

Hajdu D., Dian E., Gméling K., Klinkby E., Cooper-Jensen C.P., Osan J., Zagyvai P. (2021) Experimental study of concrete activation compared to MCNP simulations for safety of neutron sources, *Appl. Rad. Isot.*, **171**, 109644.

Hansen J. S. (2004) Application guide to tomographic gamma scanning of uranium and plutonium, LANL report, LA-UR-04-7104.

IAEA (2007) Strategy and methodology for radioactive waste characterization, IAEA-TECDPOC-1537, March 2007, http://wwwpub.iaea.org/MTCD/publications/PDF/te_1537_web.pdf

IAEA (2004) Management of Waste Containing Tritium and Carbon-14. Technical Reports Series 421; International Atomic Energy Agency, Vienna.

IAEA (2009) Determination and Use of Scaling Factors for Waste Characterization in Nuclear Power Plants, Nuclear Energy Series No NW-T-1.18.

Jang D., Lee D. Kim J. (2017) Radioactivation analysis of concrete shielding wall of cyclotron room using Monte Carlo simulation, *J. Korean Soc. Radiol.*, **11 (5)**, 335-341. https://doi.org/10.7742/jksr.207.11.5.335.

Jallu F., Lyoussi A., Passard C., Payan E., Recroix H., Nurdin G., Buisson A., Allano J. (2000) The simultaneous neutron and photon interrogation method for fissile and non-fissile element separation in radioactive waste drums, *Nucl. Instrum. Methods Phys. Res. B*, **170**, 489-500.

Jang D., Lee D., Kim J. (2017) Radioactivation analysis of concrete shielding wall of cyclotron room using Monte Carlo simulation, *J. Korean Soc. Radiol.*, **11 (5)**, 335-341. https://doi.org/10.7742/jksr.207.11.5.335.

Jo W. J., An S. J., Kim H.-I., Lee C. Y., Chung H., Chung Y. H. (2015) Design and Characterization of a Small Muon Tomography System, *Journal of the Korean Physical Society*, **66** (4), 585 – 591.

Jones J.L., Yoon W.Y., Norman D.R., Haskell K.J., Zabriskie J.M., Watson S.M., Sterbentz J.W. (2005) Photonuclear-based nuclear material detection system for cargo containers, *Nucl. Instrum. Methods Phys. Res. B*, **241**, 770-776.

Jonkmans G., Anghel V.N.P., Jewett C., Thompson M. (2013) Nuclear waste imaging and spent fuel verification by muon tomography, *Annals of Nuclear Energy*, **53**, 267-273.

Jossens G., Mathonat C., Bachelet F. (2015) Nuclear waste measurement calorimeter for very large drums with 385 litres sample volume, Fusion Science and Technology **67 (2)**, 390-393.

Jossens G,. Mathonat C., Hubinois J.-C., Godot A., Bachelet F. (2018) Flow-measuring differential calorimeter, Patent number: 10078061, Type: Grant, Filed: January 14, 2014, Date of Patent: September 18, 2018.

Kemp R.B. (1988) Nonscanning calorimetry, in Handbook of Thermal analysis and calorimetry, Vol. 1: Principles and Practice, M.E. Brown editor, Elsevier Science B.V.

Kinlaw M.T., Hunt A.W. (2006) Fissionable isotope identification using the time dependence of delayed neutron emission, *Nucl. Instrum. Methods Phys. Res. A.,* **A562**, 1081-1084.

Kistler M., Estre N., Merle E. (2018) Simulated Performances of a Very High Energy Tomograph for Non-destructive Characterization of large objects, ANIMMA 2017, International Conference on Advancements in Nuclear Instrumentation Measurement Methods and their Applications, 19-23 June, Liège, Belgium. IEEE Transactions on Nuclear Science, Vol. 65, No. 9, September 2018.

Kopp A. (2020) Non-destructive assay of nuclear waste containers using muon scattering tomography in the Horizon2020 CHANCE project, ANIMMA 2019, EPJ Web of Conferences 225, 06008.

Krings T., Mauerhofer E. (2012) Reconstruction of the isotope activity content of heterogeneous waste drums, *Appl. Rad. Isot.*, **70**, 1100-1103.

Laloy E., Rogiers B., Bielen A., Boden S. (2021) Bayesian inference of 1D activity profiles from segmented gamma scanning of a heterogeneous radioactive waste drum. *Applied Radiation and Isotopes*, **175**, 109803. https://doi.org/10.1016/j.apradiso.2021.109803.

Lee B., Kim Y., L'yi W., Kim J., Seo B., Hong S. (2021) Radiological analysis for radioactivity depth distribution in activated concrete using gamma-ray spectrometry, *Applied Radiation and Isotopes*, **169**, 109558.

Lehmuskoski, J et al. (2021) In situ monitoring of radiocarbon emissions in nuclear facilities. In preparation.

Ma J.-L., Carasco C., Perot B., Mauerhofer E., Kettler J., Havenith A. (2012) Prompt gamma neutron activation analysis of toxic elements in radioactive waste packages, *Appl. Rad. Isot.*, **70**, 1261-1263.

Mason J.A. (1982) The use of calorimetry for plutonium assay, Safeguards R&D Project, AERE Harwell, December 1982.

Marchais T., Pérot B., Carasco C., Allinei P.-G., Chaussonnet P., Ma J.-L., Toubon H. (2018) Gamma-ray spectroscopy measurements and simulations for uranium mining, *EPJ Web of Conferences*, **170**, 05003, *ANIMMA 2017*, https://doi.org/10.1051/epjconf/201817005003

Martz H.E., Decman D.J., Roberson G.P., Johansson E.M., Keto E. R. (1996) Application of gamma-ray active and passive computed tomography to nondestructively assay TRU waste, UCRL-JC-123342.

Mauerhofer E., Havenith A. (2014) The MEDINA facility for the assay of the chemotoxic inventory of radioactive waste pakcages, *J. Radioanal. Nucl. Chem.*, **302**, 483-488.

Mauerhofer E., Havenith A., Kettler J. (2016) Prompt gamma neutron activation analysis of a 200 L steel drum homogeneously filled with concrete, *J. Radioanal. Nucl. Chem.*, **309**, 273-278.

McCartt A. D., Ognibene T. J., Bench G. & Turteltaub K. W. (2016) Quantifying Carbon-14 for Biology Using Cavity Ring-Down Spectroscopy. Anal. Chem., **88**, 8714- 8719.

Mees F., Swennen R., Van Geet M., Jacobs P. (eds) (2003) *Applications of X-ray Computed Tomography in the Geosciences*, Geological Society, London, Special Publications, **215**, 1-6, 0305-8719/03/$15.

Mertz A., Hogenbirk A. (2017) Optimal shape of a gamma-ray collimator: single vs double knife edge, *EPJ Web of Conferences*, **153**, 07018.

Micklich B.J., Smith D.L., Massey T.N., Fink C.L., Ingram D. (2003) FIGARO: detecting nuclear materials using high-energy gamma-rays, *Nucl. Instr. Methods Phys. Res. A.*, **505**, 466-469.

Mildenberger F., Mauerhofer E. (2016) Prompt gamma neutron activation analysis of large heterogeneous samples composed of concrete and polyethylene, *J. Radioanal. Nucl. Chem.*, **309**, 1265-1269.

Mildenberger F., Mauerhofer E. (2017) Cyclic neutron activation analysis of large samples with a pulsed 14 MeV neutrion source, *J. Radioanal. Nucl. Chem.*, **311**, 917-927.

Morris C. L., Alexander C. C., Bacon J. D., Borozdin K. N., Clark D. J., Chartrand R., Espinoza C. J., Fraser A. M., Galassi M. C., Green J. A., Gonzales J. S., Gomez J. J., Hengartner N. W., Hogan G. E., Klimenko A. V., Makela M. F., McGaughey P., Medina J. J., Pazuchanics F. E., Priedhorsky W. C., Ramsey J. C., Saunders A., Schirato R. C., Schultz L. J., Sossong M. J., Blanpied G. S. (2008) Tomographic Imaging with Cosmic Ray Muons, *Science and Global Security*, **16**, 37–53.

Mozin V., Campbell L., Hunt A., Ludewigt B. (2012) Delayed gamma-ray spectroscopy for spent nuclear fuel assay, *Journal of Nuclear Materials Management*, Volume **XL, No. 3**, 78-87.

Naqvi A.A., Garwan M.A., Nagadi M.M., Maslehuddin M., Al-Amoudi O.S.B., Khateeb-ur-Rehman (2009) Non-destructive analysis of chlorine in fly ash cement concrete, *Nucl. Instrum. Methods Phys. Res. A*, **607**, 446-450.

Naqvi A.A., Nagadi M.M., Garwan M.A., Al-Amoudi O.S.B., Maslehuddin M., Khateeb-ur-Rehman, Raashid M. (2010) Non destructive analysis of concrete for corrosion studies utilizing nuclear technique, *Atoms for Peace an International Journal,* International Symposium on the Peaceful Applications of Nuclear Technology in the GCC Countries, Jeddah, 2008.

Naqvi A.A., Maslehuddin M., Garwan M.A., Nagadi M.M., Al-Amoudi O.S.B., Khateeb-ur-Rehman, Raashid M. (2011) Estimation of minimum detectable concentration of chlorine in blast furnace slag cement concrete, *Nucl. Instr. Methods Phys. Res. B.,* **269**, 1-6.

NEA (2017) Radiological characterisation from a waste and materials end-state perspective. Practices and experience, NEA No. 7373, Nuclear Energy Agency – Organisation for Economic Co-operation and Development, Radioactive Waste Management.

Nicol T., Pérot B., Carasco C., Brackx E., Mariani A., Passard C., Mauerhofer E., Collot J. (2014) ^{235}U and ^{239}Pu characterization in radioactive waste using neutron-induced fission delayed gamma rays, *2014 IEEE Nuclear Science Symposium and Medical Imaging Conference (NSS/MIC)*, 10.1109/NSSMIC.2014.7431204

Nicol T., Carasco C., Perot B., Ma J.L., Payan E., Mauerhofer E ., Havenith A., Collot J. (2016) Quantitative comparison between PGNAA measurements and MCNPX simulations, *J. Radioanal. Nucl. Chem.*, **308**, 671-677.

Nicol T., Pérot B., Carasco C., Brackx E., Mariani A., Passard C., Mauerhofer E., Collot J. (2016B) Feasibility study of ^{235}U and ^{239}Pu characterization in radioactive waste drums using neutron-induced fission delayed gamma rays, *Nucl. Instr. Methods Phys. Res. A*, **832**, 85-94.

Norman E.B., Prussin S.G., Larimer R.-M., Shugart H., Browne E., Smith A.R., McDonald R.J., Nitsche H., Gupta P., Frank M.I., Gosnell T.B. (2004) Signatures of fissile materials: high-energy γ rays following fission, *Nucl. Instrum. Methods Phys. Res. A.*, **521**, 608-610.

O'Keefe A. & Deacon D. A. G. (1988) Cavity ring-down optical spectrometer for absorption measurements using pulsed laser sources. Rev. Sci. *Instrum.*, **59**, 2544.

Patra S., Agarwal C., Chaudhury S. (2019) Full energy peak efficiency calibration for the assay of large volume radioactive waste drums in a segmented gamma scanner, *Appl. Rad. Isot.*, **144**, 80-86.

Pérot B., Jallu F., Passard C., Gueton O., Allinei P.-G., *et al*. (2018) The characterization of radioactive waste : a critical review of techniques implemented or under development at CEA, France. *EJP N – Nuclear Sciences & Technologies*, EDP Sciences, 2018, **4 (3)** 10.1051/epjn/2017033. cea-01794043.

Pettier J.L., Eck D., Thierry R. (2004) High energy X-ray imagery on large or dense objects: definition and performance studies of measurement devices by simulation, In: *Emerging technologies in non destructive testing, Van Hemelrijck, Anastasopoulos & Melanitis (eds), A.A. Balkema Publishers,* 211-218.

Poulson D., Durham J.M., Guardincerri E., Morris C.L., Bacon J.D., Plaud-Ramos K., Morley D., Hecht A. (2017) Cosmic ray muon computed tomography of spent nuclear fuel in dry storage casks, *Nuclear Instruments and Methods in Physics Research A,* **842**, 48–53.

Raoux A.-C., Lyoussi A., Passard C., Denis C., Loridon J., Misraki J., Chany P. (2003) Transuranic waste assay by neutron interrogation and online prompt and delayed neutron measurement, *Nuclear Instruments and Methods in Physics Research B*, **207,** 186-194.

Rimlinger M., Frosio T., Menaa N., Magistris M., Theis C. (2020) Qualification of gamma spectrometry measurement for the radiological characterization of mixed VLLW cables in particle accelerators, *Appl. Rad. Isot.*, **166**, 109419.

Rizo Ph., Robert-Coutant Ch., Moulin V., Sauze R., Antonakios M. (2000) Application of transmission tomography to nuclear waste management, *Proceedings of the 15th World Conference on Nondestructive Testing, Roma (Italy), 15-21 October 2000*, https://www.ndt.net/article/wcndt00/papers/idn205/idn205.htm

Rohée E., Coulon R., Carrel F., Dautremer T., Barat E., Montagu T., Normand S., Jammes C. (2015) Qualitative and quantitative validation of the SINBAD code on complex HPGe gamma-ray spectra, 4th International Conference on Advancements in Nuclear Instrumentation Measurement Methods and their Applications (ANIMMA).

Romanini D., Kachanov A. A., Sadeghi N. & Stoeckel F. (1997) CW cavity ring down spectroscopy. Chem. Phys. Lett. 264, 316-322.

Sabeeha J.B., Mohammed G.H.K., Battawi S.M., Falah S.H.H.U., Ahmad J.H., Alaa H.M. (2017) Assessment of gamma dose rate for hypothetical radioactive waste container, *Int. J. Appl. Sci. Res. Rev.*, **4 (1:4).**

Schultz L. J., Blanpied G. S., Borozdin K. N., Fraser A. M., Hengartner N. W., Klimenko A.V., Morris C. L., Orum C., Sossong M. J. (2007) Statistical Reconstruction for Cosmic Ray Muon Tomography, IEEE TRANSACTIONS ON IMAGE PROCESSING, 16 (8), 1985 – 1993.

Simon E., Jallu F., Pérot B., Plumeri S. (2016) Feasibility study of fissile mass quantification by photofission delayed gamma rays in radioactive waste packages using MCNPX, *Nucl. Instrum. Methods Phys. Res. A.*, **840**, 28-35.

Simpson A., Clarkson A., Gardner S., Al Jebali R., Kaiser R., Mahon D., Roe J., Ryan M., Shearer C., Yang G. (2020) Muon tomography for the analysis of in-container vitrified products, *Appl. Rad. Isot.*, **157**, 109033.

Slaughter D.R., Accatino M.R., Bernstein A., Biltoft P., Church J.A., Descalle M.A., Hall J.M., Manatt D.R., Mauger G.J., Moore T.L., Norman E.B., Petersen D.C., Pruet J.A., Prussin S.G. (2007) The nuclear car wash: A system to detect nuclear weapons in commercial cargo shipments, *Nucl. Instr. Methods Phys. Res. A,* **579**, 349-352.

Sonnenschein V. et al. (2018) A cavity ring-down spectrometer for study of biomedical radiocarbon-labeled samples. J. Appl. Phys., **124**, 33101.

Stapleton M., Burns J., Quillin S., Steer C. (2014) Angle Statistics Reconstruction: a robust reconstruction algorithm for Muon Scattering Tomography, Journal of Instrumentation, **9**, 11019.

Stowell P., Alrheli A., Kikola D., Kopp A. , Tietze-Jaensch H., Mhaidra M., Thompson L., Valcke E., Velthuis J., Weekes M., (2019) Figures Of Merit for the Application of Muon Tomography to the Characterization of Nuclear Waste Drums, WM2019 Conference, March 3 - 7, 2019, Phoenix, Arizona, USA.

Su-Ping L.., Guang-chun H., Huai-long W., Cheng-sheng C., Zhao L., Jun Z., Qing-pei X., Ge D. (2014) Detection of nuclear materials: Features and functions of effective half-life, *Nucl. Instrum. Methods Phys. Res. A.,* **735**, 480-484.

Tamagno L., Eléon C., Estre N., Plumeri S., Tisseur D. *(*2018) Atomic number reconstruction using multi-MeV X-ray DECT in concrete drums*, NSS 2018, 10-17 November 2018, Sydney, Australia.*

Tesse R., Stichelbaut F., Pauly N., Dubus A., Derrien J. (2018) GEANT4 benchmark with MCNPX and PHITS for activation of concrete, *Nucl. Instrum. Methods Phys. Res. B,* **416**, 68-72.

Thomay C., Velthuis J.J., Baesso P., Cussans D., Morris P.A.W., Steer C., Burns J., Quillinb S., Stapletonb M. (2013) A binned clustering algorithm to detect high-Z material using cosmic muons, Journal of Intrumentation, **8**, 10013.

Thomay C., Velthuis J.J., Poffley T., Baesso P., Cussans D. and Frazão L., (2016) Passive 3D imaging of nuclear waste containers with Muon Scattering Tomography, Journal of Intrumentation, 11, 03008.

Toubon H., Mehlman G., Gain T., Lyoussi A., Pérot B. et al., (2001) Innovative nuclear measurement techniques used to characterize waste produced by COGEMA's new compaction facility, Proc. of WM'01, Waste Management Conference, Tucson, AZ, USA.

Troiani F., Bienvenu P., Dale C., Delepine J.J., Fachinger J., Gallego C., Klein F., Rishehri D., Rodriguez M., Vanderlinden F., Voors P.I., Welbergen J. (2001) Destructive analyses for the quality checking of radioactive waste packages, Review of methods within the working group on "destructive analyses" of the European network of testing facilities for the quality checking of radioactive waste pakcages, Report WG-B-01.

Venialgo E., Belzunce M., Verrastro C., Garbino L.M., da Ponte E., Alarcon J., Carimatto A., Estryk D., Prieto I. (2012) Analysis and comparison of tomographic gamma scanner (TGS) architectures for nuclear waste characterization systems, *MRS Online Proceedings.*

Weekes M.J., Alrheli A.F., Barker D., Kikoła D., Kopp A.K., Mhaidra M., Stowell J.P., Thompson L.F., Velthuis J.J. (2021) Material identification in nuclear waste drums using muon scattering tomography and multivariate analysis, *Journal of Instrumentation*, **16**, P05007.

Zaffora B., Demeyer S., Magistris M., Ronchetti E., Saporta G., Theis C. (2020) A Bayesian framewok to update scaling factors for radioactive waste characterization, *Appl. Radiat. Isot.*, **159**, 109092.